UTS UNIVERSITY OF TECHNOLOGY SYDNEY

Novel customisable phases for micro solid-phase extraction and automated biological sample preparation

by Karen Duong

Thesis submitted in fulfilment of the requirements for the degree of

Doctor of Philosophy

under the supervision of Distinguished Professor Philip Doble, Dr David Bishop and Dr Raquel Gonzalez de Vega.

University of Technology Sydney
Faculty of Science

August 2021

Certificate of authorship and originality

I, Karen Duong declare that this thesis, is submitted in fulfilment of the requirements for the award of Doctor of Philosophy, in the School of Mathematical and Physical Sciences at the University of Technology Sydney.

This thesis is wholly my own work unless otherwise referenced or acknowledged. In addition, I certify that all information sources and literature used are indicated in the thesis.

This document has not been submitted for qualifications at any other academic institution.

This research is supported by the Australian Government Research Training Program.

Signature:

Production Note:
Signature removed prior to publication.

Date: 30th August 2021

Acknowledgements

This thesis wouldn't have been possible without the help and support of many people.

I would like to thank my supervisors, Distinguished Professor Philip Doble, Dr David Bishop and Dr Raquel Gonzalez de Vega for their expertise, great advice, time, and emotional support. They have been instrumental to the success of this project. Dr Raquel Gonzalez de Vega played a significant role and her contributions to this work are greatly appreciated which involved help in performing the final experiments involving the complete automated workflow work with BSA and human serum samples.

Thank you to Peter Dawes, Andrew Minett, Reno Cerra and Mark Wardle at Eprep for the opportunity to work on this project. They have provided countless hours of support. Furthermore, I'd like the express my gratitude to UTS and Eprep for the opportunity to be involved in the Industry Doctorate Program. This targeted PhD program has provided me with invaluable skills and experiences for my career and personal development.

Thank you to Dr David Clases for his assistance with my research project, helping me run instruments, and for offering great support and ideas. I would also like to thank Dr Matt Padula and Joel Steele for their help with proteomics and running samples. Thank you to Dr Ronald Shimmon and Dr Dayanne Bordin for providing great technical services.

I'd like to thank the analytical research group, Mika Westerhausen, Matthew Diplock, Phuc Nguyen, Prashina Singh, Natasha Benson-Jeffrey, Sarah Meyer, Thomas Lockwood and Brooke Mansell for their comradery, support and good times. Would like to thank my peers, Minh Nguyen for being a good lunch buddy and always bringing the best snacks, and Jacqueline Loyola-Echeverria for providing moral support. Thank you to Susan Shimmon and Mahmoud El Safadi for the great times we had in laboratory.

I want to give a huge thanks to my family who encouraged me to finish. They have showed me never-ending love and support, and to them I am so grateful. Thank you to all my friends for your support and words of encouragement. Particularly, a massive thanks to Hue for being there for me through the highs and lows. Finally, I'd like to give my utmost thanks to the LORD God for his providence and guidance over all things.

Abstract

Protein biomarkers play an important role in clinical settings as they serve as measurable indicators for normal or abnormal biological processes. They aid in accelerated disease identification, diagnosis, prognosis, and response to treatments. Recently, mass spectrometry (MS) assays have been introduced as an alternate to the conventionally used immunoassays. MS provides accurate and precise quantification due to its high sensitivity and specificity. However, major challenges lie with sample preparation involving lengthy workflows, limited automation, and challenges related to highly complex biological samples where several techniques are applied.

This thesis aims to improve sample preparation techniques to provide an accurate, rapid, and automated method for protein biomarker quantification using micro-solid-phase extraction (μSPE) technology through the development of a micro-immobilised-enzyme reactor (IMER) and a μSPE immunoaffinity cartridge to alleviate sample preparation bottlenecks caused by conventional ~18-hour digestions.

A novel and customisable material was prepared for bio-ligand immobilisation. A hybrid inorganic-organic material using silica modified with carboxymethylated dextran (CMD) was prepared. This material was packed into μSPE cartridges and 1-ethyl-3-(3-dimethylaminopropyl)carbodiimide (EDC) and N-hydroxysuccinimide (NHS) coupling was exploited to immobilise enzymes and antibodies in-situ using a programmable syringe driver allowing for the development of an automated workflow.

Reproducible trypsin digestion was observed using high performance liquid chromatography (HPLC) through the cleavage of N-α-Benzoyl-L-arginine ethyl ester (BAEE). Three model proteins (bovine serum albumin, cytochrome c and thyroglobulin) and a human serum sample were analysed, and compared to conventional in-solution digestion by employing liquid chromatography orbitrap mass spectrometry (LC-OT-MS) and liquid chromatography quadrupole time of flight mass spectrometry (LC-QToF-MS). The IMER facilitated protein digestion within 10 minutes at room temperature and overall, observed lower sequence coverages and number of identified proteins compared to the conventional in solution digestion method at 37°C.

In the same manner as trypsin, anti-BSA was immobilised and BSA isolation was confirmed using size exclusion chromatography hyphenated to triple quadrupole inductively coupled plasma mass spectrometry (SEC-ICP-MS/MS). Whilst immobilisation of anti-BSA was achieved, challenges with low level protein detection were observed.

The immunoaffinity and trypsin μSPE cartridge were combined into an automated workflow for protein pre-concentration and digestion. Using BSA as the model protein, BSA standards and BSA spiked into human serum samples were subjected to the workflow. BSA extraction and digestion was achieved, however, the complex human serum matrix negatively impacted the BSA isolation compared to neat standards. Further investigation and optimisation of the workflow must be performed.

List of Publications and Presentations

Journal Publications

Immunoaffinity extraction followed by enzymatic digestion for the isolation and identification of proteins employing automated µSPE reactors and mass spectrometry (Submitted to Analytical and Bioanalytical Chemistry).

Application Notes

Karen Duong, Simin Maleknia, Andrew Minett, David Bishop, Philip Doble, "µSPEed-Cxyl microreactor cartridges: Trypsin cartridges for digests of bovine serum albumin (BSA)", ePrep Application Note, 2019.

Karen Duong, Philip Doble, "µSPEed recovery curve with 4 nitrotoluene", ePrep Application Note, 2015.

Conference Poster Presentations

Karen Duong, Raquel Gonzalez de Vega, Andrew Minett, David Bishop, Philip Doble, *"Immunoaffinity and enzymatic reactor micro-solid-phase extraction cartridges for rapid protein isolation and digest"*, American Society for Mass Spectrometry Conference, 2019, Atlanta, Georgia, USA.

Karen Duong, Simin Maleknia, Andrew Minett, David Bishop, Philip Doble, *"Immobilised enzymes on micro-solid-phase extraction cartridges for automated protein digestion"*, American Society for Mass Spectrometry Conference, 2018, San Diego, California, USA.

Karen Duong, Simin Maleknia, Andrew Minett, David Bishop, Philip Doble, *"Customisable micro-solid-phase extraction for selective binding in biological sample preparation"*, The Pittsburgh Conference on Analytical Chemistry and Applied Spectroscopy, 2018, Orlando, Florida, USA.

Karen Duong, Simin Maleknia, Andrew Minett, David Bishop, Philip Doble, *"Immobilised enzymes on customisable micro-solid-phase extraction cartridges for proteolytic digests in minutes"*, Lorne Proteomics Symposium, 2018, Lorne, Melbourne, Australia.

Table of Contents

Certificate of authorship and originality ..... **i**

Acknowledgements ..... **ii**

Abstract ..... **iii**

List of Publications and Presentations ..... **v**

Table of Contents ..... **vi**

List of Abbreviations and Acronyms ..... **viii**

List of Figures ..... **xii**

List of Tables ..... **xvi**

Chapter 1 Introduction: Protein biomarker quantification for clinical proteomics **1**

1.1 Biomarkers for Clinical Proteomics 2

1.1.1 Protein Biomarker Quantification 3

1.1.2 Molecular mass spectrometry for the analysis and determination of potential biomarkers 5

1.1.3 Elemental mass spectrometry for the analysis and determination of potential biomarkers 7

1.1.4 Sample preparation for biomarker analysis 10

1.2 Solid Phase Extraction 15

1.2.1 Miniaturisation, automation, and progression of SPE methods 17

1.2.2 Customisable material for targeted sample preparation 20

1.3 Project Aims 30

Chapter 2 Customisable support material for biologically selective and automated sample preparation using the ePrep µSPE format **33**

2.1 Introduction 34

2.2 Experimental 37

2.2.1 Chemicals and Consumables 37

2.2.2 µSPE method 37

2.2.3 Development of customisable material for µSPE cartridges 37
2.3 Results and Discussion 41
2.4 Conclusion 50
Chapter 3 Development of rapid and automated µSPE sample preparation workflows for protein biomarkers 51
3.1 Introduction 52
3.2 Experimental 55
3.2.1 Chemicals and Consumables 55
3.2.2 µSPE sample preparation workflow development 55
3.3 Development of the IMER µSPE cartridge 59
3.3.1 Instrumentation and parameters for IMER µSPE cartridge 59
3.3.2 Sample preparation for protein digestion using model proteins and human serum sample 62
3.3.3 Results and Discussion 63
3.4 Development of the immunoaffinity µSPE cartridge 78
3.4.1 Instrumentation and parameters for immunoaffinity µSPE cartridge 78
3.4.2 Exogenous labelling of proteins 79
3.4.3 Antibody immobilisation and Ab-Ag complex formation 80
3.4.4 Results and Discussion 82
3.5 Combination of the immunoaffinity and IMER µSPE cartridges for an automated workflow 89
3.5.1 µSPE workflow 89
3.5.2 Results and Discussion 89
3.6 Conclusion 91
Chapter 4 : Overall Conclusions and Future Work 93
References 98

List of Abbreviations and Acronyms

Ab-Ag: antibody-antigen complex

ABTS: 2,2'-azino-bis(3-ethylbenzothiazoline-6-sulfonic acid)

ACN: acetonitrile

AGC: automated gain control

APS: aminopropyl silica

ATR: attenuated total reflectance

BA: N_{α}-Benzoyl-L-arginine

BAEE: N_{α}-benzoyl-L-arginine ethyl ester

BCA: bicinchoninic acid

BEC: background equivalent concentration

BIN: barrel insert and needle

BSA: bovine serum albumin

CID: collision induced dissociation

CMD: carboxymethylated dextran

Cyt c: cytochrome c

CV: coefficient of variation

Da: dalton

DMSPE: dispersive micro-solid-phase extraction

DNA: deoxyribonucleic acid

DSS: disuccinimidyl suberate

DTT: dithiothreitol

EDC: 1-ethyl-3-(3-dimethylaminopropyl)carbodiimide

ELISA: enzyme-linked immunosorbent assays

ESI: electrospray ionisation

F_{ab}: fragment antigen binding

F_c: fragment crystallisable

FDR: false discovery rate

FI: flow injection

FTIR: Fourier-transform infrared spectroscopy

GC: gas chromatography

HAPs: high abundant proteins

HPLC: high performance liquid chromatography

HRP: horseradish peroxidase

IA: iodoacetamide

IASPE: immunoaffinity-based solid-phase extraction

ICP-MS: inductively coupled plasma mass spectrometry

ID: inside diameter

Ig: immunoglobulin

IMAC: immobilised metal affinity chromatograph

IMER: immobilised enzyme reactor

ITSP: instrument top sample preparation

KHP: potassium hydrogen phthalate

LAPs: low abundant proteins

LC: liquid chromatography

LAC: lectin affinity chromatography

LLE: liquid-liquid extraction

mAb: monoclonal antibody

MALDI: matrix assisted laser desorption/ionisation

MEPS: microextraction by packed sorbents

MES: 2-(*N*-morpholino)ethanesulfonic acid

MIPs: molecularly imprinted polymers

MISPE: molecularly imprinted solid-phase extraction

MOAC: metal oxide affinity chromatography

MRM: multiple reaction monitoring

MS: mass spectrometry

MS/MS: tandem mass spectrometry

MSPE: magnetic solid-phase extraction

MW: molecular weight

m/z: mass-to-charge ratio

NHS: *N*-hydroxysuccinimide

OAI: oriented antibody immobilisation

OD: outside diameter

OT: orbitrap

pAb: polyclonal antibody

PBS: phosphate buffer saline

PEG: poly(ethylene glycol)

pI: isoelectric point

PIT: pre-immobilised trypsin

PPT: protein precipitation

PRM: parallel reaction monitoring

Q1, Q2, Q3: quadrupole 1, 2 and 3

Q-OT: quadrupole-orbitrap

QQQ: triple quadrupole

RAI: random antibody immobilisation

RNA: ribonucleic acid

SBSE: stir-bar sorptive extraction

SEC: size exclusion chromatography

SPE: solid-phase extraction

SPME: solid-phase microextraction

SPR: surface plasmon resonance

SRM: selected reaction monitoring

TCEP: tris(2-carboxyethyl)phosphine hydrochloride

TPCK: L-1-tosylamide-2-phenylethyl chloromethyl ketone

TIC: total ion chromatogram

ToF: time-of-flight

UV: ultraviolet

UV-Vis: ultraviolet-visible

List of Figures

Figure 1.1: Illustration of a QQQ mass spectrometer with mass filters (Q1, Q3), and collision cell (Q2) [58]. 6
Figure 1.2: Protein interactions with porous stationary phases used in SEC [77]. 8
Figure 1.3: MS/MS mode using an oxygen cell for mass shifting of ^{32}S (m/z 32) to $^{32}S16O$ (m/z 48) [87]. 9
Figure 1.4: Sample preparation workflow for targeted quantification of protein biomarkers [101]. 10
Figure 1.5: Bind-elute strategy for SPE [170]. 17
Figure 1.6: Non-specific interaction between silica surface and proteins. A) electrostatic interaction between negatively charged surface and positively charged residues on the protein, and B-D) protein deformation due to weak internal cohesion resulting in deformation and hydrophobic interaction with the silica surface [254]. 22
Figure 1.7: Immobilisation strategies used for biomolecules (E) [148]. 24
Figure 1.8: A) Avidin-biotin complex with four binding sites, and B) Bicyclic structure of biotin with a carbylic acid side chain that can be modified [283]. 26
Figure 1.9: Antibody immobilisation through intermediate proteins: protein A or G [280]. 26
Figure 1.10: Homo- and hetero- bifuncational crosslinkers with reactive groups held by a spacer arm [291, 292]. 28
Figure 1.11: EDC activation of a carboxylic group for form an unstable o-acylisourea intermediate that when reacted with an amine compound, forms an amide bond between the carboxylate compound and amine compound [295]. 29
Figure 1.12: Primary amine reacting with the stable NHS ester to form an amide bond [295]. 29
Figure 1.13: -SH groups obtained through disulfide bridge reduction [305]. 30
Figure 2.1: digiVOL® syringe driver used for method development and the press-fit µSPEed cartridge onto a syringe. The µSPEed offers two flow paths where solutions are aspirated through the one-way valve and dispensed onto the sorbent packing material [314]. 36
Figure 2.2: ePrep® Sample Preparation Workstation showing sample trays and liquid dispensing syringes [314]. 36

Figure 2.3: Methods for non-covalent and covalent immobilsation of HRP onto silica-CMD cartridges. 40
Figure 2.4: FTIR spectra obtained for starting materials a) APS, b) CMD (red), and the synthesised material c) silica-CMD. 42
Figure 2.5: Conductometric titration of the blank control with no silica-CMD material. 43
Figure 2.6: A) Conductometric titration of silica-CMD prepared from 120 Å material with the first derivatives for the B) starting and C) end point of the neutralisation of -COOH groups on the silica-CMD. 45
Figure 2.7: Conductometric titration of silica-CMD prepared from 300 Å material. 47
Figure 2.8: FTIR of 1000 Å APS material following attempted CMD coating. 47
Figure 2.9: Absorbance of ABTS radical cation at 620 nm using the Thermo Fisher Multiskan Ascent 96/384 Plate Reader to compare between non-covalent and covalent immobilisation of HRP onto silica-CMD material. 49
Figure 3.1: Automated µSPEed biomarker workflow for both protein immunoaffinity isolation and digestion. 58
Figure 3.2: Observing the presence of BAEE (4 min) hydrolysis to BA (2 min) by excess non-covalently bound trypsin in collected salt wash buffer aliquots. A) Chromatogram shows BAEE hydrolysis following the first salt wash buffer wash and B) a chromatogram showing no presence of trypsin in subsequent washes. 64
Figure 3.3: Comparison of two BSA digests (5 µg protein load) using different $CaCl_2$ concentrations. Aliquot A1) TIC for BSA digest in running buffer containing 1000 µM $CaCl_2$ and Aliquot A2) TIC for elution buffer aliquot following the 1000 µM $CaCl_2$ running buffer digest using 25 mM Tris, 10 mM $CaCl_2$ and 10% ACN showing minimal peptide adsorption. Aliquot B1) TIC for BSA digest in running buffer containing 500 µM $CaCl_2$ and the Aliquot B2) TIC for elution buffer aliquot following the 500 µM CaCl2 running buffer using 25 mM Tris, 10 mM $CaCl_2$ and 10% ACN showing peptide adsorption. C) TIC of 50 ng/µL BSA standard that was not digested. 66
Figure 3.4: Cyt c adsorption onto a) -COOH glycine end-capped as observed by the red appearance, and the absence of cyt c adsorption onto b) -OH ethanolamine end-capped silica-CMD. 67

Figure 3.5: HPLC-UV chromatogram at 254 nm for BAEE (4 min) digestion to BA (2 min) for a) 2-minute digest and b) 5-minute digest. 68
Figure 3.6: TICs of cartridge digests of Cyt c with varying protein amounts. A) A 5-minute digest of 10 µg of Cyt c showing remaining undigested protein whilst B) a 5-minute digest of 1 µg Cyt c shows no undigested protein. 69
Figure 3.7: TICs of cartridge digests of BSA with varying protein amounts. A) A 10-minute digest of 5 µg BSA showing undigested protein whilst B) a 10-minute digest of 1 µg BSA with minimal protein remaining. 70
Figure 3.8: A) and B) show TIC of BSA digest using two trypsin cartridges where 15 pmol of BSA was loaded with an incubation time of 10 minutes. Analysis was performed using the LC-OT-MS and the resulting injected peptides from 375 fmol of digested protein. C) TIC of a blank trypsin cartridge digest where running buffer was used. 71
Figure 3.9: Two BSA cartridge digests (top being 61% sequence coverage and bottom 59%), showing high overlap of protein sequence coverage. 72
Figure 3.10: Standard calibration curve constructed for BAEE after analysis with HPLC-UV. 73
Figure 3.11: Number of identified peptides using IMER and in-solution digests for BSA, Cyt c and Tg, and the number of peptides observed across both methods. 75
Figure 3.12: Protein sequence coverage for the A) overnight and B) cartridge digest of BSA, highlighting the amino acids that were unique to each respective sequence coverage and not observed in the other. 76
Figure 3.13: Protein sequence coverage for the A) overnight and B) cartridge digest of Cyt c, highlighting the amino acids that were unique to each respective sequence coverage and not observed in the other. 76
Figure 3.14: Protein sequence coverage for the A) overnight and B) cartridge digest of Tg, highlighting the amino acids that were unique to each respective sequence coverage and not observed in the other. 77
Figure 3.15: Example of Maxpar™ labelling through maleimide linkages on desired biomolecule containing free -SH groups [353]. 80
Figure 3.16: A) Covalent immobilisation of anti-BSA onto silica-CMD and visualisation with mouse IgG HRP polymer antibody and B) covalent immobilisation of BSA onto silica-CMD for

complex formation with anti-BSA, and visualisation with mouse IgG HRP polymer antibody. 81
Figure 3.17: Visualisation of HRP activity with mouse IgG HRP polymer and ABTS substrate for the confirmation of A) covalent immobilisation of anti-BSA onto silica-CMD as well as the B) BSA immobilisation followed by complex formation betweeen anti-BSA and BSA, and C) and D) as their respectivblank controls where no covalent immobilisation was performed using EDC/NHS. 83
Figure 3.18: Protein ladder calibration used to calculate MW of the biomolecule using the retention time using the Agilent Bio SEC-3 column. 84
Figure 3.19: SEC-ICP-MS/MS analysis using the Agilent Bio SEC-3 column for BSA (black), anti-BSA (red), and Ab-Ag complex (orange) with corresponding MW calculations using the protein ladder calibration. 85
Figure 3.20: Chromatographic separation of BSA (S signal, red) and labelled BSA-Er (Er signal, black) by SEC-ICP-MS/MS analysis using the Waters ACQUITY UPLC Protein BEH SEC. 85
Figure 3.21: Chromatograms obtained form the analysis of salt wash buffer aliquots following BSA sample loading onto an ePrep cartridge and analysed using FI-ICP-MS/MS for detection of $^{32}S^{16}O$. 87
Figure 3.22: Chromatograms obtained from the analysis of salt wash buffer aliquots following BSA-Er sample loading onto an ePrep cartridge and analysed using FI-ICP-MS/MS for detection of ^{166}Er. 87
Figure 3.23: Analysis of eluted sample following immunoaffinity extraction of BSA with an anti-BSA ePrep cartridge. Sample was analysed using SEC-ICP-MS/MS for detection of $^{32}S^{16}O$. ... 88
Figure 3.24: Analysis of eluted sample following immunoaffinity extraction of BSA with an anti-BSA ePrep cartridge. Sample was analysed using FI-ICP-MS/MS for detection of $^{32}S^{16}O$. 88
Figure 3.25: BSA protein coverage (26%) obtained by LC-OT-MS of the spiked human sample after protein isolation followed by tryptic digestion. 90

List of Tables

Table 1.1: Enzyme immobilisation techniques and their advantages and disadvantages [148]. 24
Table 2.1: Calculated mmol of -COOH groups per gram of customised silica-CMD material for n=7 batches. 45
Table 2.2: Relationship between pore size and surface area for APS, and the resulting mmol of -COOH groups from the synthesis of silica-CMD [327]. 47
Table 3.1: HPLC conditions for analysis of the trypsin digest of BAEE 59
Table 3.2: Analysis conditions for protein digestion on LC-MS instruments. 61
Table 3.3: Two cartridge digestion methods with differing running buffer salt concentrations followed by an elution buffer to observe for any peptide adsorption to the cartridge as a result. All aliquots were analysed by LC-QToF-MS. 65
Table 3.4: Effect of flow rate on BAEE digest whilst ensuring the total incubation for both digests remain the same. 69
Table 3.5: Calculated BAEE concentration following a 2-minute incubation with six trypsin cartridges. 73
Table 3.6: BSA sequence coverages for µSPE cartridge digest and BSA MS overnight in-solution digest. 76
Table 3.7: Typical operating conditions for the 8900 ICP-MS/MS. 78
Table 3.8: SEC calibration for the protein ladder standard used to calculate sample. 84
Table 3.9: Obtained BSA protein coverage after immunoaffinity extraction followed by tryptic digestion using three affinity cartridge twice. 90

Chapter 1

Introduction: Protein biomarker quantification for clinical proteomics

1.1 Biomarkers for Clinical Proteomics

A biomarker is defined as a specific characteristic, molecule or gene that is measured as an indicator of normal biological processes, pathogenic processes, or responses to an exposure or intervention, including therapeutic interventions [1]. Valid biomarkers are categorised into four groups: (1) detective biomarkers, (2) diagnostic biomarkers, (3) prognostic biomarkers, and (4) predictive biomarkers [2]. Biological systems continually express and suppress the production of molecules due to an environmental stimulus or biological processes where correlation of the up and down regulation of these molecules can be very useful in discerning various biological pathways. While biomarkers can be any molecule within any organism, generally in life science research, peptides and proteins are of highest interest and importance where the proteome is used to discover, identify, and quantify protein biomarkers. Proteins are large, complex molecules that are made up of hundreds or thousands of smaller amino acid units which determines its unique 3-dimensional structure and specific function. Proteins are essential to all biological processes as they perform a vast array of functions within an organism such as, catalysing chemical reactions, synthesising and repairing deoxyribonucleic acid (DNA), transporting materials across cells, receiving and sending chemical signals, responding to stimuli, providing structural support, and regulating cellular and physiological activities [3, 4]. Consequently, protein biomarkers play an important role in clinical settings as they are measurable indicators of homeostasis and are often used to accelerate or aid in diagnosis, prognose the course of a particular disease, and provide insights into effective treatments for cancer [5-7], Alzheimer's and Parkinson's disease [8, 9], muscular dystrophy [10], cardiovascular disease [11], lung damage [12] and kidney injury [13], amongst others.

The biomarker pipeline workflow involves several phases which include discovery, qualification, verification and clinical assay development, validation, and evaluation. Most protein biomarker analyses attempt to detect proteins specifically associated with disease by the comparative profiling of healthy control proteomes against disease affected donors [14]. The first stage is to discover protein targets that can aid in the diagnosis and detection of physiological conditions. The markers must be qualified for association between differential protein abundance and clinical outcomes following verification phases to measure the most promising candidates, and exclude false candidates, and must be able to differentiate cases

from controls for the purposes of diagnosis, prognosis or other measurable outcomes to move onto clinical phases [15, 16]. Once identified, assays with suitable analytical performance for diagnostic accuracy studies and for eventual use in routine clinical practice are developed, validated and evaluated [17]. However, in the last decade, despite the considerable interest and large number of studies that aimed to identify and quantify protein biomarkers for diseases, the average rate at which a discovered biomarker is translated into a clinical application is slow with only 1.5 new tests per year [18]. A novel and useful biomarker must be clinically relevant and provide information beyond the current biomarkers available for disease, or provide benefits financially or to patient risk [19]. To be used in a clinical application, protein quantification assays must be developed and validated with stringent standards which include high sensitivity and specificity, accuracy, reproducibility and low coefficients of variation (CV) [20]. Since clinical needs vary for different diseases, the discovery, verification and validation cannot be restricted to a single method [21]. The assays must have short analysis times, high throughput, simplicity, and low costs to be easily translated for use in clinical laboratories. However, this can be challenging from an analytical standpoint as samples from body fluids such as saliva, plasma/serum, whole blood, and urine are highly complex and contain various macromolecules. Therefore, proteomic technologies are being advanced to quantify protein biomarkers of diseases.

1.1.1 Protein Biomarker Quantification

There is a necessity for accurate quantification of proteins and peptides in complex biological matrices particularly for clinically relevant biomarker candidates identified during the discovery phase. However, the biggest hurdle with biomarker discovery and quantification is the transfer from laboratory to the clinic. There are several different technologies used for biomarker quantification including ligand-binding assays, mass spectrometry, flow cytometry and immunohistochemistry, where ligand-binding assays and mass spectrometry are the two most commonly used platforms [22].

Ligand-binding assays rely on capturing the protein of interest by an agent, often an analyte-directed antibody followed by detection through either complex formation with a detection reagent, or via a modified and easily detectable form of the protein analyte, which competes with the analyte for the binding sites on the capturing reagent [23]. In particular,

Enzyme-Linked Immunosorbent Assays (ELISAs), have been a standard tool for scientific and diagnostic laboratories worldwide [24]. In the simplest form of an ELISA, an analyte from a sample is captured to a surface containing a specific binding partner, typically an antibody. This antibody can be coupled to an enzyme to generate a detectable signal through an enzymatic reaction that can be measured via colour, light, or fluorescent signal. Using this simple principle, ELISAs has expanded to create other approaches including sandwich ELISAs [25], indirect ELISAs [26] and competitive ELISAs [27]. An advantage of the ELISA platform is its simple application, however, it can have limitations when considering high-throughput screenings [28]. Although ELISAs are regarded as a singleplex assay format, they can be made suitable for multiplex protein analysis by combining several antibodies with defined specificity in one test, allowing binding of multiple proteins [29]. This however can be limited as the ELISA may exhibit cross-reactivity [30]. Thus, ELISAs are suited for applications where only a few biomarkers need to be validated for many samples [26]. Other limitations are seen in costs as the development of an ELISA is an expensive and time-consuming process where antibodies for each targeted protein or peptide are often unavailable [31, 32].

Mass spectrometry (MS)-based assays are emerging as viable alternatives for accurate protein quantification to ligand-binding assays where comparable quantitative results are achievable [33]. Furthermore, the analytical specificity provided by MS is often superior to that of other methods by unambiguous identification of a molecule. For example, a comparative study showed the discrimination between vitamins D2 and D3 in human serum samples using liquid chromatography tandem mass spectrometry (LC-MS/MS) when immunoassays could not [34]. An example of a successful application of MS in clinical chemistry is newborn screening. Through simultaneous detection of multiple amino acids, free carnitine, and acylcarnitines from dried blood spots using tandem MS (MS/MS), critical information of congenital deficiencies of metabolism can be identified [35]. This MS-based method is suitable to screen more than 50 different metabolic disorders in one rapid and efficient test. In contrast, conventional enzyme- or immunoassays, require one test to detect one disorder [36, 37]. Thus, there is potential for MS-based assays for protein biomarker quantification in clinical settings. However, as with any assay, there are challenges that require consideration as described in the following sections.

1.1.2 Molecular mass spectrometry for the analysis and determination of potential biomarkers

Mass spectrometry is the gold standard for the identification and quantification of potential biomarkers in diagnostic and therapeutic medicine, with MS/MS frequently applied to biomarker quantification due to its high sensitivity and through-put [38]. MS/MS is a technique where two or more mass analysers are coupled together. A typical configuration involves the isolation of a predetermined *m/z* precursor ion followed by fragmentation to produce product ions, which are detected in the second stage of MS/MS producing a mass spectra [39]. This method is otherwise known as selected reaction monitoring (SRM) or multiple reaction monitoring (MRM) where multiple product ions are analysed [40]. MRM is ideal for protein quantification with a variety of platforms such as matrix assisted laser desorption/ionisation time-of-flight tandem (MALDI-ToF/ToF) [41], ion trap [42], QToF [43], and the most popularly used triple quadrupole (QQQ) mass spectrometer [44]. MRM is a scanning mode involving two stages of mass analysis commonly performed with QQQ mass spectrometers equipped with tandem quadrupole mass filters (Q1, Q3) and a collision cell (Q2) (see Figure 1.1). During the first stage, the Q1 filters a precursor ion, Q2 performs collision induced dissociation (CID) for further fragmentation of the selected precursor ion, and Q3 filters the unique fragment(s) (product ions) for unambiguous and sensitive determination of the original biomarker. Greater specificity is achieved by fragmenting the analyte, and monitoring both precursor and one or more product ions simultaneously. This reaction however must be defined (or predicted) to allow selection of the appropriate precursor/product ion pairs, or transitions for the analyte of interest.

Studies have successfully used MRM-MS to verify diseases and quantify biomarkers for cancer [45, 46], cardiovascular diseases [47] and atherosclerosis [48] with the latter reporting comparable results with well-established immunoassays. MRM-MS allows targeted multiplexed tandem MS detection of hundreds of peptides with a recent report of quantification of 63 protein biomarkers in human urine [49]. Furthermore, recent studies have shown that targeted experiments known as parallel reaction monitoring (PRM) can also be performed on hybrid quadrupole-orbitrap (Q-OT) and quadrupole time-of-flight (Q-ToF) mass spectrometers in which the Q3 is replaced by their respective mass analyser [50-56]. PRM

protein quantification is highly selective and specific as MS/MS data is acquired with high resolution and mass accuracy [50, 51]. Additionally, PRM allows acquisition of full MS/MS spectra containing all the potential product ions, eliminating prior selection of target transitions [57].

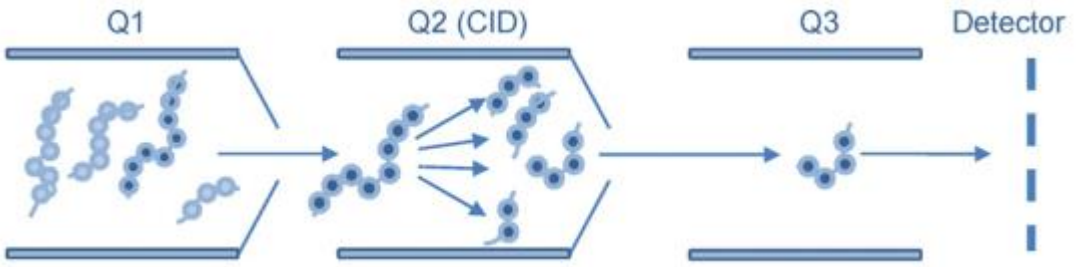

Figure 1.1: Illustration of a QQQ mass spectrometer with mass filters (Q1, Q3), and collision cell (Q2) [58].

Although MS/MS is a well-known technique that has been used for over 30 years for small molecule analysis such as drug metabolites [59-61], its application to protein quantification is still growing [45, 46, 62, 63]. Whilst MS/MS detection ensures high selectivity and works well for relatively small molecular species, up to around 4000 Da, it is inherently less suitable for larger analytes as their ions are distributed over many different charge states and these tend to fragment less readily, which considerably reduces sensitivity [64]. Consequently, for protein quantification, macromolecular analytes require division into smaller compounds to allow quantification by MS/MS. This is usually accomplished by digestion of the analyte with an enzyme, such as trypsin, into a series of peptides where a signature peptide is then quantified as a surrogate for the intact protein [65, 66]. To accurately quantify the signature peptide, and specifically in the case of molecular mass spectrometry where ionisation sources preserve molecular information of the analyte, stable isotope-labelled peptide internal standards are often used to compensate for variation in recovery and the influence of differential matrix effects as they have the same structures and similar chromatographic properties as their native compound [67, 68].

1.1.3 Elemental mass spectrometry for the analysis and determination of potential biomarkers

An alternative approach to protein biomarker detection is available using elemental mass spectrometry techniques such as inductively coupled plasma mass spectrometry (ICP-MS) [69]. Compared to molecular mass spectrometry techniques where molecular information of the analyte is preserved, ICP-MS determines the elemental composition of the sample where molecules in the sample are completely atomised during sample ionisation [70]. As a result, ICP-MS offers a quantitative and highly selective approach to elemental bioanalysis due to its virtual matrix/species-independent ionisation [71]. However, due to the nature of the atomic detection, the potential applicability of ICP-MS to biomarker quantification depends on the ability to hyphenate ICP-MS to other techniques such as liquid chromatography (LC) to obtain species information in terms of retention [72]. Additionally, LC hyphenation to ICP-MS allows intact protein quantification, which can be challenging for molecular MS techniques [73, 74]. Depending on which chromatographic method is used, different species-specific characteristics such as polarity, size, charge, or affinity can be exploited for separation and isolation of the target protein(s). For example, size exclusion chromatography (SEC) hyphenated to ICP-MS has been used for targeted analysis of proteins and peptides in complex biological matrices [75]. SEC is a separation technique based on the molecular size of the analytes where fractionation occurs through repeated exchange of the molecules between the mobile phase and a porous stationary phase [76]. As molecules pass through the column, smaller molecules enter the pores of the stationary phase while the larger ones are unable to enter due to their size (see Figure 1.2). The smaller molecules are temporarily retained by the stationary phase and will continue flowing down the column encountering other particles and pores. On the other hand, the larger molecules which do not interact with the pores flow more rapidly down the length of the column and consequently elute first. This results in the separation of different molecular sizes into distinct chromatography bands that can be detected [77]. When this technique is used with a protein standard mix containing proteins of different molecular weights (MW), a calibration curve (elution time vs. $\log_{10}$[MW]) can be constructed to calculate the MW of a target analyte [78].

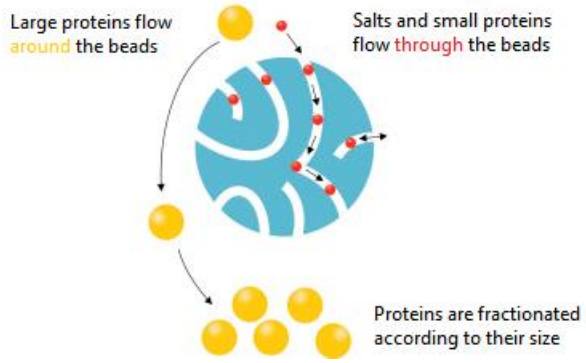

Figure 1.2: Protein interactions with porous stationary phases used in SEC [77].

ICP-MS offers multi-elemental analysis, excellent detection limits (as low as pg/g), and a large linear dynamic range [79]. ICP-MS has emerged as a technique to detect complex biomolecules, such as nucleic acids [80] and metal-proteins [81, 82] via their specific and often characteristic elemental content. Moreover, ICP-MS is ideal to measure naturally occurring heteroatoms (that is, elements other than the frequently found C, H, O, and N) in protein biomarkers such as sulphur (present in cysteine and methionine amino acids), selenium (selenoproteins) and phosphorous (phosphoproteins) for screening and quantification purposes [83]. For instance, when the amino acid sequence of a protein is known, and thus the number of sulphur-containing residues, the sulphur concentration obtained by ICP-MS can be easily translated into protein molar concentration [84]. However, whilst detectable, there are some elements that are difficult to analyse by ICP-MS such as those with high first ionisation potentials resulting in poor detection limits, as well as elements that are subject to spectral and polyatomic interferences [85, 86]. For example, the ionisation efficiency of sulphur in the argon plasma is limited due to its high first ionisation potential of 10.36 eV [87]. Additionally, polyatomic ions such as $^{16}O^{16}O^{+}$, $^{14}N^{18}O^{+}$, $^{16}O^{18}O^{+}$, and $^{16}O^{17}OH^{+}$ interfere with the main isotopes of ^{32}S and ^{34}S measurements respectively. Consequently, techniques have been developed to improve protein detection capabilities using ICP-MS including tandem MS and exogenous tagging.

One technique used to enhance protein detection is the triple quadrupole ICP-MS (also known as ICP-MS/MS). Traditionally, elements such as sulphur and phosphorous, two non-metallic and relevant heteroatoms in proteins have been refractory to sensitive ICP-MS determinations [88]. The emergence of ICP-MS/MS has improved sulphur and phosphorous analysis as it

minimises the effect of interferences by providing different detection modes with the QQQ, thereby improving analyte selectivity [89, 90]. Using sulphur as an example, the QQQ allows mass shift detection where $^{32}S^{+}$ (Q1 mass filter) reacts with oxygen in the O_2 reaction/collision cell to form a sulphur-oxygen ion ($^{32}S^{16}O^{+}$) which can be measured at *m/z* 48 (Q3) (see Figure 1.3) [84, 87]. This approach has been used for the simultaneous quantification of different sulphur-containing peptides and phosphopeptides with low detection limits in the femtomole range [91] and the absolute quantification of proteins by analysing the total amount of sulphur [92].

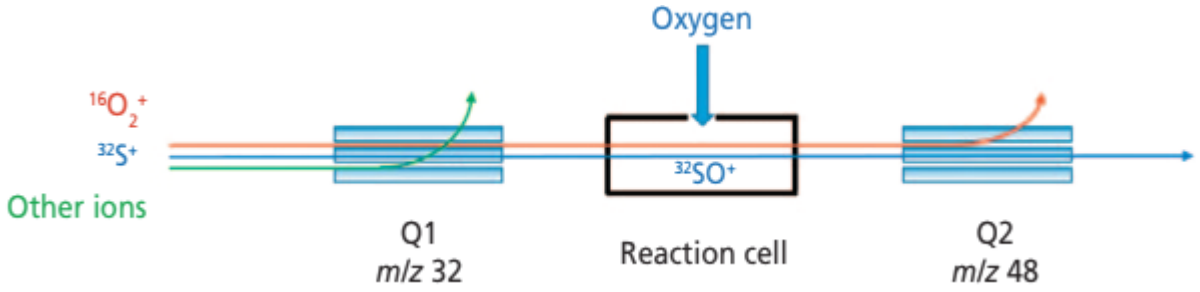

Figure 1.3: MS/MS mode using an oxygen cell for mass shifting of ^{32}S (m/z 32) to $^{32}S16O$ (m/z 48) [87].

Another technique used to enhance protein detection capabilities and sensitivity for ICP-MS analysis is through exogenous tagging or labelling of biomolecules [93]. The most popular tags are functionalised metal chelators such as 2-(4-isothiocyanatobenzyl)-1,4,7,10-tetraazacyclododecane-1,4,7,10-tetraacetic acid [94] and Maxpar™ reagent [95]. These isotopically enriched elements are used to maximise the signal measured by the ICP-MS with lanthanides being popular choices for tagging as they are not present in biological systems at detectable levels, are easily ionised, have low background equivalent concentration (BEC) and few interfering polyatomic species [96]. Additionally, these tags offer numerous metal binding sites resulting in hundreds of lanthanide atoms per biomolecule [97]. However, the labelling process is variable and can produce conjugates lacking the metal tag. Consequently, it is important to monitor the labelling process where hyphenated chromatographic separation methods such as SEC-ICP-MS are used [98].

1.1.4 Sample preparation for biomarker analysis

Sample preparation plays an important role in bioanalytical methods as biomarkers of interest are often present at low concentrations in biological matrices with complex compositions and high dynamic range [99]. This can lead to challenges for LC-MS analysis where endogenous substances such as salts, phospholipids, sugars, peptides, and nucleic acids may compromise the sensitivity and robustness of analysis [100]. To remove or minimise the effect of these endogenous substances, protein precipitation (PPT), liquid-liquid extraction (LLE), and solid-phase extraction (SPE) techniques have been regarded as effective means for the majority of biomarkers analysed, however, for larger proteins or long peptides, further processing with more complex sample preparation techniques are required including extraction of the proteins from biofluids or tissues, enrichment of the target proteins and peptides using immunoaffinity capture, protein denaturation, reduction and alkylation, and proteolytic digestion (see Figure 1.4) [101].

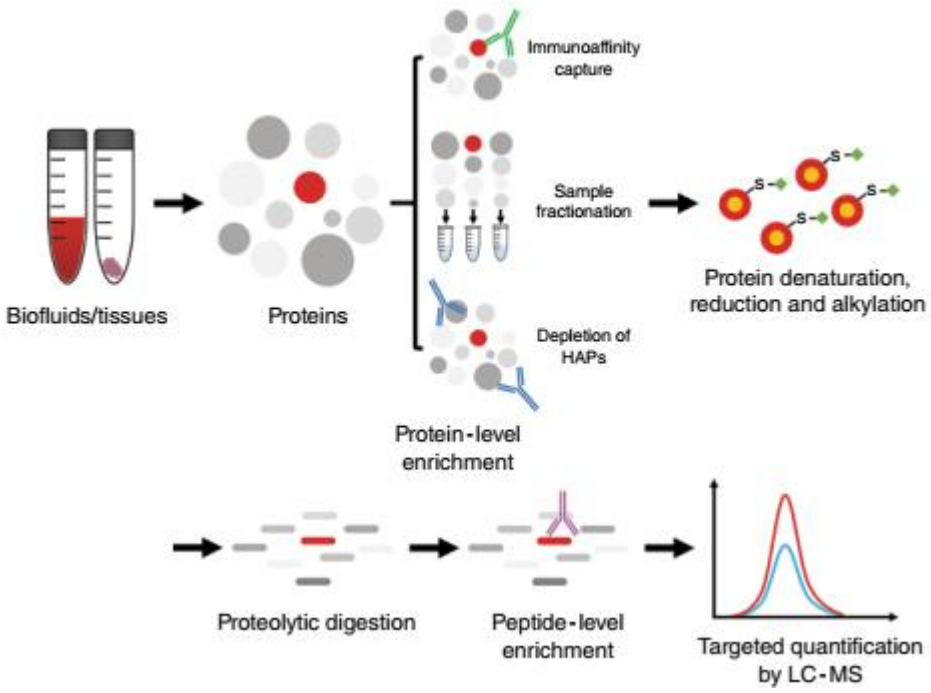

Figure 1.4: Sample preparation workflow for targeted quantification of protein biomarkers [101].

1.1.4.1 Affinity chromatography

A difficult aspect for biomarker quantification is the ability to detect one protein within a complex mixture of 10^4 to 10^6 other proteins [102]. For example, low abundant proteins (LAPs) make up about 1% of the entire human serum proteome by mass with the remaining 99% being compromised of high abundant proteins (HAPs) [103]. Therefore, sample preparation methods, particularly, affinity chromatography, has been used to either deplete HAPs or to enrich LAPs where large signals produced by HAPs can mask or interfere LAP signals [104].

Affinity chromatography is a separation method based on specific binding interactions between an immobilised ligand and a binding partner. This technique derives from a naturally occurring phenomena existing within biological macromolecules including antibody-antigen (Ab-Ag), enzyme-substrate, and enzyme-inhibitor interactions [105]. Consequently, separations using affinity ligands have become a popular method for selective purification and isolation of biological compounds. Various biological and non-biological binding agents have been used including antibodies, lectins, protein A/protein G, immobilised metal-ion chelates, and boronates [106]. For example, immobilised metal affinity chromatography (IMAC) and metal oxide affinity chromatography (MOAC) have been used for phosphoprotein enrichment [107], lectin affinity chromatography (LAC) for glycoproteomes [108], boronates for peptide biomarkers [109], and metal-ion chelates for anthrax biomarkers [110]. Additionally, a study by Zhao *et al.* used both depletion and enrichment strategies where the depletion of albumin combined with the affinity enrichment of troponin I (a cardiac biomarker) reduced sample complexity, improved the dynamic range and detection sensitivity [111].

Whilst many affinity chromatography methods exist for biomarker analysis, immunoaffinity extractions are a popular choice as they are highly specific to proteins. Immunoaffinity extractions rely on antibodies, or immunoglobulins (Ig) which are unique soluble glycoproteins produced by the immune system as a response to an exogenous compound [112]. The generated antibodies can selectively bind to one (monoclonal), or several (polyclonal) locations of the exogenous compound through non-covalent interactions where each individual location on the antigen is known as an epitope [113]. Immunoaffinity extraction can be performed both prior to and after the protein digestion step, and provides unique selectivity through interactions between the protein or peptide and the antibody [114]. Using

immunoaffinity chromatography, HAPs such as immunoglobulin G (IgG), immunoglobulin A (IgA), immunoglobulin M (IgM), transferrin, haptoglobin, and α-2-macroglobulin can be depleted using antibodies (for example, bacterial protein A/G which specifically bind to the F_c region of immunoglobulins [115] and the antibody-based removal of albumin [116]) to minimise the differences of protein concentrations within a sample [117]. However, proteins of interest may also bind to immunoglobulins and albumin which are two abundant plasma proteins [44]. As a result, target proteins may be undesirably removed with depletion methods. Alternatively, immunoaffinity ligands have also been applied to reduce sample complexity through enrichment. The ligands selectively target LAP, boosting their concentration to increase their chance of detection [118]. LAP can be pre-concentrated with antibodies, for example, the extraction of human chorionic gonadotropin proteins which are important biomarkers in pregnancy detection, cancer diagnostics, and doping analysis [119]. Additionally, anti-peptide antibodies can be used to capture and enrich peptides of interest obtained from proteolytic digestion [120].

1.1.4.2 Proteolytic Digestion

Targeted proteomics and low-level quantification of proteins are often performed by proteolytic digestion for production of smaller peptides that serve as surrogate markers and are much more amenable to targeted mass spectrometry analysis [48, 121]. Peptides that are unique to the target protein are used as surrogates for targeted MS-based quantification [122]. However, this step often takes up to 24 hours creating significant bottlenecks in the sample analysis workflow [123]. When performed by conventional protocols, the sample is digested in-solution with small amount of free trypsin being the most frequently used protease in mass spectrometry-based proteomics experiments due to its stringent cleavage specificity of carboxy terminals of arginine and lysine [124]. This approach, however, has major drawbacks with long digestion times, enzyme autolysis, low activity, non-reusability of the enzyme, and difficulty with automation [125]. Consequently, there has been a shift towards faster digestion where different techniques to accelerate this procedure have been developed. As reported by Capelo *et al.* [126], there are several ways to speed up protein identification workflows including heating, ultrasonic energy, infrared energy, microwave energy, alternating electric fields, high pressure methods, micro-spin columns and microreactors. This can be further

grouped into temperature related digestion (heating, IR and microwave assisted digestion), immobilised digestion (micro-spin columns and microreactors), and other digestion methods (ultrasonic energy, alternating electric fields, high pressure) [123, 127]. For example, Havlis *et al*. showed that reductive methylation of trypsin minimises autolysis and shifts the optimum temperature for enzyme activity to 50-60°C where the enzymatic digestion of bovine serum albumin (BSA) was 12 times faster than in-solution at 37°C [128]. Lopez *et al*. used ultrasonic energy to digest proteins separated in gel and proteins and whole proteomes dissolved in aqueous samples in 120-seconds [129]. Wang *et al*. [130] introduced a trypsin digestion method using infrared heating and Pramanik *et al*. [131] introduced microwave assisted tryptic digestion to speed up digestion through elevated heat.

Regardless of the method used, there has been a trend towards faster digestion where an immobilised enzyme reactor (IMER) is a popular choice due to its potential for automation [132]. Rather than having free enzymes, an IMER consists of enzymes immobilised onto solid support material. Enzymes are specific and efficient natural biocatalysts (typically proteins) that increase the rates of chemical reactions within a cell. Enzymes rely on binding to a substrate to facilitate a chemical reaction producing one or more products. At the end of the reaction, the enzyme releases the products without being consumed or permanently altered by the reaction and is ready to accept another substrate molecule for catalytic conversion [133]. The use of enzymes in their free native form faces several drawbacks relating to high costs, long-term operational stability and challenging recovery and reuse cycles. Therefore, enzyme immobilisation has become common practice to maximise sample preparation efficiency [134]. Immobilisation provides convenient handing, improved stability, and separation from the product allowing high recovery and reuse of costly enzymes [135]. These advances in sample preparation have led to smaller sample consumption, reduced contamination, and enhanced throughput.

A comprehensive review by Safdar *et al*. presents a summary of methods using different types of microscale proteolytic reactors with digestion times ranging from seconds to ~4 hours as enzymes are confined to a smaller space allowing high enzyme to substrate ratios which improves digestion capacity and decreases digestion times, thus improving the preparation time compared to conventional overnight times of ~24 hours [136]. Other advantages of using IMERs include the minimisation of enzyme autolysis as contact between enzymes is reduced

[137, 138], and IMER reusability as immobilised enzymes are often stabilised in both storage and operational use [139]. IMERs are available with a range of support surfaces such as particles/beads [140], monoliths [137] and membranes [141], and formats including discs [142], capillaries [143], microchips [144], columns [145], and particle suspension [146]. Depending on the format, IMERS can operate in a flow-through manner allowing automation and/or online coupling to LC-MS for high-throughput analysis [147]. Regardless, the main aim for IMERs is to provide convenient quick and efficient digestion, where many novel IMERs have been developed with the aim to produce systems that offer high digestion efficiency, good reproducibility, good stability and non-specific adsorption of peptides onto the IMER [137, 142, 148-150]. Examples include a study by Duan *et al*. [151] where an immobilised trypsin monolithic IMER for protein identification showed digestion efficiency was over 230 times greater than when in-solution digestion was performed, and a study by Stigter *et al*. [152] where immobilised pepsin on dextran modified silica capillaries provided online protein digestion for peptide mapping.

Whilst rapid digestion can be achieved, it is important the protein digests by IMERs are reproducible as there have been reports of differences between peptides obtained from a digestion arising from varying reaction conditions. For example, Kim *et al*. [153] reported yeast proteome analysis by in-solution and IMER digestion methods, and observed unique peptides that were exclusive to each method with 26% of total peptides observed by both methods unique to the IMER, whilst it was 28% for the in-solution digest. Additionally, a study by Rivera-Burgos *et al*. showed changes in digestion temperature from 27 to 70°C altered the protein structure allowing proteolysis to start at different sites and thus changes to observed peptide cleavages [154]. A multi-laboratory study of proteins in plasma reported good reproducibility for MRM-MS based assays across eight different sites [155], however, an assessment by Hoofnagle *et al*. outlined the importance of proteolytic digestion reproducibility as the CVs for site independent digestions were two-fold greater than the CV for centralised pre-digested samples provided [156]. Therefore, when the same trypsin digestion method and conditions remain constant for all samples, good reproducibility of the trypsin digests are achieved and thus reliable quantification. For example, a study performed by Toth *et al*. applied an IMER to quantify multiple apolipoproteins in serum (biomarkers for cardiovascular disease) obtaining good reproducibility of the trypsin digest through controlled

flow rates, column volume and temperature [47]. Using the IMER, high precision analysis was obtained where intra-assay variations were <4.4% RSD (n=5) for all eight apolipoproteins, and overall inter-assay variations spanning over five days (n=25) were <8%. When compared to in-solution digestions, quantification of the apolipoproteins was also comparable where the IMER showed a concentration range difference from -4.2% to +9.9% for the apolipoproteins in 25 patient samples relative to the in-solution method. Also, this study demonstrated an automated proteomics workflow through coupling the IMER to LC-MS/MS which is especially useful as rapid assays for clinical applications are vital for effective patient treatment of critical and life-threatening conditions. Consequently, effective ways to eliminate the time constraints of protein sample preparation are essential for clinical implementation in medical laboratories.

Major challenges for accurate and precise LC-MS/MS quantification lie with sample preparation which include lengthy workflows to produce signature peptides, and the diminishing accuracy of quantitative measurements in highly complex biological samples due to background interferences [157]. Therefore, it is essential to establish optimal protocols for sample clean-up and proteolytic digestion of the target protein that achieve high and reproducible recovery of the signature peptides for targeted quantification of protein biomarkers.

1.2 Solid Phase Extraction

Current technology in mass spectrometry-based proteomics analyses rely on lengthy sample preparation steps such as proteolytic digests and immunoaffinity extractions. Therefore, appropriate sample preparation prior to analysis is crucial for efficient, accurate and precise measurement of the target analyte. Depending on the sample and the analysis to be performed, one or more operations such as dilution, precipitation, filtration, extraction, and centrifugation processes may be required. Consequently, sample preparation can be the most time-consuming step with significant consideration of the analytes and their matrices, numerous sources of inaccuracy, low recovery and poor reproducibility [158]. Therefore, it is ideal that as few possible operations are used to reduce processing time and errors.

As discussed previously, sample preparation techniques for biomarkers analysis can include, protein precipitation (PPT), liquid-liquid extraction (LLE), and solid-phase extraction (SPE), enrichment, denaturation, chemical modification and proteolytic digestion. Whilst these

techniques play different roles in the sample preparation workflow, there has been considerable effort put into improving biomarker sample preparation with certain techniques being more amenable to improvement than others. For example, LLE and SPE are considered the oldest and most used methods of sample preparation of target analytes [159, 160]. Although LLE is still widely and routinely used due to its simplicity, they can however be labour intensive, difficult to automate, and subject to extraction volume errors due to the separation of phases and emulsion formation, and uses large solvent volumes [161]. In contrast, SPE presents advantageous features such as convenience, lower costs, time savings, simplicity, less consumption of organic solvents, easy automation and the ability to combine it with different detection techniques [162]. Using the SPE technique, components of a mixture are separated or extracted based on their differential interactions with two phases, a mobile phase and a stationary phase [163, 164]. SPE is a well-established sample preparation technique used in analytical chemistry and comes in several different formats such as cartridges, disks and/or fibres [165]. Despite the different forms, a typical SPE method involves introducing a liquid phase, usually containing the sample, onto a solid-phase sorbent bed, and depending on the purpose of the sample preparation task such as clean-up, analyte concentration, or analyte derivatisation, the sample components will have certain interactions with the solid phase sorbent [165]. One example is the bind-elute strategy where target analytes are retained in the sorbent due to a greater affinity than the sample matrix, and the unwanted non-retained components are washed away (see Figure 1.5) [166]. Following the washing step, the analytes are eluted from the sorbent using small volumes of solvents (in the µL to mL range), therefore maintain higher concentrations of the analyte. Alternatively, the removal/trapping strategy retains the matrix components on the sorbent while the analytes are not retained [167].

Consequently, due to the nature of solid-phase materials, new methods and materials are being developed to improve sample preparation techniques. The following sections will address the general advances in solid-phase materials as it progresses towards miniaturisation, automation and customisability [168, 169], followed by the considerations of developing customisable material for targeted sample preparation for protein biomarker workflows.

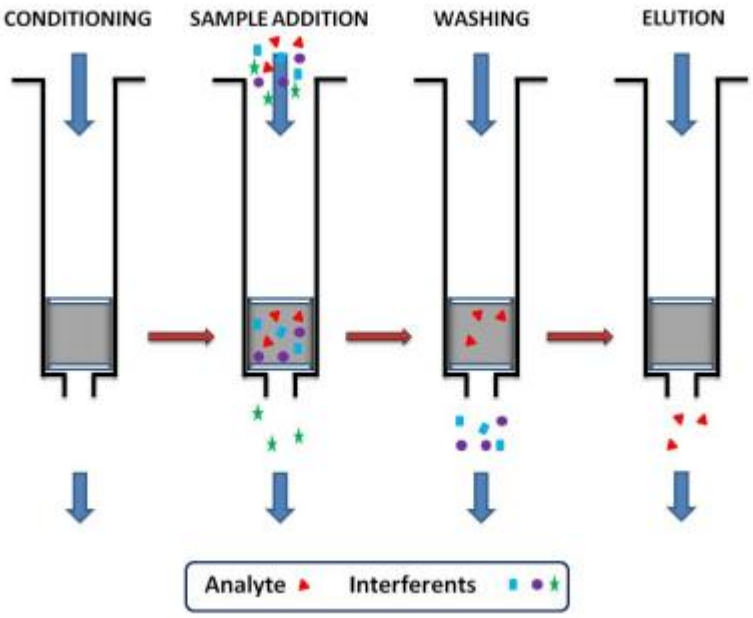

Figure 1.5: Bind-elute strategy for SPE [170].

1.2.1 Miniaturisation, automation, and progression of SPE methods

Miniaturisation of SPE

The progression towards miniaturisation is a trend in analytical chemistry affecting sample preparation techniques. The main drivers for miniaturisation are the increased speed and thus reduced costs, enhanced sensitivity and selectivity, the ability for automation and portability, and environmental sustainability [171]. This aims to minimise or eliminate the disadvantages such as consumption of large amounts of organic solvents with the concomitant generation of wastes, processing of large volumes of aqueous samples, and excessive number of operational steps [172].

As reviewed by Płotka-Wasylka *et al.* [173], many miniaturised SPE techniques have been developed including solid-phase microextraction (SPME), stir-bar sorptive extraction (SBSE), magnetic solid-phase extraction (MSPE), dispersive micro-solid-phase extraction (DMSPE) and microextraction in a packed syringe (MEPS). SPME uses a fibre coated phase for extraction of solid, liquid or gas samples [174]. This technique adsorbs the analytes onto the sorbent surface and desorbs them under high temperature reducing the need for organic solvents and allowing it to be readily coupled to gas chromatography (GC) for online analysis. Furthermore, solvent desorption allows for coupling to liquid chromatography (LC) [175]. Stir-bar sorptive

extraction (SBSE) was introduced in 1999 as a miniaturised and solventless extraction technique for aqueous samples [176], magnetic solid-phase extraction (MSPE) is a useful sample preparation technique enabling the dispersion of solid sorbents in liquid sample matrices followed by the magnetic retrieval of the sorbent [177], dispersive micro-solid-phase extraction (DMSPE) is technique used to trap compounds in loose sorbent materials, and microextraction in a packed syringe (MEPS) uses a liquid handling syringe with a sorbent packed cartridge placed in between the needle and the syringe barrel, also referred to as the barrel insert and needle (BIN) assembly [178]. Whilst these techniques can differ in its operational use, a common factor is that they aim to miniaturise through reduction in device dimensions, reduced amount of sorbents, and/or use of micro-sized or nano-sized materials (particularly the latter with their advantageously large surface area and exceptional physicochemical properties) [179]. Additionally, there has been a reduction of sorbent particle size, where the average particle size for most traditional SPE cartridges of 40 to 60 μm [180] have been reduced to less than 3 μm since the introduction of micro-SPE, providing greater surface area and extraction efficiencies [181].

Automation of SPE

Automation of the SPE procedure is an important step towards improving the throughput of the sample preparation technique where several platforms exist. These platforms can be categorised as online systems which involves coupling or integrating sample preparation to analytical systems such as LC and GC, or offline systems where sample preparation devices or platforms are standalone systems that are not integrated or hyphenated to another system. This results in the manual transfer of outputted sample from the offline platform to the analytical instruments. Due to the format of certain SPE techniques, automation of SPE is readily available as laboratory built systems by analysts, or purchased from instrument vendors [182]. For example, SBSE can be automated using a commercially available sampler system [174], and MEPS where the syringe allows for automation through online coupling to LC [183] and GC [184] without any modifications to the instrument.

Online systems typically use pre-column devices for hyphenation to analytical instruments through valve-switches for “loading” and “injecting” of samples, [185]. Coupling pre-column SPE cartridges to an analytical detection instruments such LC involves a switching valve where

the cartridge can be connected to an analytical instrument and the analytes eluted straight from the cartridge for detection [186, 187]. Other online systems include the instrument top sample preparation kit (ITSP) which use miniaturised SPE cartridges with dedicated instrument autosamplers to prepare samples prior to analysis. Both online and offline approaches have successfully been used for food [185, 188, 189], environmental [190, 191], biological [192, 193], and pharmaceutical [194] samples. Using online approaches minimises operator sample preparation handling time and a reduction of sample loss, however, disadvantages of online SPE include greater operational complexity as the sample preparation and analytical instrumentation data acquisition are integrated, and system compatibility issues may arise where extraction solvents and column pressures must be compatible with the analytical instrument [195]. Additionally, SPE columns may deteriorate due to analyte carryover, clogging, or binding of non-specific and irreversible matrix interfering compounds [196]. Alternatively, offline systems provide sample preparation flexibility and simplicity as the sample preparation systems are not integrated to analytical detection instruments allowing samples to be prepared and run independently from each other [197]. Current liquid handling robots are designed to be general-purpose machines to offer flexibility whilst not sacrificing throughput. Different robots come with unique consumables such as syringes, SPE cartridges, 96-well plates and tips, and hardware to handle tasks such as liquid handling and sample heating, agitation or transportation [198-201].

Progression of SPE

SPE is also evolving through the introduction and development of new and novel materials for targeted sample preparation such as immunoaffinity solid-phase extraction (IASPE) [202] and molecularly imprinted solid-phase extraction (MISPE) [203]. Since the development of SPE, traditional sorbents such as reverse-phase (C_{18} or C_8) and normal phase (silica, alumina) have been popular sorbent choices for SPE due to their broad applicability [204]. These sorbents however are non-specific sorbents where interactions with analytes are based on polarity and may not selectively isolate target analytes within complex biological matrixes [205]. Therefore, new and novel sorbent materials have been synthesised during the last decades to circumvent the main limitations of the traditional solid phases that is the lack of specificity, providing enhanced sorption capability, improved selectivity, or an alternative mechanism for chemical retention [206]. Using the high specificity and selectivity of antibodies, IASPE have successfully

been used for food [207], environmental [208], pharmaceutical [209], and biological [210] samples through the extraction and enrichment of analytes during sample preparation. Similarly, MISPE use molecularly imprinted polymers (MIPs) sometimes referred to as plastic antibodies, are synthetic polymers designed to have predetermined selectivity towards an analyte and or related compounds have also been used [211, 212]. MIPs are produced by forming a complex between an analyte (template) and functional monomers. The monomers are then linked together to form a three-dimensional polymer, and the template molecule is removed to leave a specific site where the polymer recognises and binds only to the template molecule resulting in a highly selective material [213].

1.2.2 Customisable material for targeted sample preparation

There has been growing interest and development in solid support materials customised with biomolecules to perform target-specific sample preparation. Depending on the analysis required, a solid-phase carrier material can be modified with different biomolecules for specific sample preparation tasks for bioanalysis. For instance, biomolecules may include avidin to form avidin-biotin complexes for sensitive assays [214], oligonucleotides as molecular recognition probes [215], enzymes for catalytic reactions on a substrate [216], and antibodies for immunoaffinity extraction [217] with the latter two being used in proteomics analysis.

To be used effectively, biomolecules are often immobilised onto the solid support materials as it allows for automation [218], convenient handing where resulting products can be separated from the support [219], and biomolecule stabilisation and reusability [220]. Although immobilisation of biomolecules onto carrier supports is well known, there is no single protocol that can be applied for every biomolecule, but rather an approach of continual optimisation is used until a satisfactory system has been developed [221]. Solid supports come in various formats such as beads, fibres, membranes and films, however regardless of the type, appropriate choice of the immobilised support material is crucial for thermal, mechanical and microbial resistance, high loading capacity, biocompatibility, minimal hydrophobicity due to undesired protein adsorption and denaturation, regeneration and reusability, stability under reaction conditions, cost effectiveness, and environmental friendliness [222, 223].

1.2.2.1 Support material

Solid support carriers used for immobilisation are commonly divided into organic, inorganic and hybrid materials [222]. Organic carriers include natural and synthetic polymers such as cellulose [224, 225], starch [226], agarose [227], chitosan [228], collagen [229], Sepharose™ [230], polyacrylamide [231], polymethacrylate [232], nylon [233] and polystyrene [234]. Natural and synthetic polymer supports are used as they possess, or can be modified with suitable functional groups on their surface providing attachment points for immobilisation, and they also mimic biological environments allowing certain biomolecules to be stabilised and retain their activity [235]. Additionally, organic polymer supports in general have broad pH working ranges (for example polystyrene divinylbenzene operating between pH 1-14) whilst inorganic phases such as silica operate only between pH 2-9 where below pH 2, Si-C bonds can be cleaved and above pH 9, silica is slowly solubilised into silicate [236, 237]. This broad pH range may be beneficial as it allows a wide range of harsh solvents to be used without degrading the phase material where an example of this is observed in immunoaffinity extractions where basic elution buffers (pH>10) such as ammonium hydroxide and triethylamine are used [238, 239].

Inorganic supports such as metal-based and silica-based materials are widely considered for immobilisation as they are microbially resistant, thermally stable and have high mechanical strength compared to organic supports [240, 241]. Inorganic supports have well developed pores and stiffness ensuring constant volume and shape allowing operation under higher pressures. They also contain greater surface areas enabling high protein loading during immobilisation [242]. For example, when immobilising a biomolecule such as an enzyme to the support without any spacers or coatings, the support should have the largest possible pore volume enabling the biomolecule to enter without any steric hindrance [243]. With decreasing pore sizes, Trevisan *et al.* [243] reported a sharp decrease in immobilised enzyme activity due to size exclusion of the enzyme molecule, however for bigger pore sizes, a decrease in activity was also observed as a result of the reduction in the surface area of the support. Consequently, a balance between pore size and surface area must be achieved.

Metal-based supports are commonly used as they can provide additional features that may be beneficial to certain applications such as biosensors. A popular support metal due to its stability towards nearly all reagents, and its high electrical conductivity is gold, making it

desirable for electro-enzymatic sensors [244, 245]. It can also be used for chemical sensing or imaging due to its surface plasmon resonance (SPR) band at 250 nm and are therefore commonly used in biosensors for molecular recognition [246]. Gold has an affinity for thiol groups where a bifunctional reagent can form a chemical "bridge" between the metal and the immobilised biomolecule [247]. Other metal-oxide supports such as titania and alumina are also used provided that their surface is reactive enough for chemical modifications allowing biomolecule immobilisation [248].

Silica-based supports are effective for immobilisation due to their large specific surface areas, large pore volumes and uniform pore sizes and has therefore been widely used [249-251]. However, non-specific interactions can occur during the immobilisation of proteins due to the coexistence of both hydrophobic and hydrophilic sites (siloxane and silanol) on the surface [252] where at pH>3, the silanol groups which are more acidic than their alcohol counterparts tend to be deprotonated leading to a negatively charged surface that reversibly interacts with positively charged amino acid groups such as arginine and lysine (see Figure 1.6 A) [253, 254]. Furthermore, depending on the protein, irreversible interaction can occur between the protein and the silica support. This occurs when proteins with weak internal cohesion deforms and rearranges on the surface (see Figure 1.6 B-D). During this change, there is an increase in the number of interactions between the surface and protein, and hydrophobic interaction may occur between the surface and the protein.

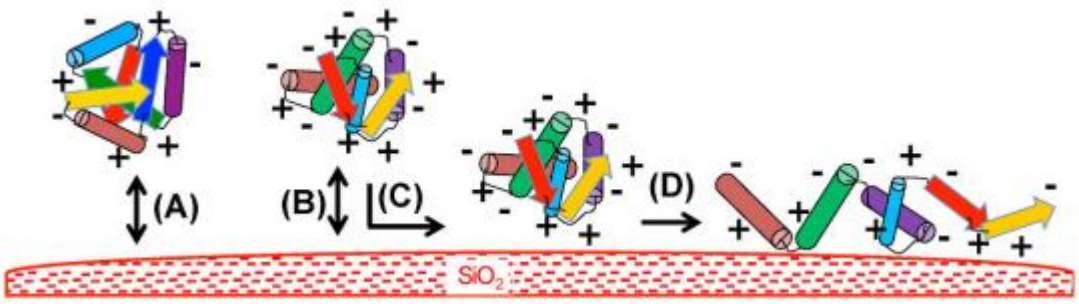

Figure 1.6: Non-specific interaction between silica surface and proteins. A) electrostatic interaction between negatively charged surface and positively charged residues on the protein, and B-D) protein deformation due to weak internal cohesion resulting in deformation and hydrophobic interaction with the silica surface [254].

Another type of material commonly used as supports are inorganic-organic hybrid materials. Inorganic-organic materials have emerged as novel materials with desired characteristics combining the benefits of both inorganic and organic materials. To obtain inorganic-organic hybrid materials, inorganic materials are coated with polymers or polysaccharides such as chitosan [255], poly(ethylene glycol) (PEG) [256], cellulose [257], and dextran [258], obtaining the biocompatibility of organic-based supports combined with the mechanical stability of inorganic-based supports. Improved surface biocompatibility can be used to increase activity of the immobilised biomolecule. A study performed by Peng *et al*. [255] demonstrated that improving the surface's biocompatibility increased the activity of the immobilised enzyme. In this study, trypsin immobilised onto microspheres modified with chitosan showed increased amounts of immobilised trypsin due to an increased affinity between trypsin and chitosan and thus greater enzyme activity compared to microspheres without modification. Additionally, polymers and polysaccharides are effective at reducing protein and silica surface interactions as they act as a shield where unwanted non-specific binding is prevented as a result of improved hydrophilicity of the carrier [259].

1.2.2.2 Immobilisation

Immobilisation of biomolecules plays an important role in developing targeted sample preparation techniques as they help to enhance the function and operation of the biomolecule. Depending on the application, immobilisation methods can be short-term or long-term localisations, for example, in the case of a drug delivery system, the immobilised drug is released from the support, either over a short or longer-term period, while an immobilised enzyme is designed to remain attached to the support over the duration of use [260]. Therefore, it is important to consider the type of immobilisation strategy used.

In general, there are three main immobilisation strategies used for biomolecules: carrier-free crosslinking, entrapment and support binding (see Table 1.1 and Figure 1.7) [261]. Immobilisation by crosslinking involves the formation of covalent bonds among the biomolecules using bifunctional chemical cross-linkers, such as glutaraldehyde [262]. This approach is commonly used for crosslinked enzymes where the method avoids the need for solid support carriers as the crosslinked enzymes aggregates act as their own support [263]. Entrapment is an irreversible method of immobilisation where biomolecules are entrapped in

a support or matrix, such as an organic polymer or gel [264]. Entrapment has several advantages including its simplicity, geometrical flexibility, and the absence of chemical modification to bind the biomolecule to a support preserving its activity, however this approach has leakage and diffusion limitations due to the incorporation of the biomolecule within a matrix [265]. The third strategy is based on support binding and includes immobilisation by non-covalent attachment (adsorption and electrostatic interactions), covalent attachment, and affinity interactions.

Table 1.1: Enzyme immobilisation techniques and their advantages and disadvantages [148].

Linkage	Mechanism	Advantages	Disadvantages
Crosslinking	Molecules are linked together using crosslinking reagents to form a large network	Simple	Distortion of the enzymes active site resulting in activity loss
Entrapment	Incorporation of the molecule within a gel or polymer	No chemical reaction between molecule and support, and multiple types of molecules can be immobilised	Suffers from performance restriction due to diffusion barriers
Non-covalent	Weak bonds such as Van der Waals forces, hydrophobic and electrostatic interactions	Preserves enzyme activity	Easily desorbed off solid supports with changes in pH and temperature and non-specific adsorption
Covalent	Chemical bond between functional groups on the molecule and support	Stable linkages between support and molecule	Not regenerable and high amounts of bio-reagents are required
Affinity	Affinity bonds between ligand and target	Bonds formed are controlled and oriented	Specific groups need to be present on target for ligand binding

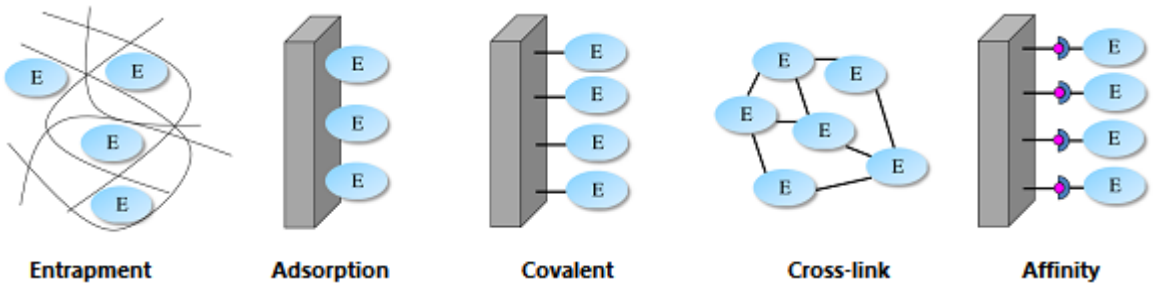

Figure 1.7: Immobilisation strategies used for biomolecules (E) [148].

Immobilisation by adsorption relies on interactions such as van der Waals forces and hydrogen bonding. Therefore, biomolecules with large hydrophobic surface area will interact with a hydrophobic support. An advantage of this technique is no change in the native structure is required, however, immobilisation by adsorption is rather weak and typically leads to leakage from the support [266]. Additionally, adsorption of an enzyme that has hydrophobic active sites onto a hydrophobic carrier can result in an irreversible opening of the enzyme leading to reduced activity [267]. Similar to non-covalent adsorption, electrostatic interaction is simple, rapid and mild as no covalent bond linkages are formed [268]. Electrostatic interactions however are stronger than adsorption and therefore minimise leakage from supports. Depending on the pKa of the surface support and the isoelectric point of the biomolecule, the immobilisation buffer should have a pH value favouring electrostatic interactions between the carrier surface and biomolecule [269]. Furthermore, using ion exchanger supports, biomolecules that have been immobilised, used, and consequently inactivated through repeated use can be reversible desorbed allowing the support to be reused for several cycles [270].

Covalent attachment is predominantly used as it offers high strength bonding between the support and biomolecule with minimal leakage issues, and high stability towards heat, pH and organic solvents benefitting operation and storage [271, 272]. Covalent attachment mainly occurs through functional groups (-NH_2, -COOH, -SH) that are activated by crosslinkers allowing the biomolecule to be immobilised [273, 274]. Consequently, carrier surfaces with functional groups for immobilisation are often used to ensure the use of mild immobilisation reactions (e.g. carbonyldiimidazole [275] and carbodiimide [276] reactions) to avoid the loss of activity due to the structure conformation (e.g. an enzyme) during immobilisation reaction [277].

Affinity binding exploits the selectivity between complementary molecules (ligand and target) for immobilisation. In most cases, affinity binding is used in conjunction with other immobilisation mechanisms where one of the two complementary molecules (ligand) is attached to the support to act as an intermediate between the support and biomolecule (this is also known as indirect immobilisation). Therefore, this approach requires the presence of specific chemical functional groups on the biomolecule through modification. For instance, the avidin-biotin interaction is widely used. Avidin is a tetrameric glycoprotein that can bind

up to four biotin molecules which is a naturally occurring vitamin found in living cells (see Figure 1.8 A). Bond formation occurs rapidly and is insensitive to pH, temperature, organic solvents and denaturing reagents [278]. The interaction with avidin relies on the bicyclic ring, thus allowing modifications through the carboxyl group on the pentanoic acid side chain (see Figure 1.8 B) [278]. Another example of indirect immobilisation is observed in immunoaffinity chromatography using intermediate proteins such as protein A/G [279]. Protein A/G bind to antibodies through the fragment crystallisable (F_c) region, preserving the fragment antigen binding (F_{ab}) region for antigen binding and results in antibodies bound in a single orientation (see Figure 1.9) [280]. Furthermore, after applying the desired antibody to the protein A/G support and washing off excess antibody, they can be covalently bound together through incubation with disuccinimidyl suberate (DSS) [281]. However, immobilisation through intermediate molecules involves two steps, being time and reagent consuming, and resulting in low concentration of ligands bound [282].

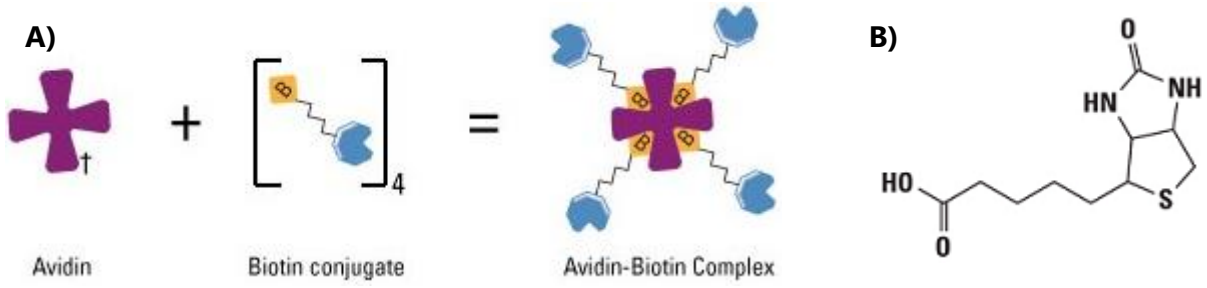

Figure 1.8: A) Avidin-biotin complex with four binding sites, and B) Bicyclic structure of biotin with a carbylic acid side chain that can be modified [283].

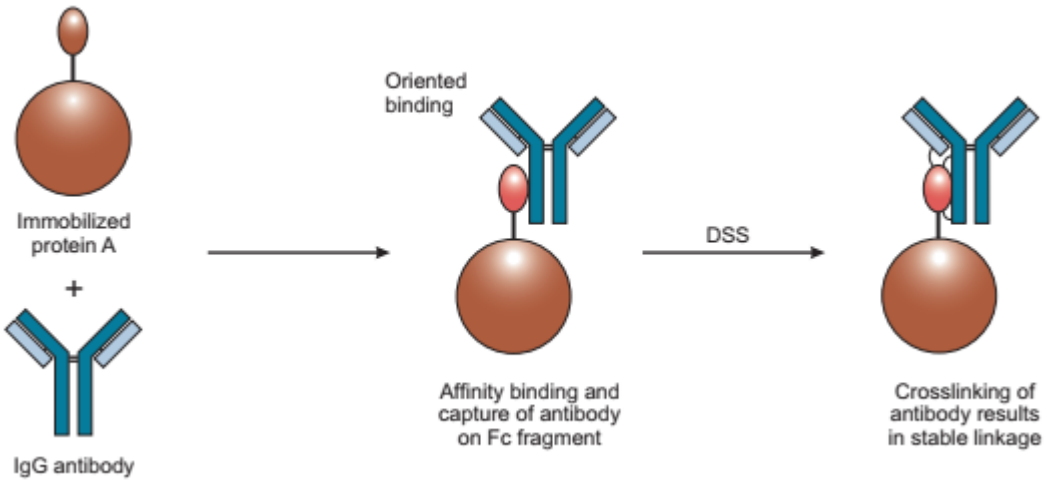

Figure 1.9: Antibody immobilisation through intermediate proteins: protein A or G [280].

Covalent Immobilisation

Whilst there are a wide range of immobilisation techniques available, covalent linkages are a desirable approach to form strong linkages between the support and a biomolecule, also referred to as bioconjugation [284]. This technique is commonly used in fields such as protein pharmaceuticals to improve the physiochemical properties of therapeutic proteins [285], medical diagnosis [286], imaging [287], and immunoaffinity chromatography for protein purification [288]. Therefore, reaction conditions for covalent linkages are often performed in near-physiological conditions to retain the biomolecules' structure and activity. Bioconjugation targets functional groups that are naturally present in the protein sequence such as primary amines and carboxyl groups at *N*-terminal and *C*-terminal amino acids and sulfhydryl in disulfide bridges [289]. Hence, bioconjugation is performed using popular crosslinking reagents that target these functional groups.

Crosslinkers are reagents employed to mediate the conjugation of two or more molecules and can exist as zero-length or multifunctional-length (bi-, tri-) [290]. Bifunctional crosslinkers are linkers that contain two reactive ends linked by a spacer arm, typically a carbon chain. When conjugation occurs, the two target molecules are linked to contain a spacer arm as part of the bond. These crosslinkers can contain identical reactive functional groups, homobifunctional, or different functional groups, heterobifunctional (see Figure 1.10) [291, 292] where heterobifunctional crosslinkers are often used as they have better control over the conjugation process avoiding creation of a broad range of poorly defined conjugates [293]. However, spacer arms may exhibit both favourable and unfavourable properties where immobilisation with a spacer arm for increased length can be used to reduce steric hindrance [233], but can possess more sites for undesired non-specific binding [294]. Alternatively, zero-length crosslinkers (such as the carbodiimide crosslinkers) are used to conjugate with no additional linker atoms and may be required in situations where an intervening linker is detrimental for the intended use, for example, antibody production from an immune response towards a hapten-carrier complex where antibodies produced may have specificity towards the crosslinking agent used to produce the complex [295].

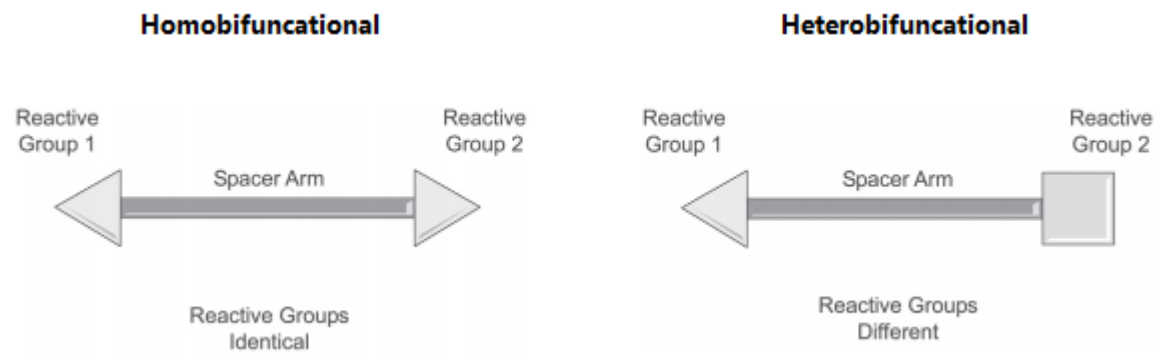

Figure 1.10: Homo- and hetero- bifuncational crosslinkers with reactive groups held by a spacer arm [291, 292].

One of the most popular carbodiimide crosslinkers used for bioconjugation is 1-ethyl-3-(3-dimethylaminopropyl)carbodiimide (EDC), a water soluble, zero-length linker used to form direct conjugations between a carboxylate and an amine group, and therefore do not become part of the link [296, 297]. When EDC is reacted with a carboxyl functional group, an *o*-acylisourea intermediate is formed which reacts with an amine group forming an amide bond yielding the isourea by-product (see Figure 1.11) [298]. However, the *o*-acylisourea intermediate is highly reactive and short-lived as it hydrolyses in aqueous solutions, therefore, a more stable reaction path can be achieved using *N*-hydroxysuccinimide esters (NHS esters) where an NHS amine reacts with the *o*-acylisourea intermediate [296]. The stable NHS esters can then react with a primary amine at pH 7-8 releasing the NHS leaving group (see Figure 1.12). Addition of NHS or sulfo-NHS (water-soluble analogue) improves reaction efficiency, intermediate stability and water solubility, increasing the conjugation yield compared to EDC alone [299].

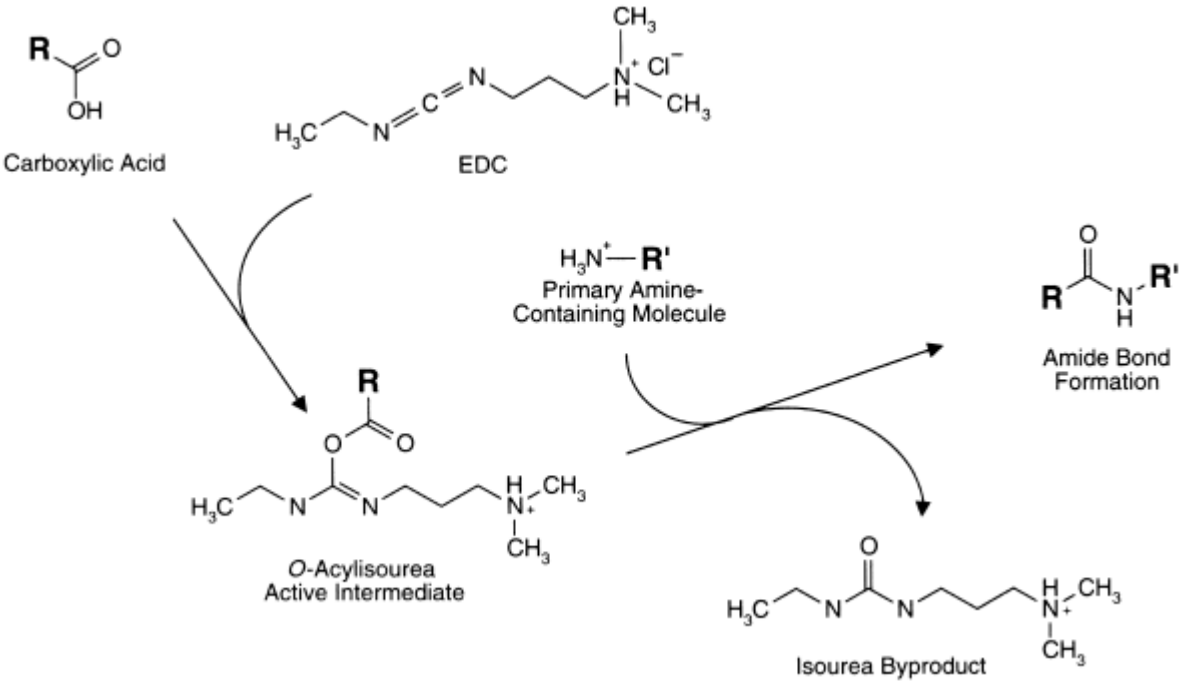

Figure 1.11: EDC activation of a carboxylic group for form an unstable o-acylisourea intermediate that when reacted with an amine compound, forms an amide bond between the carboxylate compound and amine compound [295].

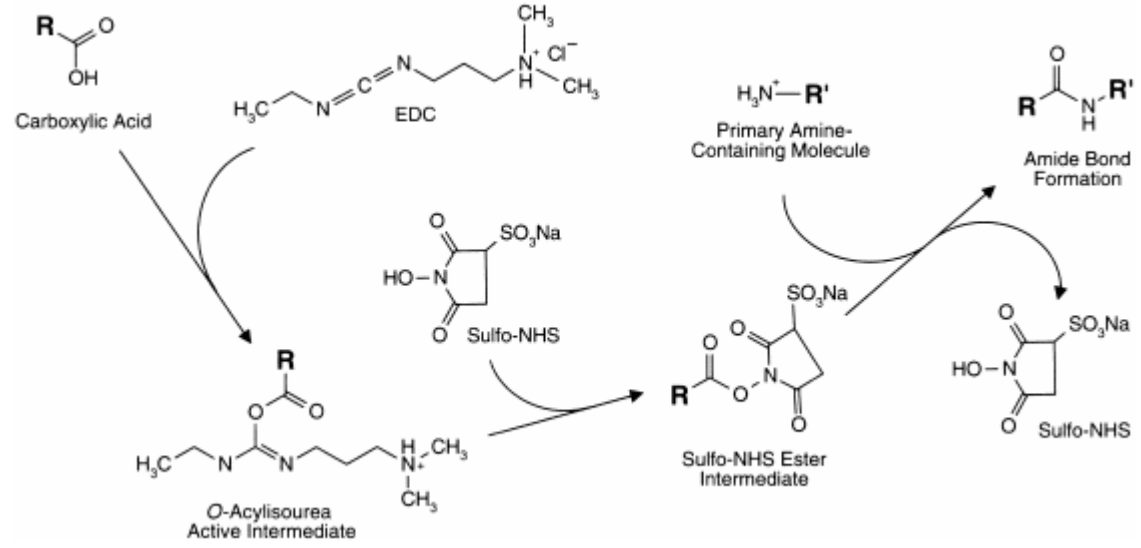

Figure 1.12: Primary amine reacting with the stable NHS ester to form an amide bond [295].

Another factor to consider in covalent immobilisation is the final orientation of the biomolecule to the solid support. As mentioned, immobilisation of biomolecules to solid supports can be achieved through primary amines and carboxyl groups as they are abundant and well distributed throughout the entire biomolecule. However, immobilisation through

these groups can result in decreased biomolecule activity due to random immobilisation. Using antibodies as an example, primary amines and carboxyl groups are present in the antigen-binding sites and random immobilisation can potentially lead to steric hindrance and reduced antibody activity [300]. However, this random antibody immobilisation approach is widely used due to its simple protocols and facilitated preparative handling. Alternatively, oriented antibody immobilisation can be achieved by selectively targeting certain functional groups for immobilisation such as targeting -SH groups through controlled reduction of the antibody in its hinge region resulting in two symmetric fragments as shown in Figure 1.13 [301, 302]. However, since disulfide bridges also exist in the F_{ab} region, the bond holding the heavy and light chains together can be reduced resulting in a denatured antibody [303]. Furthermore, oriented immobilisation can afford higher extraction recoveries but often involve lengthier immobilisation methods [304]. Consequently, regardless of the immobilisation process used, favourable and unfavourable characteristics are observed.

Figure 1.13: -SH groups obtained through disulfide bridge reduction [305].

1.3 Project Aims

Whilst literature is abundant with tailored protocols for protein isolation and digestion, there is no single universal automated protocol applicable to routine proteomic or clinical needs. In collaboration with Eprep (Mulgrave, Victoria, Australia), this thesis aims to develop the next generation of sampling by designing novel automated generic workflows that may be applied to the quantification of protein biomarkers. This thesis details the development of novel, rapid and customisable micro-solid-phase extraction (μSPE) devices for pre-concentration and proteolytic digestion of protein biomarkers for subsequent quantification by targeted

LC-MS/MS using an emerging automated offline platform, the ePrep sample preparation solutions with their µSPE devices.

This generic approach aims to dramatically decrease turn-around-time for analysis of protein targets, decrease method development and routine testing costs, and improve test accuracy for improved patient management decisions and outcomes. The development of a generic clinical protein biomarker workflow for use in clinical settings will be addressed in the following four objectives. Objective 1 will be addressed in Chapter 2, whilst Objectives 2,3 and 4 will be addressed in Chapter 3.

Objective 1: Customisable support material for biologically selective and automated sample preparation using the µSPE format

Objective 1 was to develop a customisable support material for binding biological ligands for targeted sample preparation. The material was then packed into ePrep µSPE cartridges and used to immobilise ligands through crosslinking reagents for targeted sample preparation for protein biomarker workflows.

Objective 2: Development of an immunoaffinity extraction µSPE cartridge for protein capture.

Objective 2 was to develop a µSPE method for immunoaffinity separation of proteins using antibodies. Using the customisable support material from Objective 1 and the ePrep platform, an immunoaffinity cartridge was developed for protein extraction using anti-BSA and BSA as the model Ab-Ag. This involved optimisation of immobilisation approaches for binding the antibody to the cartridge material, followed by protein capture.

Objective 3: Development of a rapid and automated µSPE immobilised enzyme reactor for protein digestion.

Objective 3 was to develop a µSPE method for rapid proteolytic digestion of proteins using an enzymatic µSPE cartridge fabricated from the customisable support material from Objective 1 and the ePrep platform. This involved optimisation of immobilisation approaches for binding the enzyme to the cartridge material, followed by optimisation of protein digestion protein and comparison against the conventional in-solution method.

Objective 4: Development of a rapid and automated µSPE sample preparation workflow for protein biomarkers

Objective 4 was to link objectives 1 to 3 for turnkey workflows for complete automation of sample clean-up, pre-concentration, and digestion for protein biomarker quantification by targeted mass spectrometry. An automated workflow combining immunoaffinity extraction of BSA followed by trypsin digestion was used as model system. The method was applied to a real-life clinical sample and its performance evaluated.

Chapter 2

Customisable support material for biologically selective and automated sample preparation using the ePrep µSPE format

2.1 Introduction

This chapter addresses the growing interest and development of solid support material customised with biomolecules such as antibodies, enzymes, affinity proteins, nucleic acids, and receptors due to their target-specific functions [306, 307]. Depending on the application, a solid-phase carrier material can be prepared or modified for use with various biomolecules for sample preparation prior to bioanalyses. As discussed previously, inorganic-organic hybrid materials display excellent potential as support materials for biomolecules providing enhance stability, mechanical resistance, and compatibility with biological molecules. Accordingly, this chapter addressed objective 1 which aimed to synthesise an inorganic-organic solid-phase support based on silica particles for biomolecule immobilisation for automated sample preparation.

Preparation of a customisable solid-support material

To increase biocompatibility, hydrophilicity and functionality of the surface, silica particles were modified with carboxymethylated dextran (CMD) [308]. Dextran is a natural polysaccharide consisting of predominantly straight-chain polymers of glucose with α-1,6 linkages [309], and contain very low non-specific interactions with proteins due to the hydrophilicity of hydroxyl functional groups [310]. This is evident in a study by Penzol *et al*. [311] where the long hydrophilic and inert arms of dextran prevented protein side interactions as well as steric hindrance between the immobilised enzyme and support surface, thus improving the performance of the immobilised enzyme. Additionally, the flexible polymer chains of dextran contributes to the suppression of non-specific adsorption of biomolecules [258]. CMD is also suitable for covalent binding of biomolecules and has been used for the immobilisation of proteins [244], antibodies [312], and DNA [313].

Once prepared, the material was packed into ePrep micro-solid-phase extraction (µSPEed) cartridges for use with the ePrep automated sample preparation solutions, a digiVOL® Programmable Digital Syringe Driver (see Figure 2.1), and an ePrep® Sample Preparation Workstation (see Figure 2.2) [314]. Whilst both solutions offer sample preparation with controlled volume and flow rate dispensing, syringe washing and exchange to eliminate contamination, high pressure dispensing and sealed vial operations, the digiVOL® Programmable Digital Syringe Driver is ideally suited for method development due to its

handheld and simple operation. Once developed, the method parameters can be translated to the ePrep® Sample Preparation Workstation, to provide automated sample preparation where multiple methods are run in sequence. Along with standard liquid handling capabilities, the solutions offer µSPE extraction using ePrep µSPEed cartridges, allowing fully automated µSPE and micro-fractionation methods to be performed. The cartridges are press-fit onto a high-pressure liquid syringe with pressure limits of up to 1600 psi, suitable for cartridge packing material sizes of 3 µm. In comparison, traditional SPE is usually performed at low pressure and requires 40-60 µm particle sizes [315]. µSPEed cartridges have two flow paths eliminating carry-over. One flow path is used for direct aspiration of liquids into the syringe barrel using a one-way check valve, and the second flow path for dispensing the liquid through the sorbent bed, providing an ultra-low dead volume connection (see Figure 2.1) [315]. As the analytes are dispensed, they are focused at the top of the sorbent bed resulting in a high concentration factor [316]. This provides a higher surface area for high efficiency and rapid extractions for quicker isolation of target analytes. Furthermore, this technology can also be used with the customisable material for specific sample preparation as explored in this thesis.

This work details the synthesis and characterisation of an inorganic-organic solid-phase support material based on 3 µm silica particles and CMD. Using the µSPE cartridges and ePrep syringe drivers, two *in-situ* immobilisation techniques (non-covalent and covalent) were assessed with horseradish peroxidase as a model enzyme, dictating the immobilisation method applied in Chapter 3.

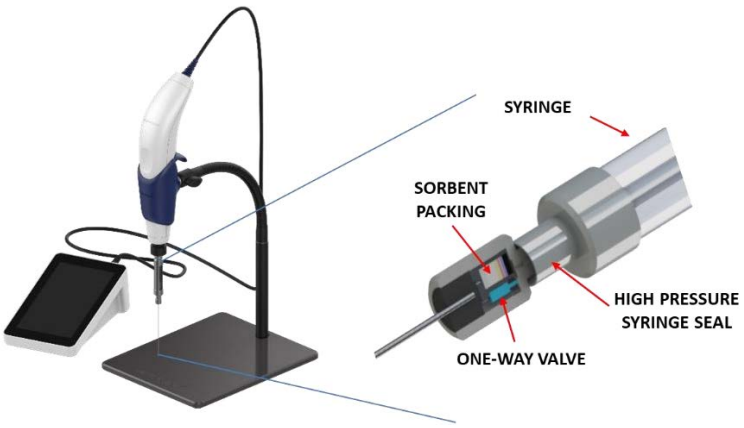

Figure 2.1: digiVOL® syringe driver used for method development and the press-fit µSPEed cartridge onto a syringe. The µSPEed offers two flow paths where solutions are aspirated through the one-way valve and dispensed onto the sorbent packing material [314].

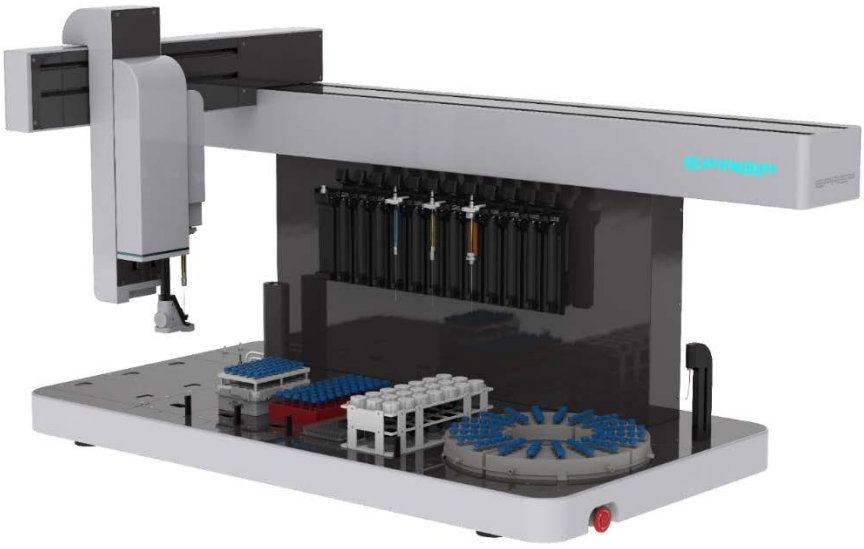

Figure 2.2: ePrep® Sample Preparation Workstation showing sample trays and liquid dispensing syringes [314].

2.2 Experimental

2.2.1 Chemicals and Consumables

DAISOGEL® aminopropyl silica (APS) (3 µm particle size with 120 Å, 300 Å and 1000 Å pore size) was obtained from Osaka Soda (Amagasaki, Hyogo, Japan). Carboxymethyl-dextran sodium salt (CMD), ethanolamine, 1-ethyl-3-(3-dimethylaminopropyl)carbodiimide (EDC), *N*-hydroxysuccinimide (NHS), 2-(*N*-morpholino)ethanesulfonic acid (MES), 10X phosphate buffer saline (PBS) pH 7.4 solution (30 mM Na_2HPO_4, 10.5 mM K_2HPO_4, 1.5 M NaCl), 2,2'-azino-bis(3-ethylbenzothiazoline-6-sulfonic acid) (ABTS) liquid substrate, horseradish peroxidase (HRP), sodium hydroxide pellets and potassium hydrogen phthalate (KHP) were purchased from Sigma Aldrich (Castle Hill, NSW, Australia). Ultra-pure water (18.2 MΩ cm^{-1}) obtained from a Sartorius 611 Arium® pro water generation system (Sartorius Stedim Plastics GmbH, Germany) was used for all preparation and dilutions unless stated otherwise.

2.2.2 µSPE method

The µSPE procedure and method development were performed with a digiVOL® Programmable Digital Syringe Driver. The µSPEed cartridges were packed with the synthesised customisable material by Eprep (Mulgrave, Victoria, Australia). The µSPE method was developed to immobilise biomolecules *in-situ* where the reagents, buffers, volumes and flow rates were optimised and transferred to the ePrep® Sample Preparation workstation.

2.2.3 Development of customisable material for µSPE cartridges

2.2.3.1 Synthesis of material

An inorganic-organic hybrid material was synthesised with aminopropyl silica (APS) beads and carboxymethylated dextran (CMD). Crosslinking chemistry using the carbodiimide reaction with EDC/NHS reagents were used to covalently bind the carboxyl group present on CMD to the amine groups on the APS. This carbodiimide reaction was performed under optimal pH conditions in a 50 mM MES pH 4.5 buffer. In a reaction vessel, 100 mg of CMD, 40 pmol of EDC, 80 pmol of NHS, and 10 mL of reaction buffer was added and mixed for 2 hours at ambient temperature. The solution was then mixed with 100 mg of APS and allowed to react

overnight at room temperature (1:1 ratio of CMD to APS by weight). The resulting material (silica-CMD) was vacuum filtered, washed with water and allowed to dry.

2.2.3.2 Characterisation of material

Fourier transform infrared spectrometer (FTIR) and conductometric titrations were performed for silica-CMD material characterisation to confirm the synthesis of the customisable material, and to quantify the amount of free -COOH groups available following the CMD coating. A Nicolet 6700 FTIR spectrometer (Thermo Fisher, Massachusetts, USA) using attenuated total reflectance (ATR) was used to qualitatively analyse the raw and synthesised material.

Conductometric titrations were performed to determine the amount of free -COOH groups per gram of silica-CMD material present for subsequent ligand immobilisation. Based on the method by Wu *et al*. [317], 100 mg of silica-CMD material was suspended into 100 mL of deionised water using ultrasonication, 200 µL of 0.10 M HCl was mixed into the suspension and was titrated under nitrogen against 25 mM of NaOH titrant. A Hach HQ14D meter (Hach, Dandenong South, Victoria, Australia) was used to monitor the conductivity over the course of the titration. To standardise the NaOH titrant, it was titrated against three aliquots of KHP prepared in deionised water. The concentration was calculated, averaged, and reported to 4 significant figures.

2.2.3.3 Covalent and non-covalent immobilisation

Prior to developing µSPE methods for biological sample preparation presented in the Chapter 3, the immobilisation method of biomolecules to the novel material was evaluated. As described in Chapter 1, there are non-covalent and covalent binding approaches for immobilising a biomolecule to a solid support material each with their advantages and disadvantages. Covalent immobilisation generally ensures robust bonding between the support and biomolecule however can require multiple reaction steps whilst non-covalent immobilisation occurs with less steps but are rather weak which typically leads to leakage from the support. Using horseradish peroxidase (HRP) as a model enzyme and a colorimetric assay, both non-covalent and covalent immobilisation methods were assessed for maximum enzyme activity and minimal enzyme wash-off. The immobilisation, washing and running buffers were also optimised to ensure unwanted non-specific binding of the HRP was minimised.

Silica-CMD was packed into µSPE cartridges and a comparison between covalent and non-covalent immobilisation was performed using a colorimetric assay with HRP and ABTS with the ePrep® Sample Preparation Workstation. Catalysed by HRP, ABTS undergoes a redox reaction in the presence of an oxidising agent such as hydrogen peroxide. This results in the formation of an ABTS cation radical that exhibits an intense turquoise colour with absorption maxima wavelengths (λ_{max}) of 415, 645, 734, and 815 nm and can be spectrophotometrically monitored using a Thermo Fisher Multiskan Ascent 96/384 Plate Reader (Thermo Fisher Scientific, North Ryde, NSW, Australia) [318].

For non-covalent binding of HRP, µSPE cartridges were conditioned with 500 µL of 10 mM MES buffer pH 4.5 (aspirate: 4500 µL/min and dispense: 1000 µL/min) and loaded with 50 µg of HRP (volume: 100 µL of 0.5 mg/mL HRP in 10 mM MES buffer, aspirate: 4500 µL/min and dispense: 300 µL/min). The cartridge was then washed with 500 µL of 10 mM MES buffer (aspirate: 4500 µL/min and dispense: 1000 µL/min) prior to applying the 100 µL of ABTS liquid substrate which was collected into a 96-well microplate. The wash step and ABTS steps were repeated to obtain ten further collections of the substrate.

For covalent binding of HRP, µSPE cartridges were conditioned with 500 µL of 10 mM MES buffer (aspirate: 4500 µL/min and dispense: 1000 µL/min), activated with 0.1 M EDC/NHS in 10 mM MES (volume: 500 µL, aspirate: 4500 µL/min and dispense: 300 µL/min), loaded with 50 µg of HRP (volume: 100 µL of 0.5 mg/mL HRP in 10 mM MES buffer, aspirate: 4500 µL/min and dispense: 300 µL/min), and end-capped with 0.1 M ethanolamine pH 8 (volume: 500 µL, aspirate: 4500 µL/min and dispense: 300 µL/min). The cartridge was then washed with 500 µL of 1X PBS buffer (aspirate: 4500 µL/min and dispense: 1000 µL/min) prior to applying the 100 µL of ABTS liquid substrate which was collected into a 96-well microplate (aspirate: 4500 µL/min and dispense: 300 µL/min). The wash step and ABTS steps were repeated to obtain ten further collections of the substrate.

These two methods are summarised in the flow chart seen in Figure 2.3.

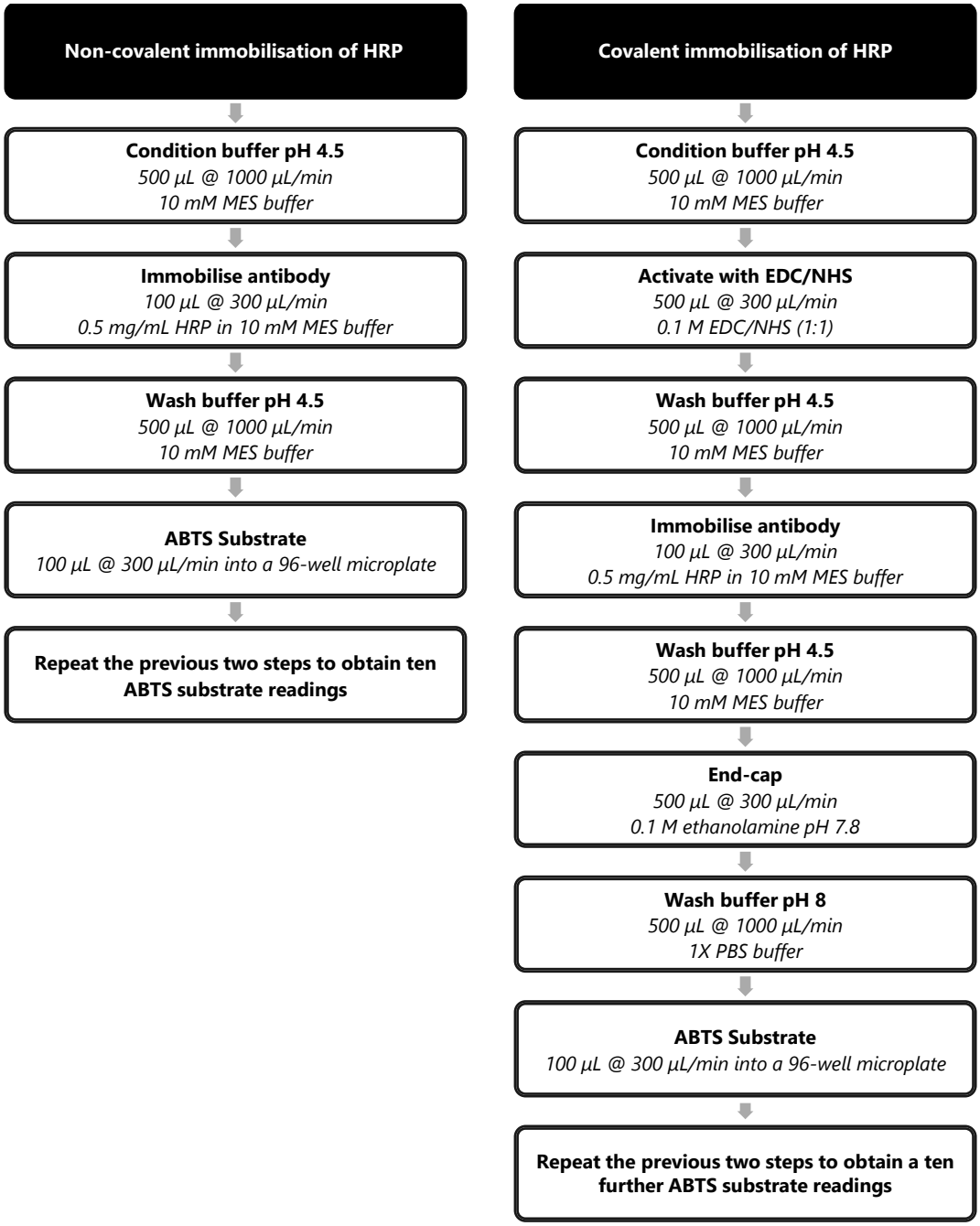

Figure 2.3: Methods for non-covalent and covalent immobilsation of HRP onto silica-CMD cartridges.

2.3 Results and Discussion

Inorganic-organic hybrid support materials for IMERs have excellent stability and compatibility with appropriate functional groups for facile biomolecule immobilisation. The 3 µm carboxymethylated dextran (CMD) covered silica support particles was fabricated and to ensure that this synthesis was successful, FTIR was used to qualitatively determine the production of customised silica-CMD material. Three samples were analysed using FTIR, the two starting raw materials, APS and CMD, and the final resulting silica-CMD product after synthesis. The FTIR spectrum of the starting silica material (Figure 2.4 A) showed two bands at 1050 cm^{-1} and 800 cm^{-1} corresponding to Si-O-Si stretch vibration [319] and the spectrum of the starting CMD-salt material (Figure 2.4 B) showed characteristic bands for carboxymethylated dextran for O-H stretch, C-H stretch, C=O stretch, C-O-H bend, C-O stretch, and the α-glucopyranose ring at 3400 cm^{-1}, 2920 cm^{-1}, 1580 cm^{-1}, 1410 cm^{-1}, 1000 cm^{-1} and 916 cm^{-1} respectively [320, 321]. The successful formation of the CMD coated silica support material was apparent in the spectrum for synthesised silica-CMD material (Figure 2.4 C) where a combination of all absorption bands was observed corresponding to both CMD (3200 cm^{-1}, 2900 cm^{-1}, 1580 cm^{-1} and 1400 cm^{-1}) and silica (1050 cm^{-1}).

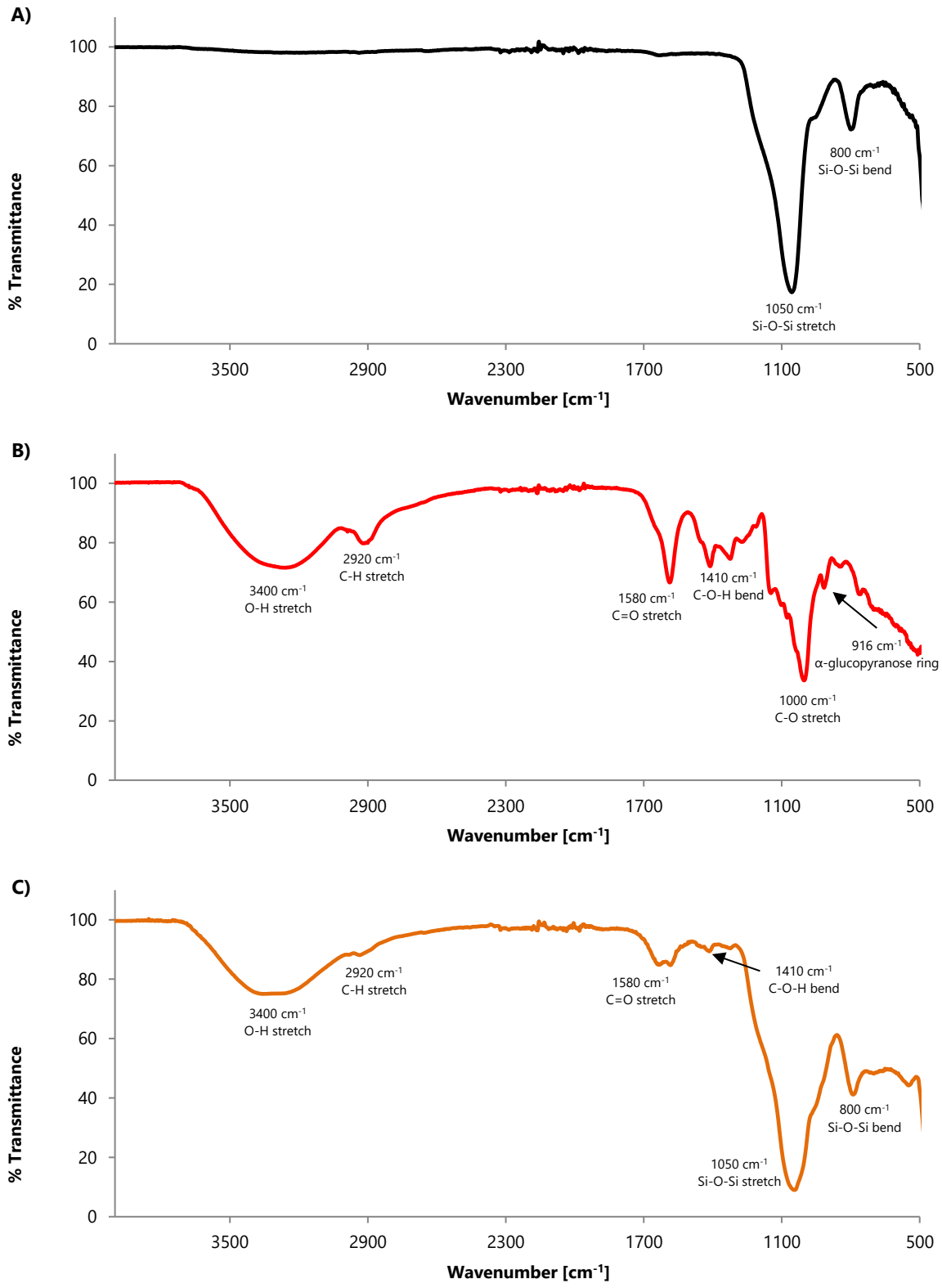

Figure 2.4: FTIR spectra obtained for starting materials a) APS, b) CMD (red), and the synthesised material c) silica-CMD.

After qualitative confirmation of the production of the silica-CMD material by FTIR, conductometric titration was used to quantify the amount of -COOH present on the material after synthesis as future ligand binding will occur at these sites. Therefore, to determine the amount of free -COOH groups per gram of novel material that was present for future ligand binding, conductometric acid-base titrations were performed. Based on a method previously described by Wu *et al.* [212], HCl was added to the sample prior to titration to ensure the -COOH groups on the material were acidified for the acid-base titration. Therefore, a control conductometric titration was first performed without any silica-CMD material to observe the titration between the added HCl and NaOH titrant. This titration produced an expected "v" shaped conductivity curve (see Figure 2.5). HCl has a high conductance due to the presence of mobile H^+ ions (with a molar conductivity of 35.01 $mS{\cdot}m^2{\cdot}mol^{-1}$ at infinite dilution and 298 K) and Cl^- ions (7.64 $mS{\cdot}m^2{\cdot}mol^{-1}$) [322]. When NaOH was added, the conductivity of the solution was affected by the addition of Na^+ ions (5.01 $mS{\cdot}m^2{\cdot}mol^{-1}$) and OH^- ions (19.92 $mS{\cdot}m^2{\cdot}mol^{-1}$) where the net effect was a decrease in conductance due to the neutralisation of H^+ and OH^- ions [322]. At the equivalence point, all H^+ ions were neutralised and the conductance increased with further additions of NaOH due to the conductivity of Na^+ and OH^- ions [323], thus giving the titration a "v" shaped curve.

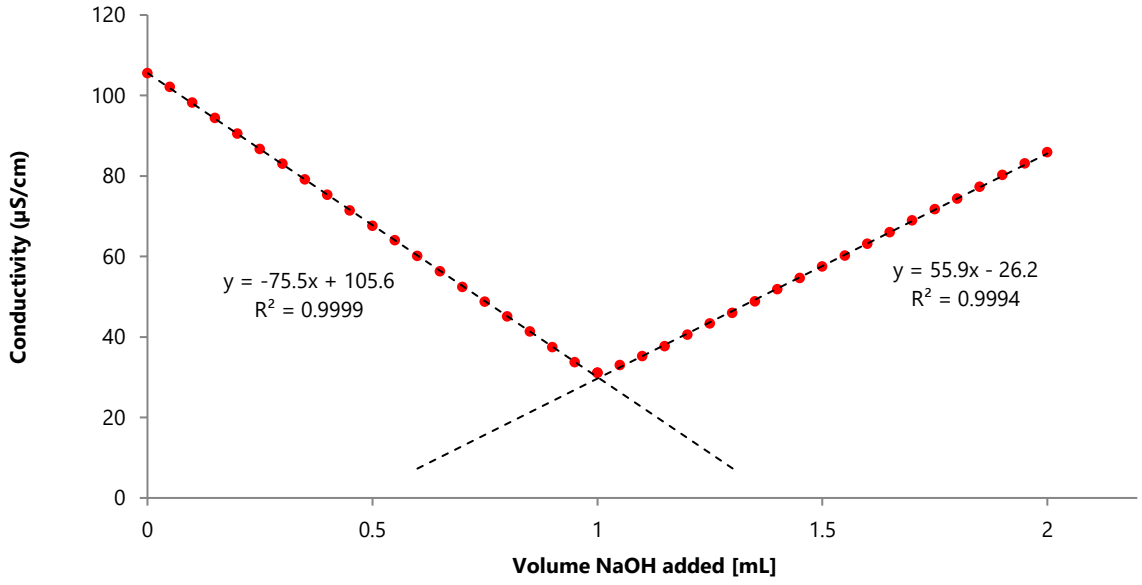

Figure 2.5: Conductometric titration of the blank control with no silica-CMD material.

Following the control titration, the conductometric titration of silica-CMD from 120 Å material produced a conductivity titration curve showing three stages (see Figure 2.6). In the first stage (1) of the titration, there was a decrease in conductivity with NaOH additions as the H^+ ions from HCl were neutralised. A similar rate of decrease in conductivity was observed when compared to the control titration with gradients of m=-72 and m=-75 for the silica-CMD titration and control titration, respectively. This indicated the neutralisation of the acidic groups from the HCl addition occurred before the neutralisation of -COOH groups on the silica-CMD. Following the HCl neutralisation, the acidic -COOH groups on the silica-CMD were neutralised and was observed in the second stage (2) of the titration curve where a net increase in conductivity was observed due to the low ionic molar conductivity of COO^- (4.09 $mS \cdot m^2 \cdot mol^{-1}$) compared to the conductivity of Na^+ and OH^- [322]. After all acidic groups reacted, the third stage (3) shows the linear increase of conductivity with further additions of excess NaOH, and when compared to the control titration, also had similar increase in conductivity as seen with the gradient, m=51 for the silica-CMD titration and m=55 for the control titration. The ΔV for NaOH in the second stage of the titration (2) was used to calculate the number of moles of -COOH groups available and was determined by computing the first derivatives of the titration curve seen in Figure 2.6 B and C where ΔV for NaOH was calculated by subtracting V_2 from V_1. From seven batches, the moles of COOH per gram of material averaged 0.60 ± 0.01 mmol/g, that is moles of -COOH groups per gram of material silica-CMD material with a 2% RSD. This shows a robust and reproducible method for synthesising silica-CMD material with free -COOH groups for future ligand immobilisation.

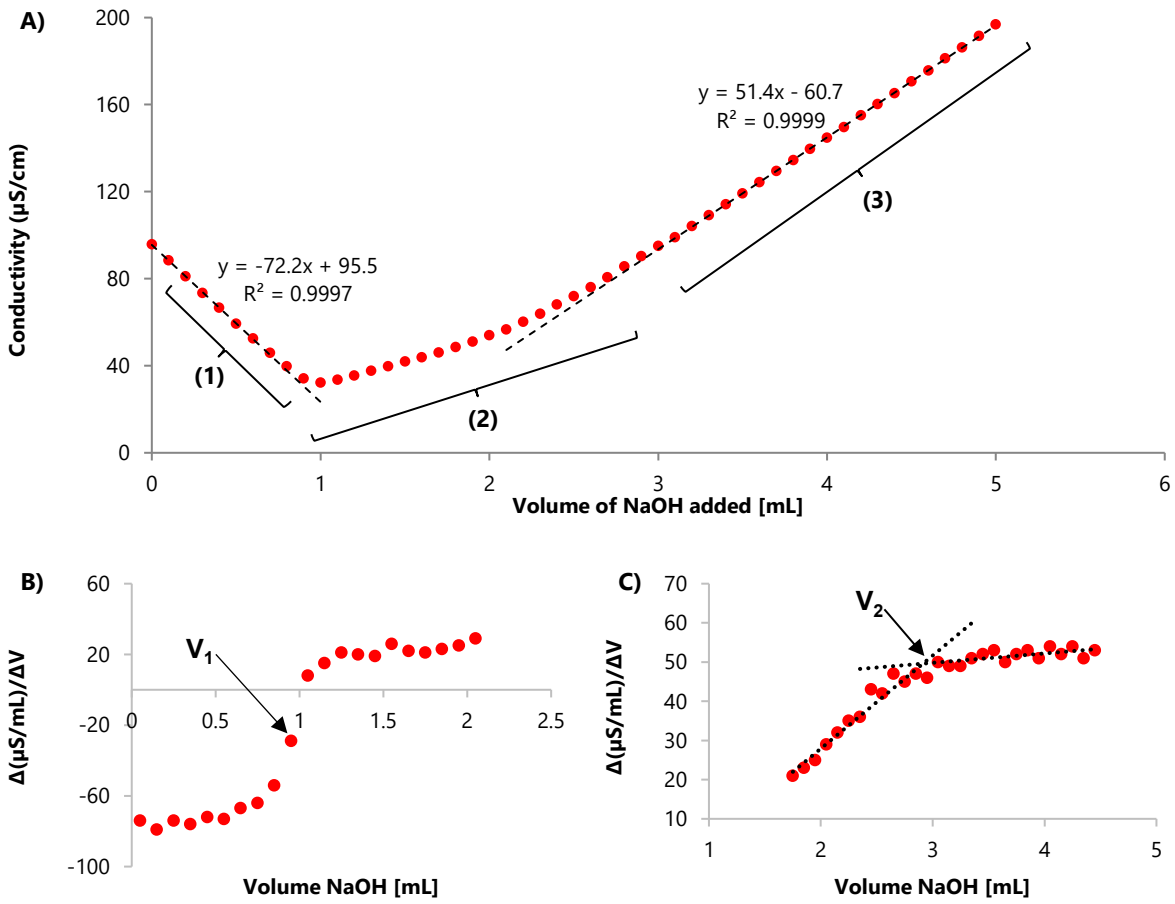

Figure 2.6: A) Conductometric titration of silica-CMD prepared from 120 Å material with the first derivatives for the B) starting and C) end point of the neutralisation of -COOH groups on the silica-CMD.

Table 2.1: Calculated mmol of -COOH groups per gram of customised silica-CMD material for n=7 batches.

Silica-CMD	**mole of -COOH per gram of material [mmol/g]**
1	0.60
2	0.59
3	0.59
4	0.61
5	0.59
6	0.60
7	0.60
Average	0.60 ± 0.01
% RSD	2.0

When developing a material to be used with biomolecule immobilisation, it is important to consider the pore size and surface area of the particle. There is an indirect relationship between the two where a decreasing pore size generally results in an increased surface area, however a smaller pore size may restrict larger biomolecules such as proteins from entering the pores and thus limiting immobilisation sites [324]. This was highlighted in a study performed by Trevisan *et al.* where silica with smaller pore diameters showed a sharp decrease in immobilisation activity of an enzyme, whilst on the other hand, larger pore sizes also a showed a decrease in activity due to the reduction of surface area of the support [325]. Additionally, in an analysis of 182 experiments on the effect on pore size for immobilised enzymes, Bayne *et. al* [326] showed that an increased protein loading was observed with increasing surface area, however this was soon limited by small pore diameters and restricted access as pore diameters of <100 Å revealed a general decrease in protein loading. Additionally, their analysis found that in the pore size range of 100-1000 Å, protein loading generally increased with increasing pore size, however above 1000 Å, loading decreased due to a reduction of surface area. Consequently, a balance between pore size and surface area must be achieved.

Three different pore sizes, 120 Å, 300 Å and 1000 Å were evaluated, where the smaller pore size material has a greater surface area compared to larger pore size material (see Table 2.2) [327]. Following CMD coating, titration of 120 Å and 300 Å resulted in an average of 0.60 ± 0.01 and 0.44 ± 0.01 mmol/g, moles of -COOH groups per gram of material, respectively. Less volume of NaOH was required to titrate against the 300 Å pore size material (see Figure 2.7). Additionally, 3 µm, 1000 Å APS material which was specially prepared and not commercially available was also tested. This larger pore size material however showed the absence of CMD coating as characterised in the FTIR spectrum (see Figure 2.8). Consequently, the 120 Å material was chosen due to increased surface area which resulted in greater moles of -COOH groups for future biomolecule binding. This result indicates improved CMD coating was achieved with increased particle surface area observed on smaller pore sized material. However, whilst determination of the free -COOH groups was achieved, the location of these groups, whether on the surface, or within the pore of the particle was not able to be determined.

Table 2.2: Relationship between pore size and surface area for APS, and the resulting mmol of -COOH groups from the synthesis of silica-CMD [327].

Particle Size [µm]	Pore Size [Å]	Surface area [m^2/g]	mole of -COOH per gram of silica-CMD [mmol/g]
3	120	300	0.60 ± 0.01 (n=7)
3	300	100	0.44 ± 0.01 (n=2)
3	1000	not reported by manufacturer	no result as CMD was not observed on the material

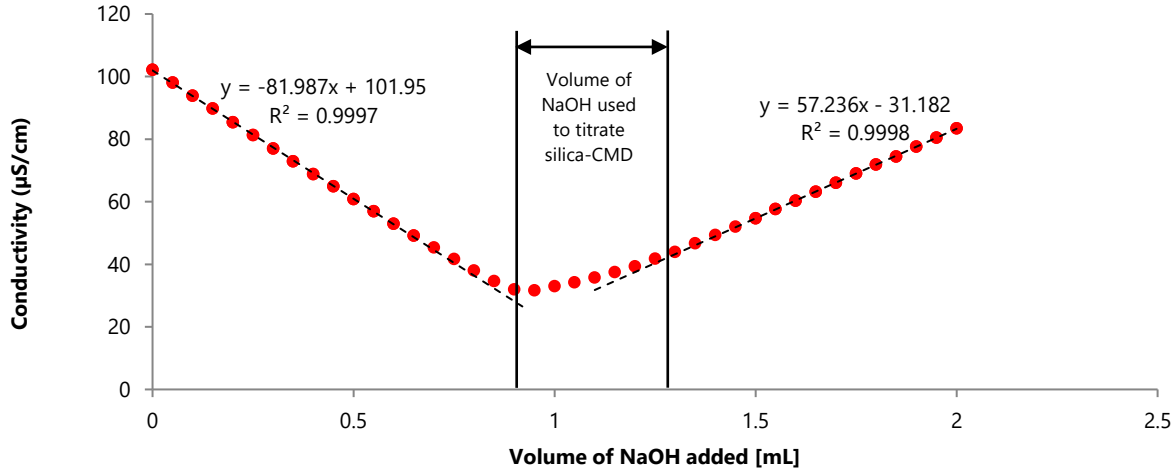

Figure 2.7: Conductometric titration of silica-CMD prepared from 300 Å material.

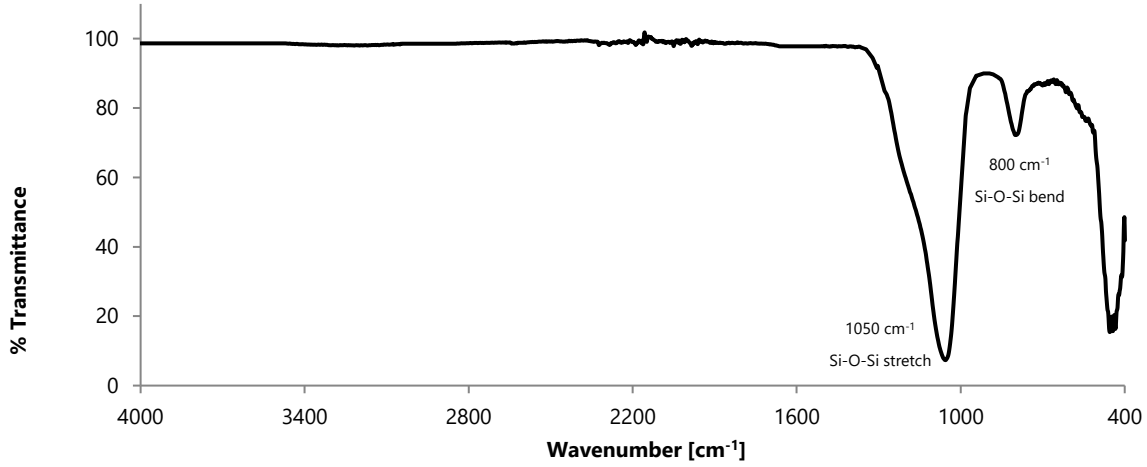

Figure 2.8: FTIR of 1000 Å APS material following attempted CMD coating.

Non-covalent vs. covalent ligand immobilisation

Prior to developing μSPE methods for biological sample preparation, immobilisation of biomolecules to the novel material was evaluated using horseradish peroxidase (HRP). A comparison between covalent and non-covalent immobilisation was performed using a colorimetric assay with HRP and ABTS.

When analysed using the spectrophotometer at 620 nm, a decreasing trend in absorption was observed for the non-covalently immobilised HRP following each repetition indicating a leaching of HRP from the material (see Figure 2.9). As noted in the method, between each of the first ten readings the non-covalently bound HRP, a mild wash buffer of 10 mM MES buffer was used. However, after the tenth reading, the cartridge was washed with a salt containing buffer, 1X PBS pH 7.4 solution, which resulted in no absorbance signal at 620 nm indicating that the adsorbed HRP was removed and no longer present on the cartridge.

Alternatively, HRP was covalently immobilised to silica-CMD packed into μSPE cartridges. In contrast to above, there was consistent absorbances for the ABTS radical cation across all readings (see Figure 2.9), indicating stable immobilisation without leakage of the biomolecule. The same washing buffer that stripped the adsorbed HRP from the non-covalently immobilised cartridge (1X PBS buffer) was used without detrimental effects. Therefore, covalent immobilisation provided more stable linkages between the biomolecule and the support phase, whilst still retaining the biomolecule's activity. Furthermore, successful immobilisation was observed as HRP activity was still seen after washing with 1X PBS buffer which had removed HRP from the adsorbed, non-covalently bound cartridge.

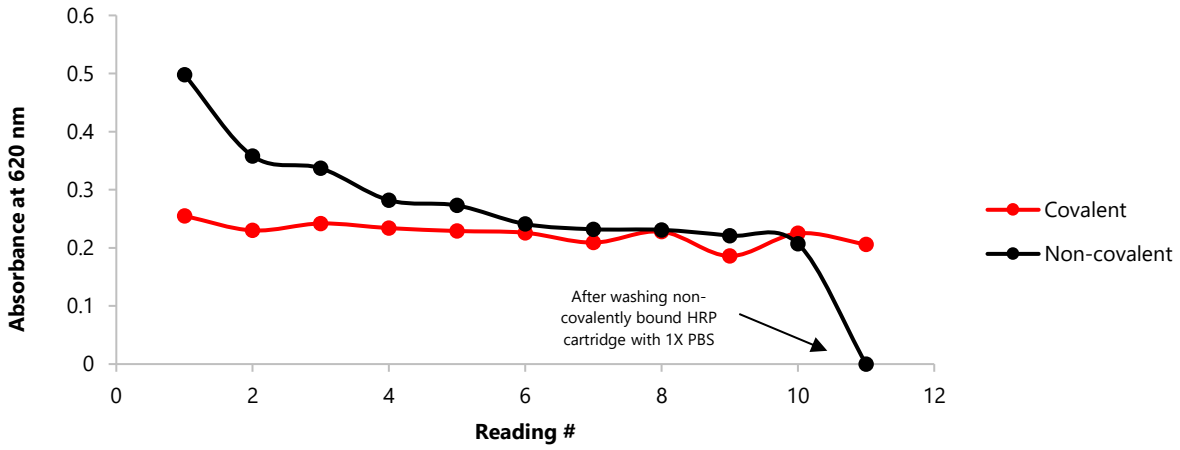

Figure 2.9: Absorbance of ABTS radical cation at 620 nm using the Thermo Fisher Multiskan Ascent 96/384 Plate Reader to compare between non-covalent and covalent immobilisation of HRP onto silica-CMD material.

120 Å material scale-up

Using the 120 Å material, an experiment was performed to determine if the reaction to produce silica-CMD could be upscaled for potential production on a larger commercial scale. The reaction was scaled up 50 times to produce approximately 5 g of silica-CMD. FTIR qualitatively confirmed the production of silica-CMD and an average of 0.57 ± 0.02 mmol/g was achieved from conductometric titrations of n=3 batches. Whilst the commercial viability of the material was not assessed, the synthesis reaction was able to be upscaled from 100 mg of material to 5 g showing potential for the material to be upscaled and produced on a larger commercial scale.

2.4 Conclusion

In this chapter, a customisable material prepared from APS and CMD was characterised using FTIR, conductometric titrations and enzymatic colorimetric assays. FTIR confirmed the binding of CMD to APS, and through conductometric titrations the number of moles of free -COOH groups per gram of customised material for future ligand immobilisation was calculated. Furthermore, a smaller pore size of 120 Å for the carrier material demonstrated its advantages for providing a greater surface area for the CMD to bind, resulting in 1.36 times more -COOH functional groups for binding of biomolecules compared to 300 Å, whilst no CMD was observed on 1000 Å material. Additionally, larger 5 g batches were successfully prepared indicating the ability to scale up the synthesis showing potential for the material to be upscaled and produced on a larger commercial scale. As demonstrated in this study, EDC/NHS crosslinking chemistry provided a simple and rapid way to bind biological ligands to the material which will allow the immobilisation of many various proteins of different functions for targeted sample preparation.

Chapter 3

Development of rapid and automated µSPE sample preparation workflows for protein biomarkers

3.1 Introduction

This chapter addresses the major challenges for protein biomarker quantification including lengthy workflows to produce signature peptides, and the diminishing accuracy of quantitative measurements in highly complex biological samples due to background interferences. Specifically, this chapter addresses objectives 2, 3 and 4 which aimed to develop an accurate and reproducible automated method for the isolation, pre-concentration and tryptic digestion of trace level proteins using customised µSPE cartridges with the ePrep automated workstation. This work builds upon recent advancements in automated platforms such as those presented by Bonichon *et al.*, who developed a rapid online immunoaffinity extraction and IMER protein digestion method coupled to LC-MS to analyse human butyrylcholinesterase as a marker for organophosphorus nerve agent exposure [328]. The workflow presented in this chapter was also inspired by various developments of automated platforms which integrate the multiple steps of protein sample preparation workflow which include protein depletion, fractionation, denaturation, digestion, and peptide enrichment into an integrated sample preparation system allowing increased throughput [329, 330].

Development of an immunoaffinity extraction and IMER µSPE cartridge

Targeted proteomics and low-level quantification of proteins is often performed by immunoaffinity extraction and proteolytic digestion as peptides are much more amenable to mass spectrometry analysis. The conversion of proteins to peptides is one of the most important steps in proteomic sample preparation where trypsin is the most widely used enzyme due to its highly specific cleavage and operating near physiological pH of 7.5-8.5. Whilst trypsin is most predominantly used in-solution for protein digestion, it has many drawbacks such as long digestion times, autolysis, and intolerance to high temperatures and organic solvent content [331]. To overcome these issues, trypsin can be immobilised onto a solid support resulting in improved enzyme activity, usability, and digestion times.

To develop both the immunoaffinity extraction and enzymatic protein digestion cartridge, the immobilisation method must be optimised by considerations of the carrier, the biomolecule, and the immobilisation strategy. Covalent coupling is a popular chemical immobilisation method used for biomolecules due to its linkage stability. It is used to form chemical bonds between functional groups on the support and biomolecule where commonly used coupling

reagents are amine reactive [146, 149, 332-335]. Linkages via the amine group are predominantly used for proteins as primary amines exist on the *N*-terminus of each polypeptide chain and in the side chain of lysine residues [336]. In physiological conditions, the amine groups on the proteins are positively charged and face outward making them easily accessible for conjugation [297]. Therefore, to maximise immobilised ligand activity and eliminate ligand leakage from the cartridge, covalent immobilisation with carbodiimide chemistry was used as presented in Chapter 2. With the customisable µSPE sorbent cartridges prepared in Chapter 2, trypsin and anti-BSA were covalently bound to silica-CMD for targeted µSPE sample preparation.

For the IMER digestion cartridge development, enzymatic protein digestion was performed with model proteins standards including bovine serum albumin (BSA), cytochrome c (Cyt c) and thyroglobulin (Tg). The IMER's performance was evaluated and compared against standard in-solution digestion protocols of proteins. The amino acid sequence coverage is often used as a measure for both the completeness of the protein digestion and the detection efficiency of the various tryptic peptides [337]. However, sequence coverage is influenced by use of different mass spectrometers and different search parameters in subsequent data analysis [127]. Therefore, to overcome this issue, comparisons between the IMER and in-solution digests were prepared and performed on the same day and analytical run. To obtain information of the digestion efficiency, and as a check before performing the data analysis, the possible presence of undigested protein in the total ion chromatogram (TIC) was used. Additionally, N_{α}-benzoyl-L-arginine ethyl ester (BAEE), a non-protein substrate that is cleaved by trypsin to produce N_{α}-benzoyl-L-arginine (BA) was used to monitor the digestion efficiency and reproducibility [338].

For the immunoaffinity cartridge development, anti-BSA and BSA were chosen as the model Ab-Ag. Immobilisation of anti-BSA to µSPE cartridges was qualitatively analysed through the colorimetric reaction between HRP antibody polymer and ABTS substrate. To quantify immunoaffinity cartridge capacities, SEC-ICP-MS/MS was employed to analyse BSA, as well as lanthanide-labelled BSA using Maxpar™ reagent for increased sensitivity where quantification of immunocaptured proteins [339] and intact BSA protein [340] have successfully been reported in literature.

Finally, the two developed cartridges were combined to create a single workflow method which addressed the isolation, pre-concentration and digestion of proteins. This workflow was applied to human serum samples and compared against standard digestion protocols.

3.2 Experimental

3.2.1 Chemicals and Consumables

Trypsin from bovine pancreas (TPCK treated), bovine serum albumin (BSA), cytochrome c (Cyt c), thyroglobulin (Tg), ethanolamine, 1-ethyl-3-(3-dimethylaminopropyl)carbodiimide (EDC), *N*-hydroxysuccinimide (NHS), Tris base, 2-(*N*-morpholino)ethanesulfonic acid (MES), sodium chloride, 10X phosphate buffer saline (PBS) pH 7.4 solution (30 mM Na_2HPO_4, 10.5 mM K_2HPO_4, 1.5 M NaCl), ammonium bicarbonate, lithium chloride, urea, iodoacetamide (IA), dithiothreitol (DTT), bicinchoninic acid (BCA) kit, *N*-α-benzoyl-l-arginine ethyl ester (BAEE), tris(2-carboxyethyl)phosphine hydrochloride (TCEP), horseradish peroxidase (HRP), 2,2'-azino-bis(3-ethylbenzothiazoline-6-sulfonic acid) liquid substrate (ABTS), ammonium acetate and formic acid were obtained from Sigma Aldrich (Castle Hill, NSW, Australia). Acetonitrile (ACN) was obtained from ChemSupply (Gillman, South Australia, Australia). Anti-BSA antibody (ab9092) was obtained from Abcam (Melbourne, Victoria, Australia). Mouse IgG VisUCyte HRP Polymer Antibody was obtained from R&D Systems (Minneapolis, MN, USA). A Maxpar™ Labelling Kit was purchased from Fluidigm (formerly DVS Sciences, San Francisco, CA). Water obtained from an Arium® pro water generation system (Sartorius Stedim Plastics GmbH, Germany) was used for all preparation and dilutions unless stated otherwise. µSPEed cartridges were obtained from Eprep (Mulgrave, Victoria, Australia).

3.2.2 µSPE sample preparation workflow development

The final µSPE sample workflow developed for protein biomarkers consisted of two cartridges, one for immunoaffinity extraction using antibodies, and the other for protein digestion using enzymes (see Figure 3.1). In both cases, the ligands were covalently immobilised to the customisable sorbent material using EDC/NHS coupling. The µSPE methods were identical in the first eight steps for both cartridges, except for select differences in the composition and concentration of reagents and buffer solutions. Section 3.3 and 3.4 details these optimisations for the IMER protein digestion cartridge and immunoaffinity extraction cartridge respectively.

Initial method development for both cartridges were performed using the ePrep digiVOL® syringe driver fitted with a 250 µL syringe and custom packed µSPEed cartridges. Sample volumes and aspirate and dispense flow rates were optimised using the digiVoL®, and once

fully developed, the method was migrated to the ePrep Sample Preparation Workstation for automation. Using the ePrep workstation, the samples, reagents and buffers for both cartridges were placed on the workstation bed and the immunoaffinity extraction and enzymatic protein digestion method was setup to run sequentially, thus creating an automated workflow method combining the two cartridges.

Cartridge 1: µSPE for immunoaffinity extraction cartridge

Immunoaffinity µSPE cartridges were prepared where anti-BSA and BSA were used as the model Ab-Ag. Anti-BSA was covalently immobilised onto silica-CMD µSPEed cartridges *in-situ* with the ePrep Workstation. An immobilisation buffer was prepared using MES to a final concentration of 10 mM. Tris buffer was prepared from Tris base to a concentration of 500 mM and adjusted to pH 8 with HCl. The Tris buffer was used to prepare two buffers, a running buffer to be used as a diluent for protein samples and cartridge conditioning (25 mM Tris with 1 mM NaCl) and a salt wash buffer (25 mM Tris with 20 mM NaCl). Ethanolamine (0.1 M) was prepared and adjusted to pH 8 with concentrated hydrochloric acid to use for end-capping.

To immobilise the antibody, the cartridge was conditioned twice with 500 µL of 10 mM MES buffer (aspirate: 4500 µL/min and dispense: 1000 µL/min), activated with 0.1 M EDC/NHS in immobilisation buffer (volume: 500 µL, aspirate: 4500 µL/min and dispense: 600 µL/min), loaded with 20 ng/µL of antibody in immobilisation buffer (volume: 500 µL, aspirate: 4500 µL/min and dispense: 600 µL/min), and end capped with 0.1 M ethanolamine pH 8 (volume: 500 µL, aspirate: 4500 µL/min and dispense: 300 µL/min) with 500 µL of immobilisation buffer in between each step (aspirate: 4500 µL/min and dispense: 1000 µL/min). The cartridge was then washed 3 times with 500 µL salt wash buffer and conditioned twice with 500 µL running buffer (aspirate: 4500 µL/min and dispense: 1000 µL/min). The sample prepared in running buffer was then cycled (repeated aspirating and dispensing through the µSPE) twice for the protein to be captured (volume: 100 µL, aspirate: 4500 µL/min and dispense: 300 µL/min), washed 3 times with 500 µL salt wash buffer to remove non-specifically bound components (aspirate: 4500 µL/min and dispense: 1000 µL/min), and eluted with 90 µL elution buffer (0.1% HCl) into an LC vial (aspirate: 4500 µL/min and dispense: 1000 µL/min) to which 10 µL of 500 mM Tris pH 8 was added for sample for compatibility with enzyme cartridge digest which was to be performed immediately after. The cartridge was immediately

reconditioned to pH 8 twice with 500 µL of salt wash buffer (aspirate: 4500 µL/min and dispense: 1000 µL/min) to prevent antibody denaturation for possible further use (see Figure 3.1, Cartridge 1).

Cartridge 2: µSPE for enzymatic protein digestion

Enzymatic protein digestion cartridges were prepared using trypsin. Trypsin was covalently immobilised onto silica-CMD µSPEed cartridges *in-situ* with the ePrep Workstation. An immobilisation buffer was prepared using MES to a final concentration of 10 mM. Tris buffer was prepared from Tris base to a concentration of 500 mM and adjusted to pH 8 with HCl. The tris buffer was used to prepare three buffers, a running buffer to be used as a diluent for protein samples and cartridge conditioning (25 mM Tris with 0.5 mM $CaCl_2$), a salt wash buffer (25 mM Tris with 10 mM $CaCl_2$), and an elution buffer (25 mM Tris with 10 mM $CaCl_2$ and 10% ACN). Ethanolamine (0.1 M) was prepared and adjusted to pH 8 with concentrated hydrochloric acid to use for end-capping.

To immobilise the trypsin enzyme, a µSPE cartridge was conditioned twice with 500 µL of 10 mM MES buffer (aspirate: 4500 µL/min and dispense: 1000 µL/min), activated with 0.1 M EDC/NHS in 10 mM MES (volume: 500 µL, aspirate: 4500 µL/min and dispense: 300 µL/min), immobilised with 50 ng/µL trypsin in 10 mM MES buffer (volume: 500 µL, aspirate: 4500 µL/min and dispense: 300 µL/min), and end-capped with 0.1 M ethanolamine pH 8 (volume: 500 µL, aspirate: 4500 µL/min and dispense: 300 µL/min) with 500 µL of immobilisation buffer in between each step (aspirate: 4500 µL/min and dispense: 1000 µL/min). The cartridge was then washed 3 times with 500 µL salt wash buffer (aspirate: 4500 µL/min and dispense: 1000 µL/min) to remove any non-specifically bound trypsin. The cartridge was then conditioned twice with 500 µL running buffer (aspirate: 4500 µL/min and dispense: 1000 µL/min) before applying the protein samples. Collected into an LC vial, protein sample (100 µL of 10 ng/µL resulting in 1 µg total protein) was aspirated and dispensed through the µSPE cartridge 30 times for 10 minutes of digest contact time (aspirate: 1000 µL/min, dispense: 300 µL/min). Following this, 100 µL of elution buffer was passed through the cartridge to elute remaining peptides (aspirate: 1000 µL/min, dispense: 1000 µL/min), and collected into the same LC vial, and 1 µL of concentrated formic acid was added for LC-MS analysis (instrument settings specified in section 3.3.1) (see Figure 3.1, Cartridge 2).

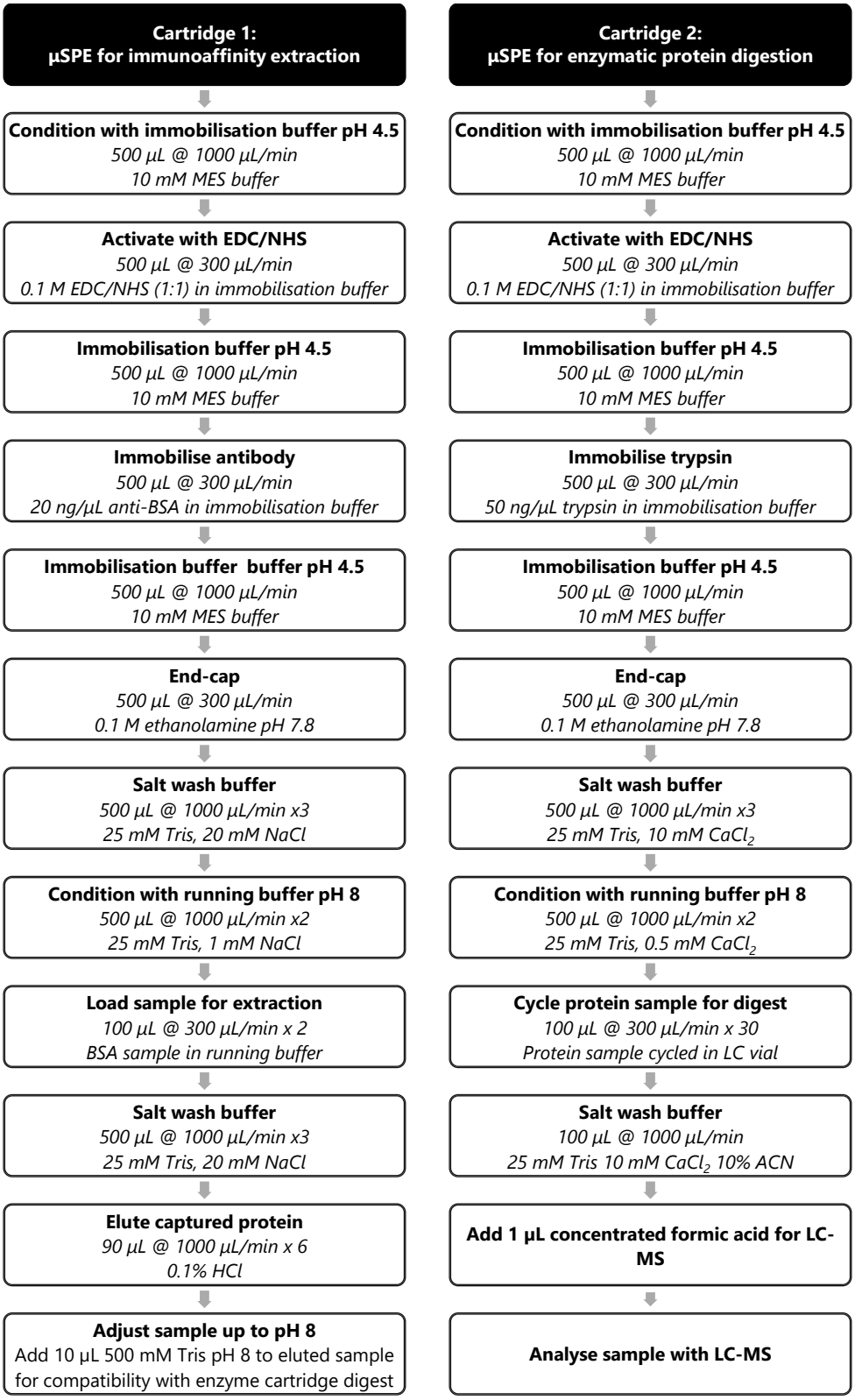

Figure 3.1: Automated µSPEed biomarker workflow for both protein immunoaffinity isolation and digestion.

3.3 Development of the IMER µSPE cartridge

To develop the µSPE trypsin cartridge, BSA, Cyt c and Tg were chosen as model proteins. The IMER's performance was evaluated and compared against standard in-solution digestion protocols of proteins. Additionally, a non-protein substrate, BAEE was also used to assess trypsin activity, assist with buffer and reagent optimisations, and determine cartridge digest reproducibility. Once optimised, the method was applied to a human serum sample.

3.3.1 Instrumentation and parameters for IMER µSPE cartridge

To analyse BAEE, a non-protein substrate that was chosen to assess the performance and reproducibility of the trypsin reactor, high performance liquid chromatography (HPLC) with an ultraviolet (UV) detector at 254 nm was used. In the presence of trypsin, BAEE is cleaved to produce N_{α}-Benzoyl-L-arginine (BA) and ethanol as trypsin cleaves at the carboxyl side of the amino acid arginine. This cleavage can be monitored under the following HPLC conditions (see Table 3.1).

Table 3.1: HPLC conditions for analysis of the trypsin digest of BAEE.

Conditions	Description
Instrument	Thermo Fisher Ultimate 3000
Column	Zorbax 300 SB-C8 Rapid Resolution 2.1 x 100 mm 1.8 µm
Mobile phase	%A: 85% Water + 0.1% formic acid, %B: 15% ACN + 0.1% formic acid
Flow rate	0.2 mL/min
UV detection	254 nm
Run time	6 minutes
Injection volume	1 µL

Peptide analysis was performed using two LC-MS setups, liquid chromatography time-of-flight mass spectrometry (LC-QToF-MS) using the Agilent 1290 Infinity II LC coupled to the Agilent 6510 (Agilent Technologies, Santa Clara, CA, USA), and liquid chromatography orbitrap mass spectrometry (LC-OT-MS) using the Waters ACQUITY M-Class Nano LC (Waters, Rydalmere, NSW, Australia) coupled to Thermo Fisher Q Exactive Plus Orbitrap (Thermo Fisher Scientific, North Ryde, NSW, Australia) (see Table 3.2). The LC-QToF-MS instrument setup was first used, however, a lack in sensitivity resulted in the use of the LC-OT-MS system.

For the LC-QToF-MS system, the MS data was processed using Agilent MassHunter B.07.00 to obtain a peptide list of charge state ≥2+. The mass list was searched against the contaminants database using MASCOT Peptide Mass Fingerprint (Matrix Science) with the following parameter settings: variable modifications carbamidomethyl (C); enzyme: trypsin; number of allowed missed cleavages: 2; and peptide mass tolerance: 1.2 Da.

For the LC-OT-MS system, MS/MS data files were searched using Peaks Studio X against the contaminants database with the following parameter settings: variable modifications: carbamidomethyl (C), deamidated (NQ), oxidation (M); enzyme: trypsin; number of allowed missed cleavages: 3; and peptide mass tolerance: 10 ppm. MS/MS mass tolerance: 0.05 Da. The results of the search were then filtered to include peptides with a $-\log_{10}P$ score that was determined by the False Discovery Rate (FDR) of <1%.

Table 3.2: Analysis conditions for protein digestion on LC-MS instruments.

Conditions	**Description**
Instrument	Agilent 1290 Infinity II LC coupled to an Agilent 6510 QToF
Column	Accucore C18+ column (100 mm x 2.1 mm, 1.5 µm)
Injection volume	20 µL
Flow rate	0.2 mL/min
Mobile phase	%A: Water + 0.1% formic acid, %B: Acetonitrile + 0.1% formic acid
Program	0 min: 5%B, 2-25 min: 5% to 60% and held for 5 minutes
MS parameters	Positive ion mode, electrospray ionisation (ESI) Vcap: 3500 V and drying gas flow of 5 L/min at 325°C Fragmentor voltage: 175 V Mass range: 400-2000 *m/z*
Conditions	**Description**
Instrument	Waters ACQUITY M-Class Nano LC coupled to a Thermo Fisher Q Exactive Plus Orbitrap MS
Columns	nanoEase Symmetry C18 trapping column PicoFrit column (300 mm x 75 µm (ID); New Objective, Woburn, MA, USA) packed with Magic C18AQ resin (3 µm, Michrom Bioresources, Auburn, CA, USA)
Injection volume	5 µL
Flow rate	15 µL/min
Mobile phase	%A: Water, %B: 98% Acetonitrile + 0.2% Formic Acid
Program	Sample was loaded at 15 µL/min for 3 minutes onto the trap column before being washed into the PicoFrit column using the following: 0-15 min: 5 to 30%B, 15-28 min: 30-80%B held for 2 minutes, 30-33 min: 80-5%B held for 2 minutes
MS parameters	The eluting peptides were ionised at 2400V. A Data Dependant MS/MS (dd MS2) experiment was performed, with a survey scan of 350-1500 Da performed at 70,000 resolution for peptides of charge state 2+ or higher with an Automated Gain Control (AGC) target of 3e6 and maximum injection time of 50 ms. The top 12 peptides were selected fragmented in the (higher-energy collisional dissociation) HCD cell using an isolation window of 1.4 *m/z*, an AGC target of 1e5 and maximum injection time of 100 ms. Fragments were scanned in the orbitrap analyser at 17,500 resolution and the product ion fragment masses measured over a mass range of 120-2000 Da. The mass of the precursor peptide was then excluded for 30 seconds.

3.3.2 Sample preparation for protein digestion using model proteins and human serum sample

Prior to enzymatic digestion, the model proteins (BSA, Cyt c and Tg), and human serum samples were prepared. Cyt c and Tg were weighed out into an Eppendorf tube and made to volume with 500 mM Tris pH 8 buffer for a final concentration of 1 mg/mL of protein. BSA and human serum samples were denatured, reduced and alkylated with urea, DTT and IA according to Kinter *et al.* [341]. BSA protein solutions and human serum samples were prepared by dissolving 1 mg protein or 100 µL of human serum in 100 mM Tris buffer containing 6 M urea. 5 µL of DTT (200mM in 100 mM Tris) were added to 100 µL of the protein solution and samples were reduced at room temperature for 1-hour and subsequently alkylated with 20 µL of IAA (200 mM in 100 mM Tris) for another hour. Additionally, 20 µL of DTT were added to consume any unreacted IAA. Finally, 855 µL of water was added to the mix to decrease the urea concentration below 1 M giving the sample a final volume of 1 mL. Prior to digestion, all protein standards and samples were diluted to working concentrations with a final composition being that of the running buffer (25 mM Tris with 500 µM $CaCl_2$). Cyt c and Tg protein samples were digested without any further pre-treatment.

The cartridge digests were compared to the conventional in-solution trypsin digests. In-solution digestion was carried out by adding 50 µL of sample, 47 µL of 500 mM Tris buffer pH 8 and 2 µL of 5 ng/µL trypsin (1:200 enzyme to protein ratio). Samples were incubated at 37°C for 18 hours and 1 µL of concentrated formic acid was added to stop the digestion.

3.3.3 Results and Discussion

As seen in Chapter 2, covalent immobilisation was successfully achieved through EDC/NHS coupling with greater enzyme stability and minimal leaching from the support when compared to non-covalent immobilisation. Therefore, covalent immobilisation was also used for the development of the tryptic IMER μSPE cartridge. The covalent binding required the immobilisation of the enzyme to the support, washing the support which removed unwanted non-covalently bound enzyme, followed by final conditioning of the support before enzymatic protein digestion was performed. Therefore, to develop a tryptic IMER, the immobilisation process as well as digestion parameters were optimised to ensure rapid and efficient proteolytic digests. Key parameters that were assessed include composition and concentration of reagents and buffer solutions, as well as protein loading amount and the digestion incubation times. Once optimised, the developed IMER was employed in the analysis of three model proteins (BSA, Cyt c and Tg) and a human serum sample.

Salt wash buffer optimisation

As discussed in Chapter 2, non-specific binding can occur through weak forces such as hydrophobic and ionic interactions, therefore it was important to ensure that wash buffer solutions removed non-covalently bound trypsin. During the immobilisation process, the pH was kept constant at pH 4.5 using a MES buffer. This resulted in negatively charged carboxyl groups on the silica-CMD, which ionically interacted with the positively charged protein residues [342]. In the case of proteins, the net surface charge was dependent on pH as they are made up of many different amino acids containing weak acidic and basic groups. Thus, trypsin with an isoelectric point (*pI*) of 10.2-10.8 exhibited a net positive charge at pH 4.5. Therefore, to remove non-covalently bound trypsin, salt solutions were used to disrupt the ionic interactions as found in ion exchange chromatography principles [343]. High ionic strength salt ions (typically Na^+ and Ca^{2+}) are commonly used in ion exchange to compete with bound components for the charged surface, and in turn release the target molecules [344].

To ensure the concentration $CaCl_2$ in the salt wash buffer was sufficient to remove non-specifically bound trypsin, BAEE was used as model substrate to detect the presence of trypsin that was being removed from the cartridge. The cartridge was washed 3 times with salt wash buffer aliquots and were collected into Eppendorf tubes containing BAEE, where the presence or absence of trypsin was observed through the detection of the hydrolysis product, BA. A 25mM Tris salt wash buffer containing 10 mM $CaCl_2$ was used and all three wash aliquots were collected into Eppendorf tubes containing 5 µL of 1000 µM BAEE. The three wash aliquots were analysed by HPLC where the first salt wash buffer wash following trypsin immobilisation showed BAEE digest to BA, indicating that non-covalently bound trypsin was washed off the cartridge into the tube (see Figure 3.2 A). After the second salt wash buffer wash aliquot, the hydrolysis product, BA, was no longer observed indicating the non-specifically bound trypsin had been washed off in the first aliquot (see Figure 3.2 B). Therefore, cartridges must be washed with a high concentration of salt (10 mM $CaCl_2$) for removal of non-covalently bound trypsin prior to protein digestion.

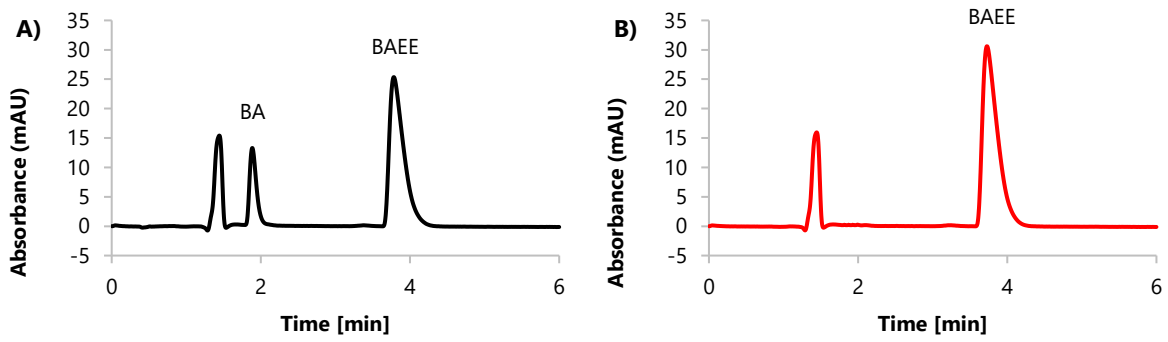

Figure 3.2: Observing the presence of BAEE (4 min) hydrolysis to BA (2 min) by excess non-covalently bound trypsin in collected salt wash buffer aliquots. A) Chromatogram shows BAEE hydrolysis following the first salt wash buffer wash and B) a chromatogram showing no presence of trypsin in subsequent washes.

Running buffer optimisation

To ensure that trypsin activity was maintained, and no enzyme denaturation occurred, a running buffer was optimised and used as the protein digestion diluent for all samples. Tris-HCl with $CaCl_2$ salt is commonly used in digestion protocols as it has been reported in literature that Ca^{2+} ions stabilise the trypsin structure resulting in preserved enzyme activity [345, 346]. However, due to the ionic interactions of protein to silica-CMD, the concentration

of $CaCl_2$ in the running buffer was optimised to ensure efficient flow-through digest whilst minimising protein and peptide adsorption. Two BSA cartridge digests were performed using two different running buffer compositions. Both cartridge digests were performed with their respective running buffers followed by an elution buffer aliquot collected into a separate vial observing for any peptide adsorption to the cartridge because of the differing running buffers. Both running buffer digest aliquots and elution buffer aliquots were analysed by LC-QToF-MS (see Table 3.3 and Figure 3.3).

For the running buffer containing 1000 µM $CaCl_2$, minimal BSA peptide adsorption to the cartridge was observed as seen in the elution aliquot (see Figure 3.3 A2), however, inefficient digestion was seen with BSA protein remaining at 18 minutes (see Figure 3.3 A1 and Figure 3.3 C which shows the TIC of 50 ng/µL BSA standard that has not been digested). At 500 µM $CaCl_2$, more efficient digest occurred with minimal undigested BSA remaining as seen in the running buffer digest aliquot (see Figure 3.3 B1). However, in Figure 3.3 B2, peptide adsorption to the cartridge was seen when the relatively lower 500 µM $CaCl_2$ concentration was used, and thus required the elution buffer to release the peptides off the cartridge. Due to the higher salt concentrations ($CaCl_2$ 1000 µM), the interactions between the BSA protein and the immobilised trypsin were reduced resulting in less efficient digestion compared to $CaCl_2$ at 500 µM. The increasing the ionic strength of a buffer weakened the electrostatic interactions between the protein/peptides and the substrate surface, and thereby minimising contact with the immobilised enzyme. Consequently, 500 µM $CaCl_2$ was used as the optimised running buffer as improved contact between trypsin and protein was observed resulting in more efficient digestion. Additionally, an elution step following protein flow-through digestion was used to release any adsorbed peptides from the cartridge support material where 25 mM Tris, 10 mM $CaCl_2$ and 10% ACN was successfully used.

Table 3.3: Two cartridge digestion methods with differing running buffer salt concentrations followed by an elution buffer to observe for any peptide adsorption to the cartridge as a result. All aliquots were analysed by LC-QToF-MS.

Cartridge digestion	**Running Buffer**	**Elution Buffer**
BSA Digestion A	Aliquot A1) Digested peptides using 25 mM Tris, 1000 µM $CaCl_2$	Aliquot A2) Eluted peptides using 25 mM Tris, 10 mM $CaCl_2$ and 10% ACN
BSA Digestion B	Aliquot B1) Digested peptides using 25 mM Tris, 500 µM $CaCl_2$	Aliquot B2) Eluted peptides using 25 mM Tris, 10 mM $CaCl_2$ and 10% ACN

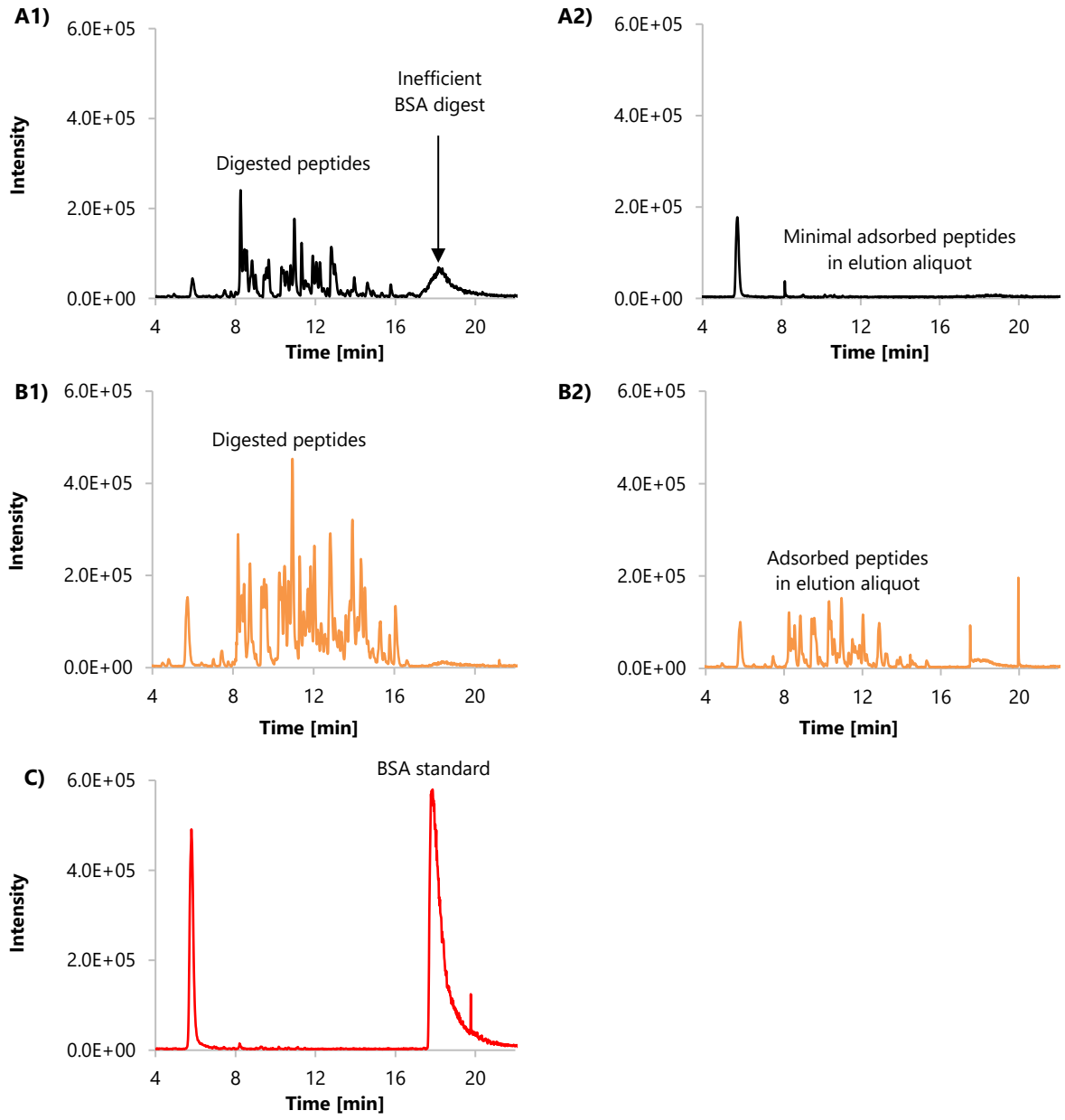

Figure 3.3: Comparison of two BSA digests (5 µg protein load) using different $CaCl_2$ concentrations. Aliquot A1) TIC for BSA digest in running buffer containing 1000 µM $CaCl_2$ and Aliquot A2) TIC for elution buffer aliquot following the 1000 µM $CaCl_2$ running buffer digest using 25 mM Tris, 10 mM $CaCl_2$ and 10% ACN showing minimal peptide adsorption. Aliquot B1) TIC for BSA digest in running buffer containing 500 µM $CaCl_2$ and the Aliquot B2) TIC for elution buffer aliquot following the 500 µM CaCl2 running buffer using 25 mM Tris, 10 mM $CaCl_2$ and 10% ACN showing peptide adsorption. C) TIC of 50 ng/µL BSA standard that was not digested.

End-cap reagent optimisation

End-capping refers to the replacement or modification of accessible functional groups present on solid support materials and is an important step in minimising unwanted non-specific binding which may induce steric hindrance and blocking of otherwise accessible binding sites [347]. When using EDC/NHS chemistry for immobilisation of biomolecules onto silica-CMD, remaining unreacted NHS ester groups undergo hydrolysis thereby regenerating the original carboxyl group. Since proteins can form non-specific ionic interactions with other charged molecules, selection of an end-capping reagent can help to minimise protein-surface ionic interactions. A comparison between -COOH end-capped groups and -OH end-capped groups using glycine and ethanolamine was evaluated for protein adsorption where Cyt c, a small hemoprotein that is highly water soluble and red coloured in solution was chosen for visualisation. Upon loading Cyt c onto both -COOH and -OH end-capped cartridges conditioned at pH 8, adsorption was present on the -COOH end-capped cartridge (as observed by the red appearance), and absent on the -OH end-capped cartridge (as observed by the lack of red appearance) (see Figure 3.4). At the running cartridge conditions of pH 8, negatively charged $-COO^-$ groups can interact with positively charged entities found on proteins resulting in ionic interactions between the protein and surface. Therefore, by end-capping with ethanolamine, -COOH groups are replaced by the amino alcohol, minimising the ionic interactions between the protein and surface.

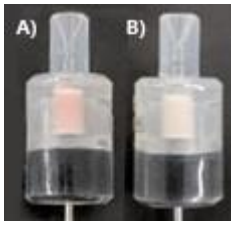

Figure 3.4: Cyt c adsorption onto a) -COOH glycine end-capped as observed by the red appearance, and the absence of cyt c adsorption onto b) -OH ethanolamine end-capped silica-CMD.

Incubation time

Incubation time and flow rates play an essential role in the development of the μSPE method. Particularly with enzymes, the longer an enzyme is incubated with a substrate, a greater number of products will form which can be achieved by optimising the flow rate and the incubation time of the substrate on the enzyme [331]. Using BAEE, a non-protein substrate for

trypsin, the activity of the enzyme can be assessed spectrophotometrically through the cleavage of BAEE to produce BA [348, 349]. Firstly, incubation time was evaluated where a 2-minute and 5-minute digest of 1 mM BAEE was performed at the same flow rate (2-minute digest had 6 cycles of 100 µL BAEE at 300 µL/min and the 5-minute digest 15 cycles of 100 µL BAEE at 300 µL/min). This resulted in a HPLC-UV chromatogram at 254 nm containing two peaks, remaining undigested BAEE (4 min) and the resulting digested product BA (2 min) (see Figure 3.5). The peak area ratio of BA/BAEE was calculated for each digest where the 2-minute digest resulted in a ratio of 0.10 compared to 0.33 for the 5-minute digest, showing that an increased incubation time resulted in greater product formation.

As incubation time was shown to have an influence on the digestion ratio of BAEE, an experiment was performed to determine whether the flow rate also influenced the digestion. Whilst keeping the BAEE substrate incubation time the same between two cartridges, two flow rates and their respective number of cycles to ensure the same incubation time were tested (see Table 3.4). The BA/BAEE peak area ratio was 0.10 and 0.11 for 300 µL/min and 600 µL/min, respectively indicating no major difference. Consequently, digestion efficiency was not affected by flow rate used but rather the incubation time.

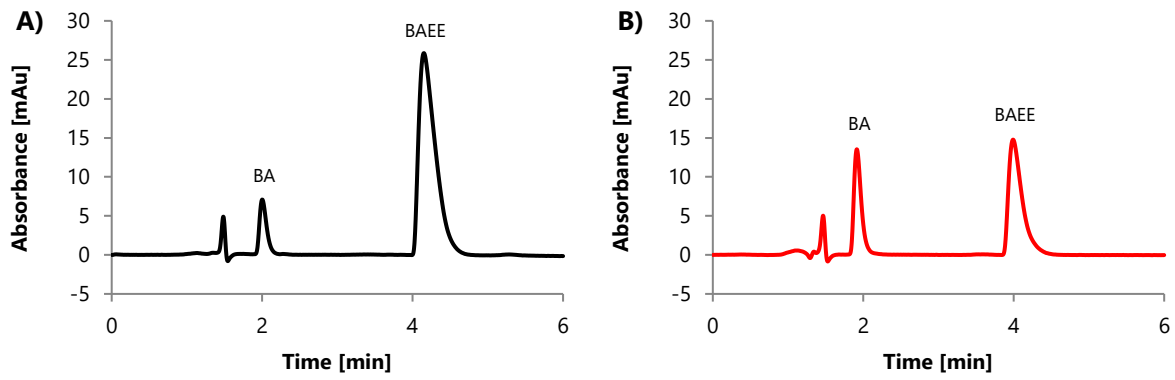

Figure 3.5: HPLC-UV chromatogram at 254 nm for BAEE (4 min) digestion to BA (2 min) for a) 2-minute digest and b) 5-minute digest.

Table 3.4: Effect of flow rate on BAEE digest whilst ensuring the total incubation for both digests remain the same.

Cartridge	Total incubation time [min]	Flow rate [µL/min]	Number of cycles to obtain desired incubation time	BAEE:BA peak area ratio
BAEE digest 1	2	300	6	0.10
BAEE digest 2	2	600	12	0.11

Following trypsin activity experiments, preliminary protein loading capacity and digestion incubation times were investigated by loading Cyt c and BSA from 1-10 µg and 5 and 10 minutes, respectively where optimum digestion conditions are protein-dependent [350]. Figure 3.6 and Figure 3.7 shows the TICs from LC-QToF-MS analysis after tryptic digestion with the IMER. Initially, a 5-minute room temperature digestion of Cyt c was attempted with 10 µg of Cyt c loaded onto the cartridge. There was a large peak at 16 minutes representing undigested Cyt c (Figure 3.6 A). Loading of 1 µg of Cyt c under the same conditions resulted in complete digestion of the protein with no evidence of residual intact Cyt c (Figure 3.6 B). Similarly, loading of 10 µg of BSA and after 10 min of incubation, a large peak of undigested BSA was observed at 18 min (Figure 3.7 A). Reducing the protein load to 1 µg resulted in improved digestion and minimal undigested BSA (Figure 3.7 B). Therefore, efficient digestion of these two proteins requires ≤ 1 µg, and higher amounts should be avoided to prevent IMER overloading.

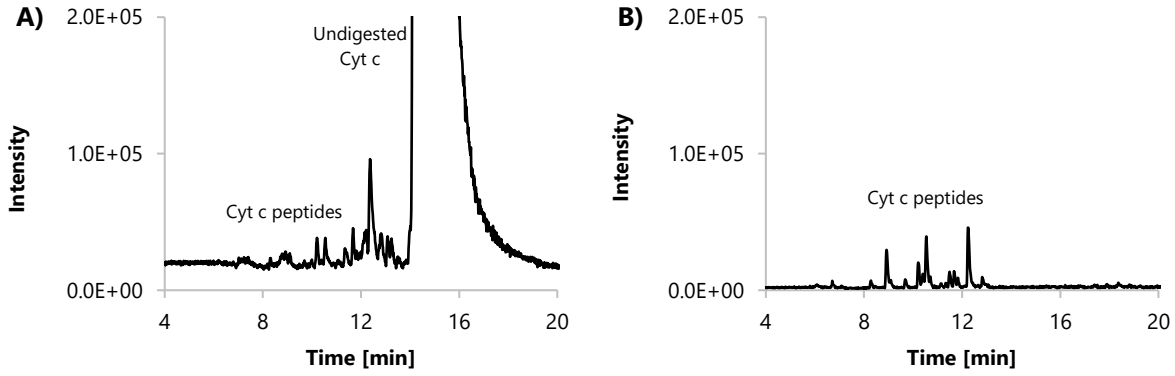

Figure 3.6: TICs of cartridge digests of Cyt c with varying protein amounts. A) A 5-minute digest of 10 µg of Cyt c showing remaining undigested protein whilst B) a 5-minute digest of 1 µg Cyt c shows no undigested protein.

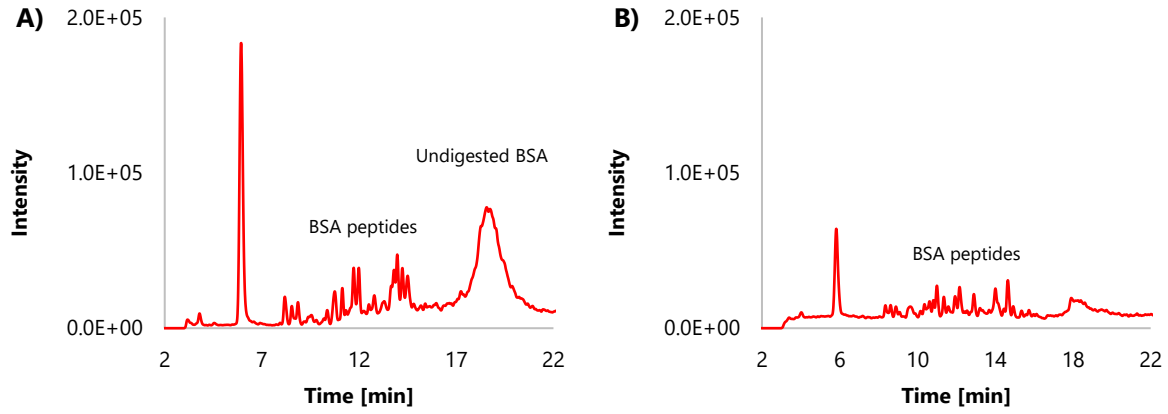

Figure 3.7: TICs of cartridge digests of BSA with varying protein amounts. A) A 10-minute digest of 5 µg BSA showing undigested protein whilst B) a 10-minute digest of 1 µg BSA with minimal protein remaining.

Optimised trypsin µSPE method for enzymatic digestion

Using the optimisations addressed above, trypsin digests were performed on BSA protein using the final conditions shown in Figure 3.1, Cartridge 2. BSA (100 µL of 10 ng/µL standard, 1 µg protein load), and a blank control (100 µL running buffer) was digested in duplicate with a 10-minute incubation time. The digests were analysed using the LC-OT-MS and the chromatograms for both digests and a blank control digest are shown in Figure 3.8. When searched using the PEAKS database, BSA digests obtained with the two cartridges resulted in sequence coverages of 61% (48 unique peptides identified) and 59% (41 unique peptides identified) respectively with peptides observed between retention times of 15.6 and 22.8 minutes. Peptide coverage between the two cartridges showed high levels of overlap as 39 peptides were observed in both cartridges (see Figure 3.9).

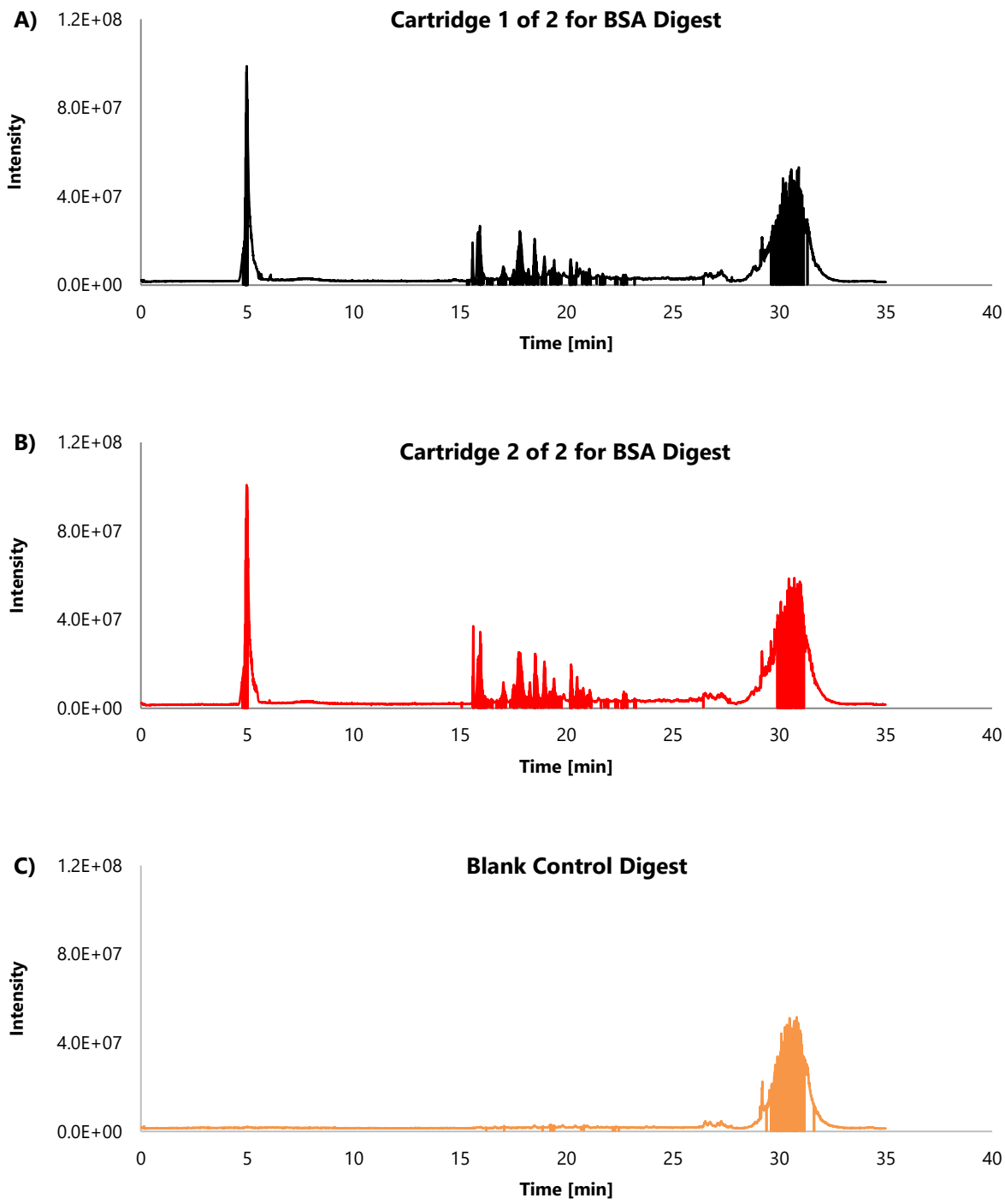

Figure 3.8: A) and B) show TIC of BSA digest using two trypsin cartridges where 15 pmol of BSA was loaded with an incubation time of 10 minutes. Analysis was performed using the LC-OT-MS and the resulting injected peptides from 375 fmol of digested protein. C) TIC of a blank trypsin cartridge digest where running buffer was used.

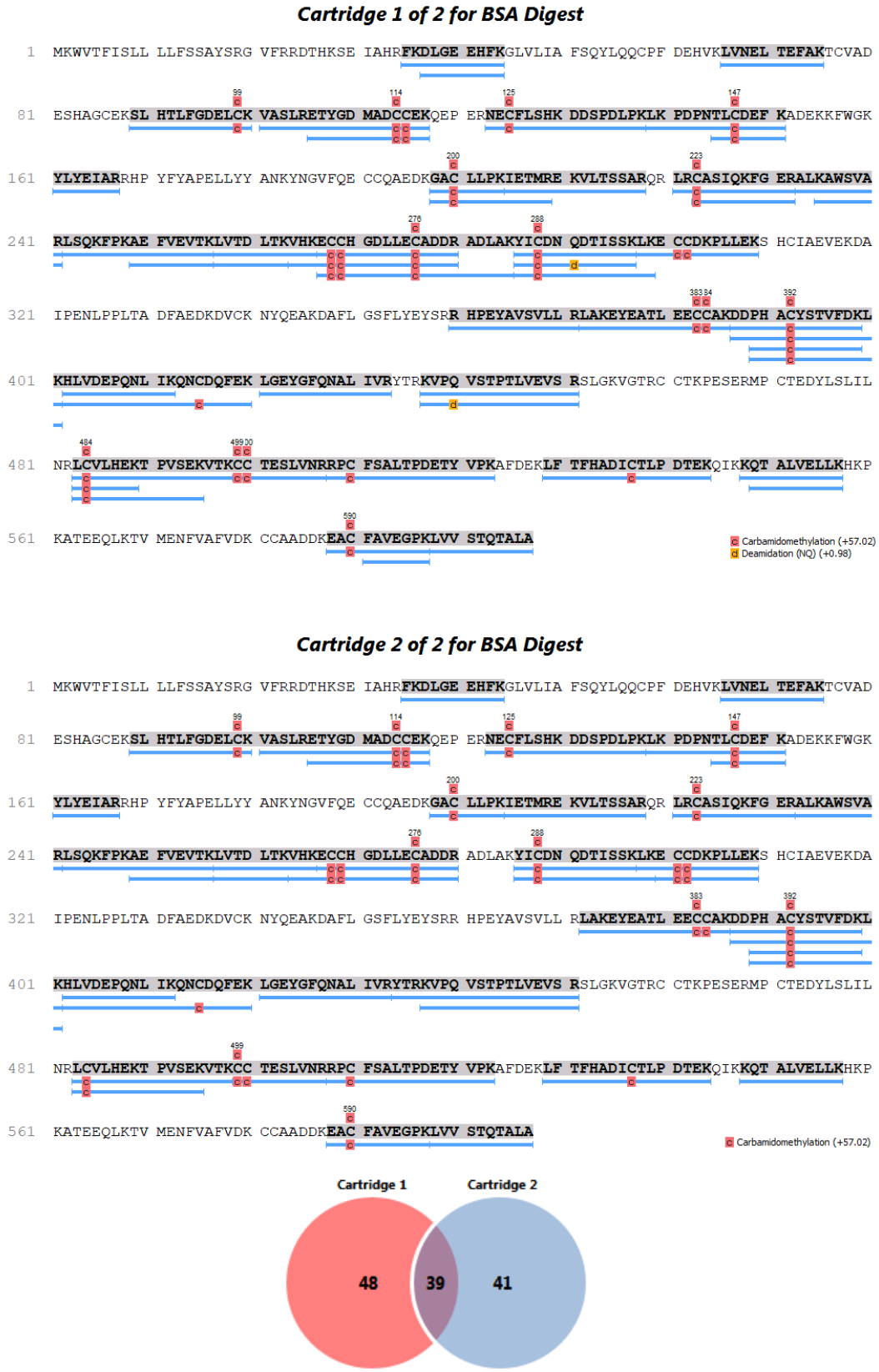

Figure 3.9: Two BSA cartridge digests (top being 61% sequence coverage and bottom 59%), showing high overlap of protein sequence coverage.

Furthermore, trypsin cartridge digestion reproducibility was evaluated with BAEE substrate by preparing a calibration curve to calculate the concentration of BAEE remaining after a 2-minute incubation digest with six trypsin cartridges. Using the HPLC-UV, the concentration of BAEE for six samples averaged 513.4 ± 26.8 mol/L with a good % RSD of 5.22% indicating reproducible digestion.

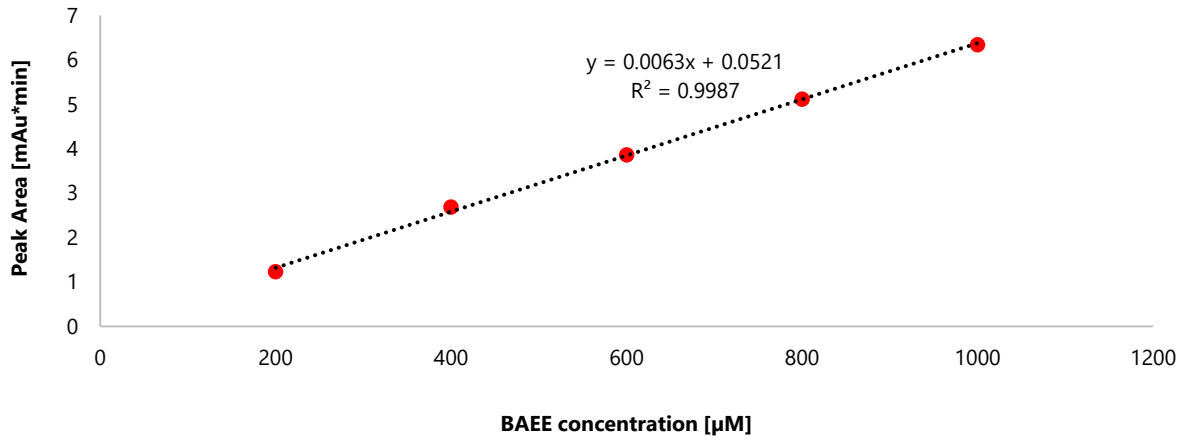

Figure 3.10: Standard calibration curve constructed for BAEE after analysis with HPLC-UV.

Table 3.5: Calculated BAEE concentration following a 2-minute incubation with six trypsin cartridges.

Cartridge	BAEE concentration [µM]
BAEE digest 1	490.1
BAEE digest 2	527.6
BAEE digest 3	478.6
BAEE digest 4	518.1
BAEE digest 5	511.1
BAEE digest 6	554.0
Average	513.4 ± 26.8
% RSD	5.22

Application to protein standards BSA, Cyt c and Tg, human serum sample, and comparison with conventional digest method

The capability of the IMER to digest and identify proteins by their peptide fragmentation fingerprint and comparison with conventional in-solution digests was evaluated by digestion of three common disparate proteins (BSA 66kDa, Cyt c 12kDa and Tg 660kDa). The IMER digestion was compared to the conventional 18-hour in-solution at 37°C digestion method [341], and all samples analysed by LC-OT-MS prior to sequence coverage determinations using PEAKS Studio X against the against either the human or bovine proteome and the common contaminants databases. Overall, sequence coverage for the conventional in-solution digest resulted in a higher coverage for all proteins. For BSA, 54% sequence coverage was obtained for the in-solution compared to 41% for the *in-situ* cartridge digest for BSA (see Table 3.6). Whilst there were 35 unique peptides for BSA that were common across both methods, the in-solution digest resulted in great sequence coverage as 49 unique peptides identified in the in-solution digest were absent in the cartridge digestion (see Figure 3.11). Whilst there were 49 more peptides observed, many of these were overlapping peptides as these 49 unique peptides resulted in only a further 13% of the sequence coverage being identified compared to the cartridge digest (see Figure 3.12 highlighted in red). Overall, the in-solution method identified more peptides and performed better than the cartridge digestion for BSA, however the cartridge digest allowed rapid digestion compared to the in-solution method from 18 hours, down to ~10 minutes.

This result was also seen for the other two proteins where the IMER performance for Cyt c digestion was similar but slightly lower compared to in-solution digestion with protein sequence coverages of 80% and 87%, respectively, and for Tg, the IMER had a lower sequence coverage (3%) than in-solution digestion (10%). Whilst both Cyt c and Tg were digested without protein reduction and alkylation to observe the performance of the IMER, low sequence coverages were observed for both Tg digests as without reduction of disulfide bonds and alkylation of sulfhydryl groups, peptides involved in the disulfide bonds are difficult to identify during database searching [351]. Cyt c on the other hand being a smaller and less complex protein was sufficiently digested by the µSPE method. Furthermore, most if not all the unique peptides observed in the cartridge digests for Cyt c and Tg were observed in the

overnight digested, showing that the conventional method performed better (see Figure 3.11, Figure 3.13 and Figure 3.14).

Finally, the digestion of the human serum samples (n=3) was performed. Human serum sample was reduced and alkylated prior to the tryptic digestion and the number of digested proteins obtained by IMER digestion was compared to the in-solution digestion which resulted in 375 ± 65 and 425 ± 54 protein identifications respectively. These results show that the µSPE method required protein alkylation and reduction to achieve efficient digestion and protein/sequence identification. Overall, µSPE method sequence coverages for neat protein standards and protein identification in human serum sample were inferior to the conventional in-solution digests. Whilst the µSPE method results show promise as a proof-of concept, further investigations and optimisations through future research is required as these results show the potential for µSPE digests to improve on the digestion time required in comparison to conventional overnight digestion.

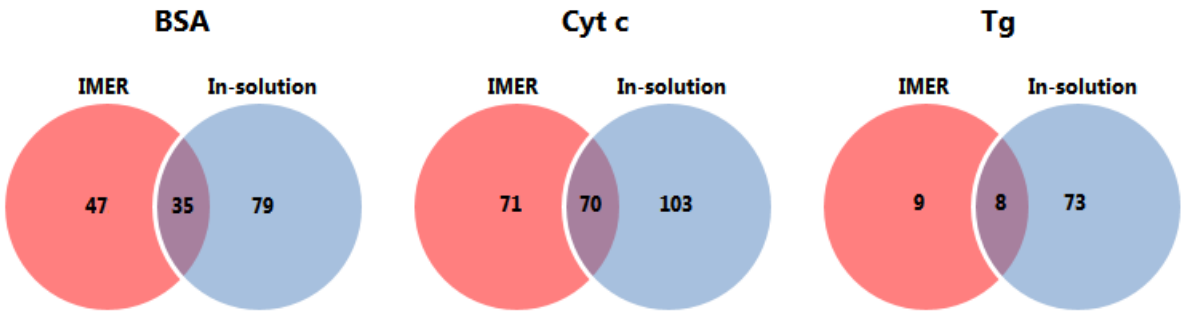

Figure 3.11: Number of identified peptides using IMER and in-solution digests for BSA, Cyt c and Tg, and the number of peptides observed across both methods.

Table 3.6: BSA sequence coverages for µSPE cartridge digest and BSA MS overnight in-solution digest.

	µSPE-IMER digestion (room temperature, 10 minutes)		**In-solution digestion (37°C, 18 hours)**	
Protein	Sequence coverage [%]	Number of identified peptides	Sequence coverage [%]	Number of identified peptides
BSA (66 kDa)	41	47	54	84
Cyt c (12 kDa)	80	71	87	103
Tg (660 kDa)	3	9	10	73
Sample	Proteins groups identified		Protein groups identified	
Human serum sample	375 ± 65		425 ± 54	

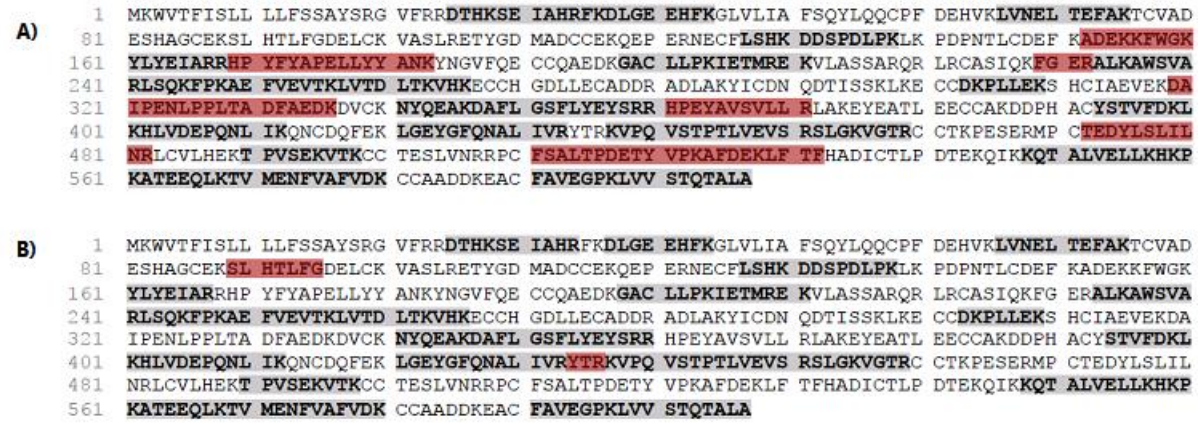

Figure 3.12: Protein sequence coverage for the A) overnight and B) cartridge digest of BSA, highlighting the amino acids that were unique to each respective sequence coverage and not observed in the other.

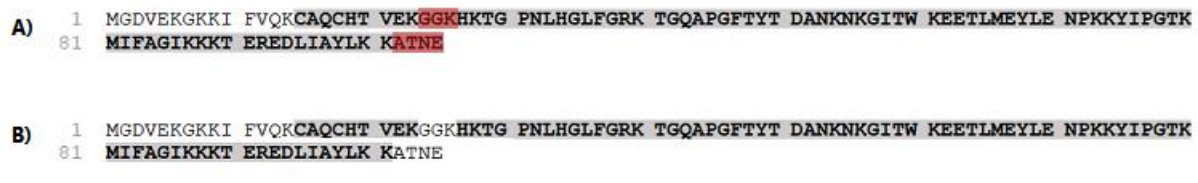

Figure 3.13: Protein sequence coverage for the A) overnight and B) cartridge digest of Cyt c, highlighting the amino acids that were unique to each respective sequence coverage and not observed in the other.

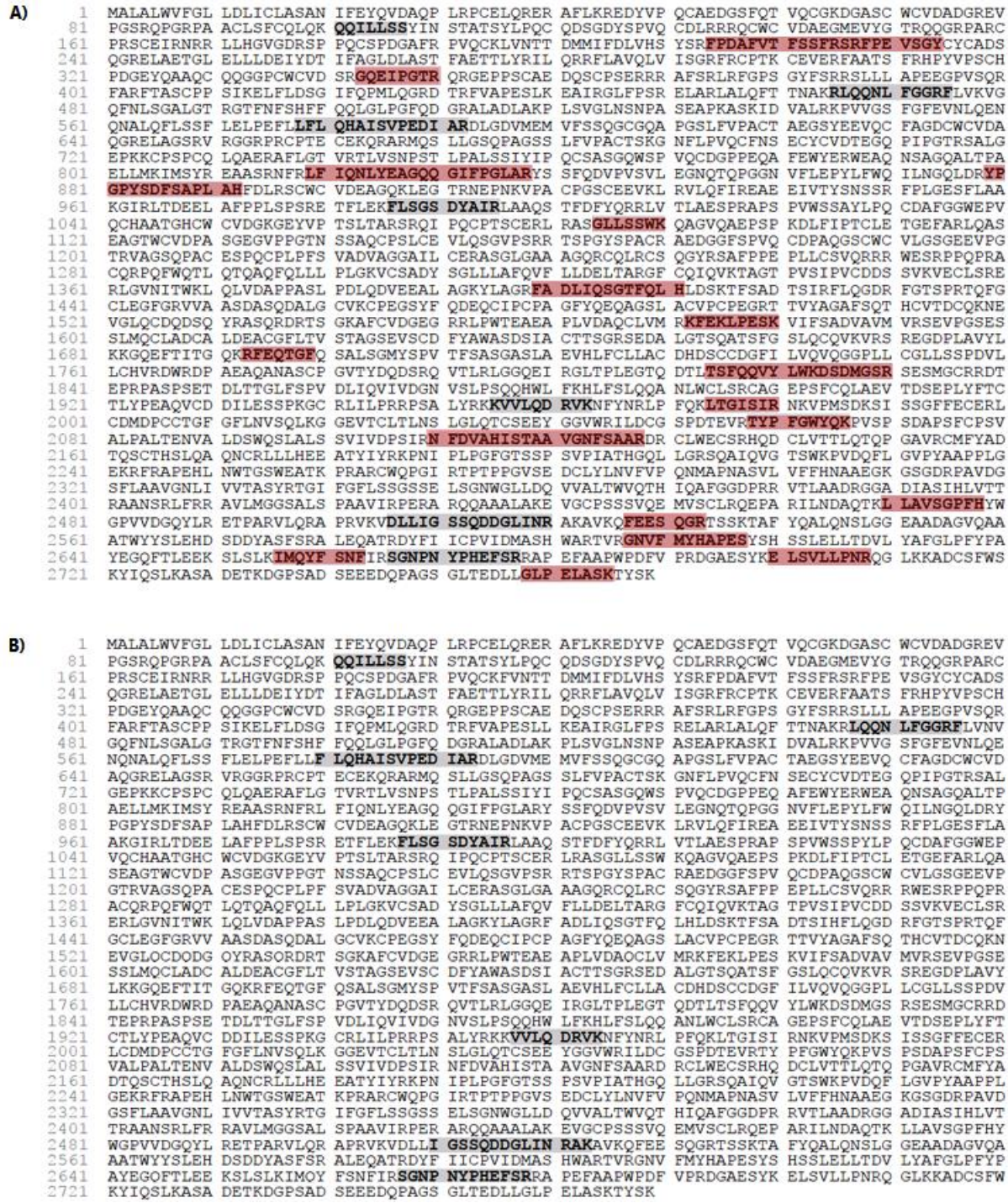

Figure 3.14: Protein sequence coverage for the A) overnight and B) cartridge digest of Tg, highlighting the amino acids that were unique to each respective sequence coverage and not observed in the other.

3.4 Development of the immunoaffinity µSPE cartridge

To develop an immunoaffinity extraction cartridge, anti-BSA and BSA were chosen as the model Ab-Ag. Size exclusion chromatography inductively coupled plasma tandem mass spectrometry (SEC-ICP-MS/MS) was used to monitor and analyse the immunoaffinity cartridge development and extraction. To obtain species information, SEC was used to separate the proteins in order of decreasing MW. Furthermore, exogenous protein tagging with lanthanides were used to label BSA for enhanced ICP-MS detection.

3.4.1 Instrumentation and parameters for immunoaffinity µSPE cartridge

To monitor the antibody immobilisation method and immunoaffinity cartridge protein isolation, an Agilent 8900 Triple Quadrupole ICP-MS instrument (Agilent Technologies, Santa Clara, CA, USA) operating in MS/MS mode was used with instrument parameters listed in Table 3.7. Oxygen was used as the reaction gas for the collision cell (ultra-high purity, BOC, North Ryde, NSW, Australia), and the tune parameters for mass-shifting ^{32}S and ^{34}S were optimised with a 100 ng/mL sulphur standard. The ICP-MS/MS instrument was operated with MassHunter software (Agilent Technologies).

Table 3.7: Typical operating conditions for the 8900 ICP-MS/MS.

Plasma		**Lens**		**Cell**	
RF power [W]	1550	**Extract 1 [V]**	4	**OctP bias [V]**	-4
Sampling depth [mm]	7.0	**Extract 2 [V]**	-230	**Axial acceleration [V]**	0.2
Nebuliser gas (Ar) flow rate [L/min]	1.10	**Omega [V]**	10.8	**Cell gas**	O_2
Make up gas (Ar) flow rate [L/min]	0.10	**Omega bias [V]**	-120	**Cell gas flow rate [%]**	10

The ICP-MS/MS was hyphenated to a liquid chromatography system, and the separations were carried out on an Agilent 1290 Infinity II LC (Agilent Technologies, Santa Clara, CA, USA). Two size exclusion columns were used, an Agilent Bio SEC-3 Column 4.6 mm x 300 mm, 3 µm, 150 Å (Agilent Technologies, Mulgrave, VIC, Australia) and a Waters ACQUITY UPLC Protein BEH SEC

Column 2.1 mm x 150 mm, 1.7 µm, 200 Å (Waters, Milford, MA, USA). All analyses were performed on the Agilent Bio SEC-3 column except for one instance where the secondary column was employed due to the Agilent Bio SEC-3 column being used on another project. An ammonium acetate buffer (0.1 M, pH 6.8) was used as mobile phase and the flow rate was optimised to 0.5 mL/min for the Agilent column and 0.15 mL/min for the Waters column. The injection volume was set to 5 µL. The LC system was directly coupled to the ICP-MS/MS using PEEK Tubing, red, 1/16″ outside diameter (OD) × 0.005″ inside diameter (ID) (1.59 × 0.13 mm) with the shortest connection possible to minimise dead volume.

To determine the MW of protein and antibody samples, a SEC MW calibration was performed with a protein standard containing thyroglobulin (660 kDa), globulin (150 kDa), albumin (66.5 kDa), superoxide dismutase (32.5 kDa) and ribonuclease A (13.7 kDa). The retention times were plotted against the $\log_{10}$[MW] with a linear regression fit applied.

A Thermo Scientific™ NanoDrop 2000 spectrophotometer was used as a quick approach to estimate protein concentration. The sample was aliquoted onto the pedestal (4 µL) and the *A280* mode was used with appropriate sample type whereby the unknown (sample) protein concentrations are calculated using the mass extinction coefficient. For example, *BSA* sample type has a mass extinction coefficient of 6.7 at 280 nm for a 1% (10 mg/mL) BSA solution, and *IgG* analysis with a mass extinction coefficient of 13.7 at 280 nm for a 1% IgG solution [352].

3.4.2 Exogenous labelling of proteins

To increase sensitivity of ICP-MS/MS analysis of proteins, Maxpar™ labelling kit (Fluidigm; formerly DVS Sciences, San Francisco, CA) was used to label BSA with isotopically enriched erbium (^{166}Er). Maxpar™ reagent is a proprietary polymer based elemental tag which uses lanthanide group elements chelated in 1,4,7,10-Tetraazacyclododecane-1,4,7,10-tetraacetic acid (DOTA) groups. Rather than labelling antibodies which the kit was developed for (see Figure 3.15), BSA was labelled according to the manufacturer's instructions [95]. A 0.5 M solution of TCEP was prepared fresh in water and used to reduce disulfide bonds in BSA to allow maleimide linkage to the polymer, and thus lanthanide labelling. In accordance with the protocol, the starting concentration of BSA protein was 1 mg/mL in a sample volume of 100 µL. The final concentration of the labelled BSA-Er was calculated by measuring the absorbance at

280 nm using the NanoDrop spectrophotometer with the *BSA* sample type option and was stored at 2-8°C until required where the final volume of sample was also 100 µL.

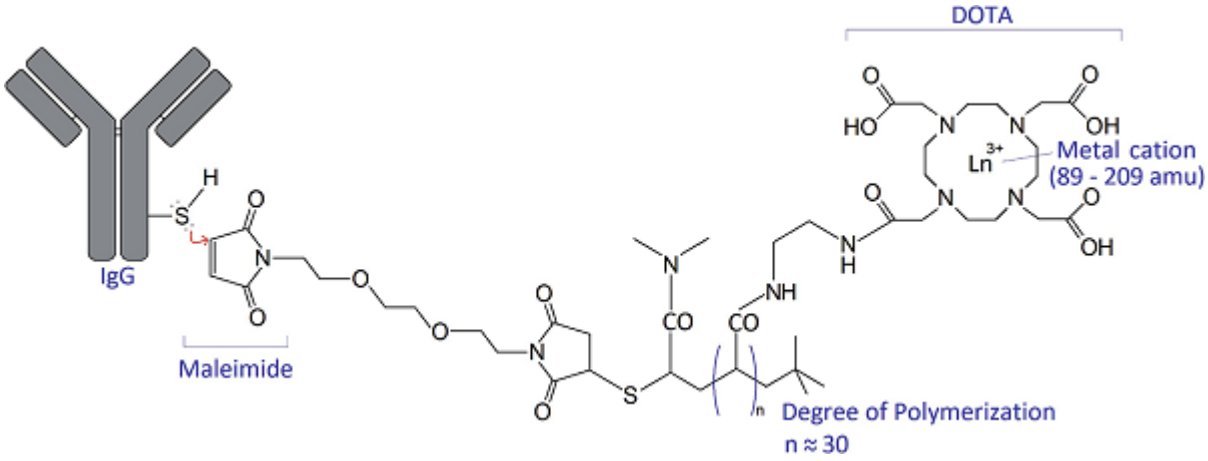

Figure 3.15: Example of Maxpar™ labelling through maleimide linkages on desired biomolecule containing free -SH groups [353].

3.4.3 Antibody immobilisation and Ab-Ag complex formation

To ensure covalent immobilisation of the antibody onto silica-CMD, a colorimetric visualisation using HRP which catalyses the reaction of ABTS in the presence of hydrogen peroxide was performed. Approximately 10 mg of loose silica-CMD was added to an Eppendorf tube followed by 200 µL of 10 mM MES buffer, 10 ug of anti-BSA, 1 mg of NHS and 2 mg of EDC and allowed to react for 1 hour. The material was washed with 500 µL of PBS buffer by a vortex, spun down with a microcentrifuge, and the solution decanted off. This was performed 5 times with PBS (10X) followed by 5 times with PBS (1X). 20 µL of mouse IgG HRP polymer was then incubated with the material for 30 minutes for binding to anti-BSA (raised in mouse) (see Figure 3.16 A). The material was then washed with 10 times with 500 µL of PBS (1X) to remove excess mouse IgG HRP polymer before adding 200 µL of ABTS liquid substrate for visualisation.

Likewise, colorimetric visualisation using HRP was used to ensure Ab-Ag complex binding. This was performed using two methods. First, BSA was covalently bound to silica-CMD material, incubated with anti-BSA, mouse IgG HRP polymer, and visualised using the ABTS substrate (see Figure 3.16 B). In a second experiment, SEC-ICP-MS/MS was performed to confirm the Ab-Ag complex formation. 10 µL of 1 mg/mL anti-BSA was added to 10 µL of 0.45 mg/mL BSA, incubated at room temperature for 2 hours and analysed.

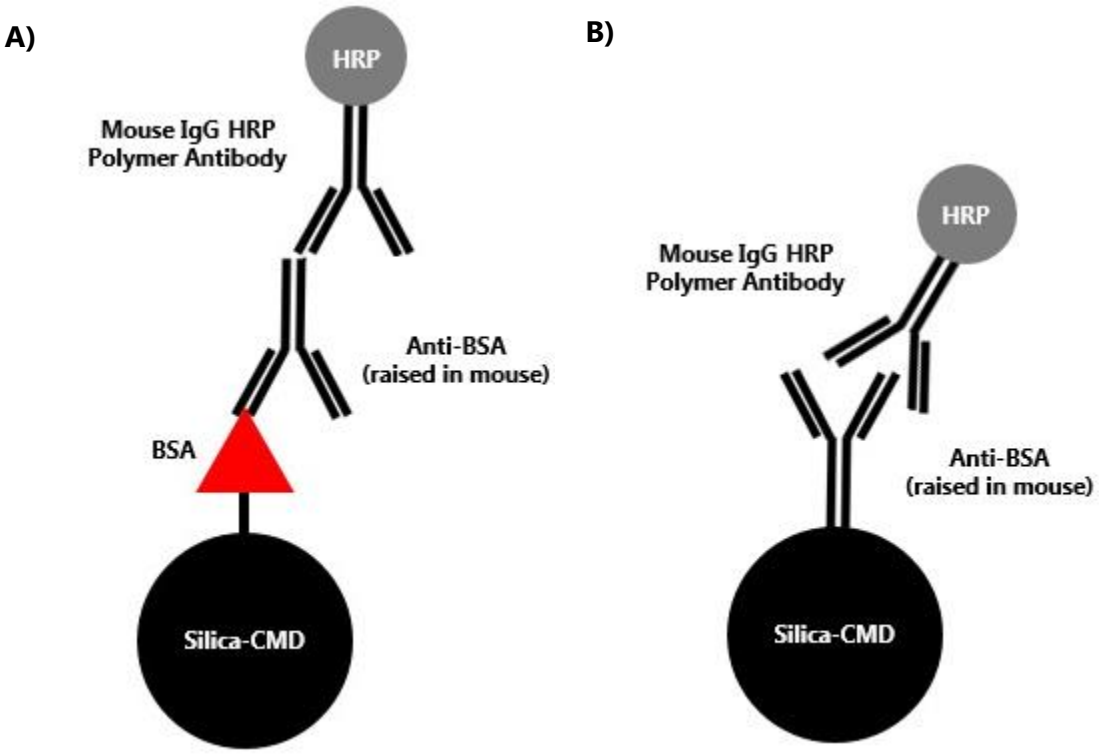

Figure 3.16: A) Covalent immobilisation of anti-BSA onto silica-CMD and visualisation with mouse IgG HRP polymer antibody and B) covalent immobilisation of BSA onto silica-CMD for complex formation with anti-BSA, and visualisation with mouse IgG HRP polymer antibody.

3.4.4 Results and Discussion

In the same way trypsin was immobilised, antibody immobilisation to the silica-CMD support material was also performed. Antibodies were immobilised using EDC/NHS coupling, a salt wash buffer was used to remove non-covalently bound antibody, and a running buffer was used to condition the cartridge before immunoaffinity capture was performed. To develop an immunoaffinity extraction µSPE cartridge, anti-BSA and BSA were chosen as the model Ab-Ag. Covalent antibody immobilisation, Ab-Ag complex formation, exogenous lanthanide tagging and immunoaffinity capture of BSA were analysed using colorimetric visualisation and SEC-ICP-MS/MS.

Confirmation of covalent immobilisation and Ab-Ag complex formation

Anti-BSA and BSA protein were used to develop the immunoaffinity extraction µSPE cartridge. To ensure covalent immobilisation of the antibody onto silica-CMD material and Ab-Ag formation, a colorimetric visualisation using HRP and ABTS substrate was performed following the scheme described in Figure 3.16 A and Figure 3.16 B respectively. A turquoise colour was observed for the covalently bound anti-BSA indicating successful immobilisation to the silica CMD material (see Figure 3.17 A). Similarly, the Ab-Ag formation was assessed by covalently immobilised BSA onto the support material. This resulted in a turquoise colour solution demonstrating the successful formation of the anti-BSA and BSA complex (see Figure 3.17 C). For both experiments control analyses were carried out where no colour change was observed (see Figure 3.17 B and Figure 3.17 D).

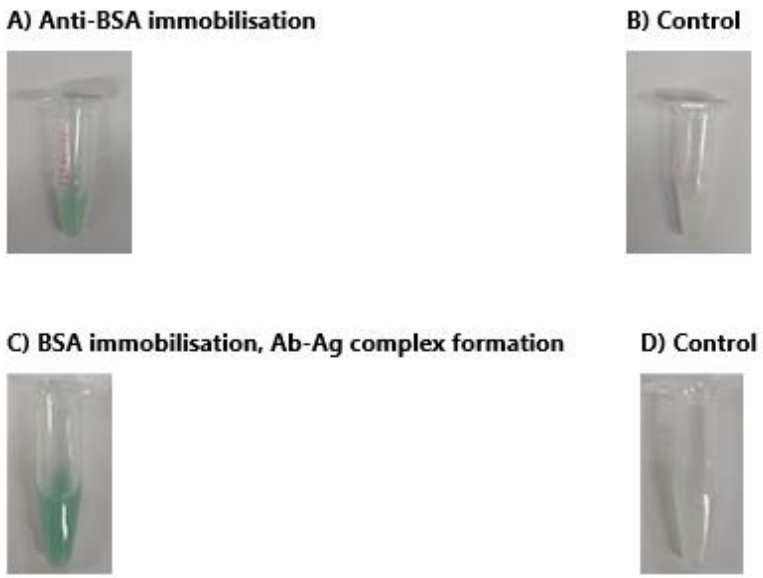

Figure 3.17: Visualisation of HRP activity with mouse IgG HRP polymer and ABTS substrate for the confirmation of A) covalent immobilisation of anti-BSA onto silica-CMD as well as the B) BSA immobilisation followed by complex formation betweeen anti-BSA and BSA, and C) and D) as their respectivblank controls where no covalent immobilisation was performed using EDC/NHS.

SEC-ICP-MS/MS was used to confirm the Ab-Ag complex formation between anti-BSA and BSA. The protein ladder analysed by the Agilent Bio SEC-3 column was plotted (see Table 3.8 and Figure 3.18) to calculate the size of anti-BSA and BSA in Figure 3.19. Tg showed poor resolution due to the column exclusion limits of the 150 Å column range (500-150,000 Da) and was therefore removed from the calibration and the other five proteins were used to construct a protein ladder calibration curve. Anti-BSA sample and BSA sample were observed to elute at 275 seconds and 285 seconds respectively (see Figure 3.19). For the Ab-Ag complex where anti-BSA and BSA were incubated together at a concentration ratio of 2:1 respectively, an earlier retention time was observed at 240 seconds with a shouldering peak at 275 seconds. Using the protein ladder for MW calculation, a MW of 132 kDa was calculated for the BSA sample (as well as the presence of BSA dimer at 252 seconds, 216 kDa) [354], 159 kDa was calculated for the anti-BSA only sample, and 300 kDa was calculated for the anti-BSA and BSA complex. For the anti-BSA–BSA complex sample, the earlier peak at 240 seconds (300 kDa) was a result of an increase in molecular size indicating successful complex formation between the Ab-Ag whilst the shouldering peak at 270 seconds corresponded to the excess unbound antibody (159 kDa) that did not complex with BSA. However, whilst the calculated 159 kDa for

anti-BSA aligned with the expected weight of ~150 kDa for IgG antibodies [355], the calculated MW for BSA at 132 kDa did not align with the expected ~66 kDa [356]. As seen in the sample chromatogram, wide peaks (~40-60 seconds in width) for the antibody and BSA samples were observed, and thus impacted the MW determination. Therefore, improved chromatography resolution with sharper peaks would ensure accurate determination. Regardless, this technique allowed the confirmation of Ab-Ag complex formation between anti-BSA and BSA.

Table 3.8: SEC calibration for the protein ladder standard used to calculate sample.

Protein	**MW [kDa]**	**Elution Time [sec]**	**$\log_{10}$[MW]**
Globulin	150	283	2.18
Albumin	66.5	318	1.82
Superoxide dismutase	32.5	367	1.51
Ribonuclease A	13.7	411	1.11

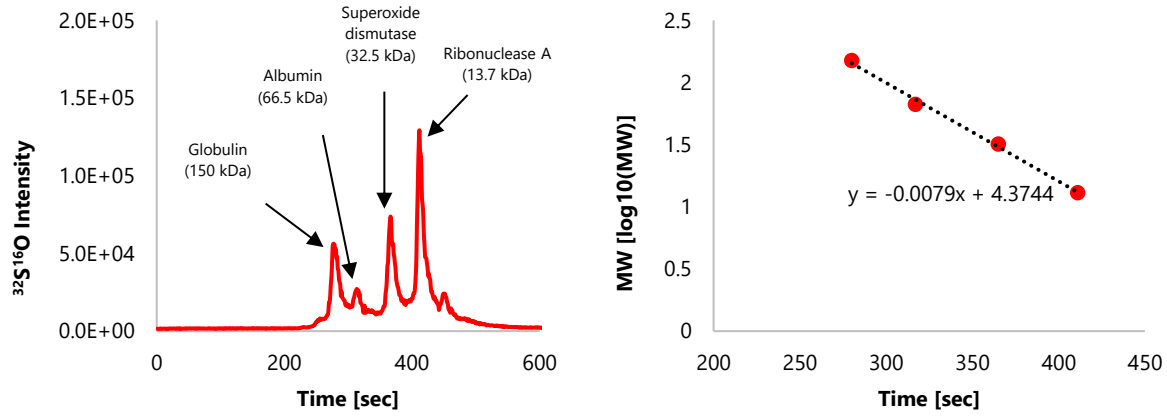

Figure 3.18: Protein ladder calibration used to calculate MW of the biomolecule using the retention time using the Agilent Bio SEC-3 column.

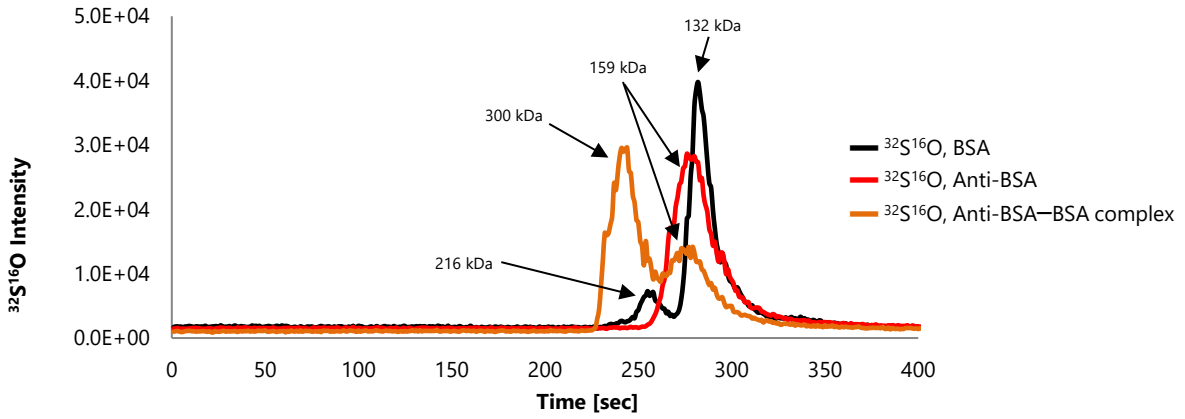

Figure 3.19: SEC-ICP-MS/MS analysis using the Agilent Bio SEC-3 column for BSA (black), anti-BSA (red), and Ab-Ag complex (orange) with corresponding MW calculations using the protein ladder calibration.

Evaluation of using unlabelled BSA and labelled BSA for ICP-MS/MS analysis

BSA was labelled with Maxpar™ polymer containing ^{166}Er to improve protein ICP-MS detection. Following labelling, the concentration of the labelled BSA-Er was estimated to be 0.225 mg/mL by measuring the absorbance at 280 nm using a spectrophotometer resulting in a loss of 77.5% from the starting protein concentration of 1 mg/mL. The labelling process was confirmed by SEC-ICP-MS/MS where BSA and labelled BSA-Er were analysed. Eluting at 260 seconds (using Waters ACQUITY UPLC Protein BEH SEC), unlabelled BSA was observed at *m/z* 48 (^{32}S^{16}O), and labelled BSA showed a peak at 190 seconds (*m/z* 166, ^{166}Er) which indicated successfully BSA labelling with the Maxpar™ polymer as an earlier elution compared to native BSA was observed because of increased MW. Additionally, shouldering peak starting at 260 seconds corresponding to unconjugated polymer (see Figure 3.20).

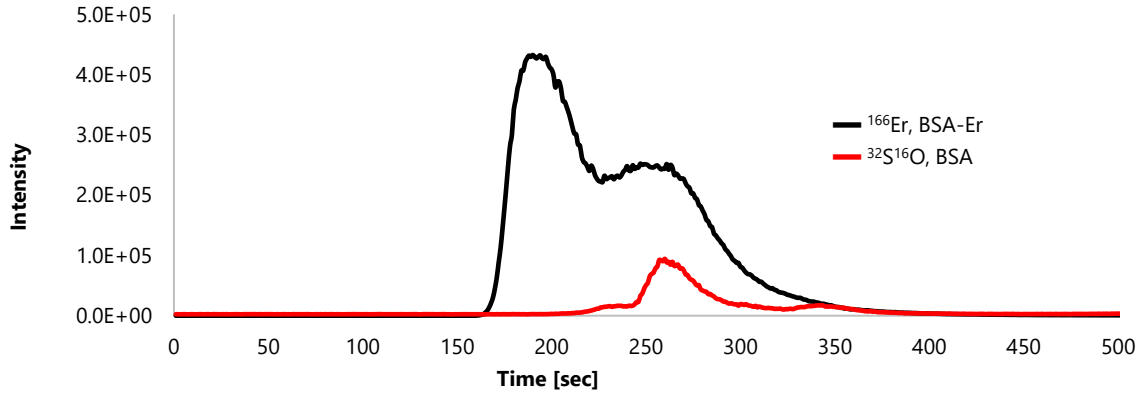

Figure 3.20: Chromatographic separation of BSA (S signal, red) and labelled BSA-Er (Er signal, black) by SEC-ICP-MS/MS analysis using the Waters ACQUITY UPLC Protein BEH SEC.

As immunoaffinity extraction aims to reduce sample matrix complexity, it is important that unwanted non-specific components are washed from the cartridge after sample loading. Non-specifically bound components may interact with the surface support through several interactions such as Van der Waals forces and electrostatic forces depending on the physiochemical properties. Therefore, a wash buffer must be of a certain composition to disrupt these forces and remove them from the cartridge. As seen in Chapter 2 and the development of the IMER, non-specifically bound protein can be removed using high salt concentration buffers such as PBS (1X) solution. This is because the silica-CMD material exhibits electrostatic forces that can interact with charged amino acid residues found in proteins and antibodies. As a result, a wash solution containing NaCl was investigated where concentrations must be optimised. However, salt solutions containing a high ionic strength can also disrupt the Ab-Ag protein-protein binding interactions [112]. Therefore, the salt wash buffers must have enough ionic strength to remove non-specific binding components whilst mild enough to not disrupt the Ab-Ag interaction.

Whilst lanthanides such as erbium provide improved ICP-MS analysis over sulphur, it was important to ensure that labelled BSA-Er would behave similarly to unlabelled BSA in the silica-CMD cartridge and have no unwanted interactions. Therefore, wash buffer optimisation experiments were performed on both labelled and unlabelled BSA. BSA and labelled BSA-Er were both applied to two separate cartridges and washed with 50 mM Tris 20 mM NaCl pH 8 buffer. Twelve wash aliquots were collected for each cartridge and analysed by flow injection ICP-MS/MS (FI-ICP-MS/MS).

This buffer was sufficient for removing non-specifically bound BSA from the cartridge as after the third washing with 500 µL salt wash buffer, no remaining BSA was observed (see Figure 3.21). On the other hand, the labelled BSA-Er exhibited stronger interactions with the cartridge material and could not be removed from the cartridge with 20 mM NaCl. When the salt concentration was increased to 1 M NaCl to encourage removal, BSA-Er was still observed after three 500 µL washes at this higher concentration (see Figure 3.22). This indicated that BSA-Er did not interact similarly to unlabelled BSA in the silica-CMD cartridge and unwanted interactions were observed between the cartridge and the labelling polymer which could not be removed electrostatically. Furthermore, increased ionic strength buffer concentrations at 1 M NaCl for washing are not ideal as they can disrupt the Ab-Ag interactions [357, 358].

Therefore, labelled BSA-Er was not used for future experiments due to its unwanted interactions with the cartridge, despite its increase in sensitivity obtained by ICP-MS analysis.

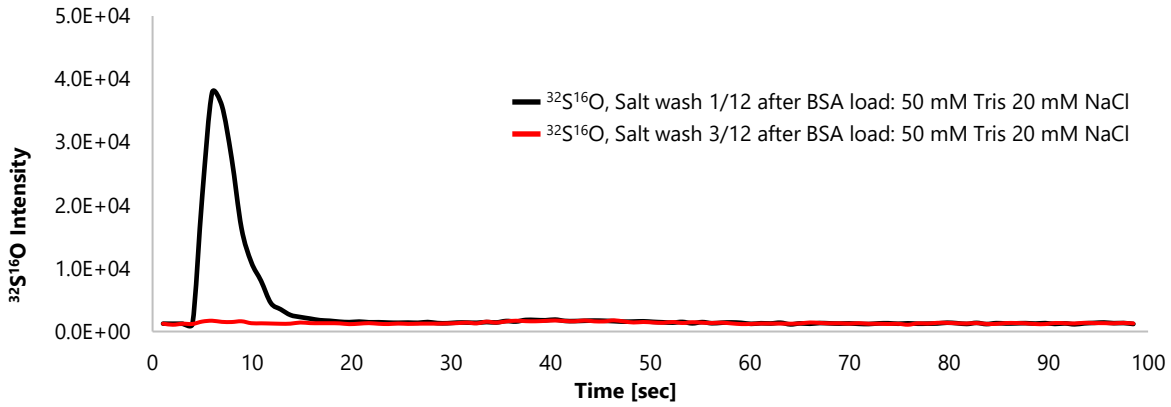

Figure 3.21: Chromatograms obtained form the analysis of salt wash buffer aliquots following BSA sample loading onto an ePrep cartridge and analysed using FI-ICP-MS/MS for detection of $^{32}S^{16}O$.

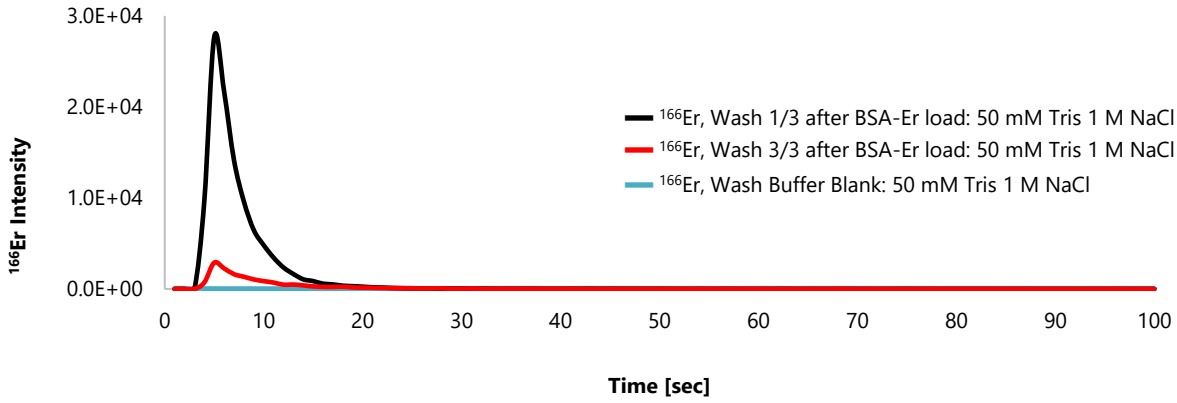

Figure 3.22: Chromatograms obtained from the analysis of salt wash buffer aliquots following BSA-Er sample loading onto an ePrep cartridge and analysed using FI-ICP-MS/MS for detection of ^{166}Er.

Using the anti-BSA immobilised immunoaffinity cartridge for BSA extraction

The immunoaffinity cartridge was used to extract BSA from a 10 ng/µL BSA sample prepared in running buffer following the method in Figure 3.1, Cartridge 1, with aims to determine cartridge extraction capacities using SEC-ICP-MS/MS. Analysis of the eluted fraction at *m/z* 48 ($^{32}S^{16}O$) is shown in Figure 3.23 where the presence of BSA was not observed as the immunoaffinity extracted BSA concentration fell below the LOD of the instrument. Alternatively, to detect the BSA from the eluted fraction, the SEC column was removed from the setup, and flow injection (FI) approach was used to analyse the eluate fraction under the same instrument parameters. Analysis of the eluted fraction by FI-ICP-MS/MS is shown in

Figure 3.24 where the presence of sulphur was observed. However, with the removal of the SEC column, species information is lost and the FI results obtained only show the total elemental content in the sample. Because a total sulphur content with no speciation was obtained using FI analysis, this result is not specific towards BSA. Therefore, an alternative method must be conducted to confirm the BSA in the final eluted fraction is shown in Section 3.5 where immunoaffinity extracted BSA was digested and identified using peptide database search.

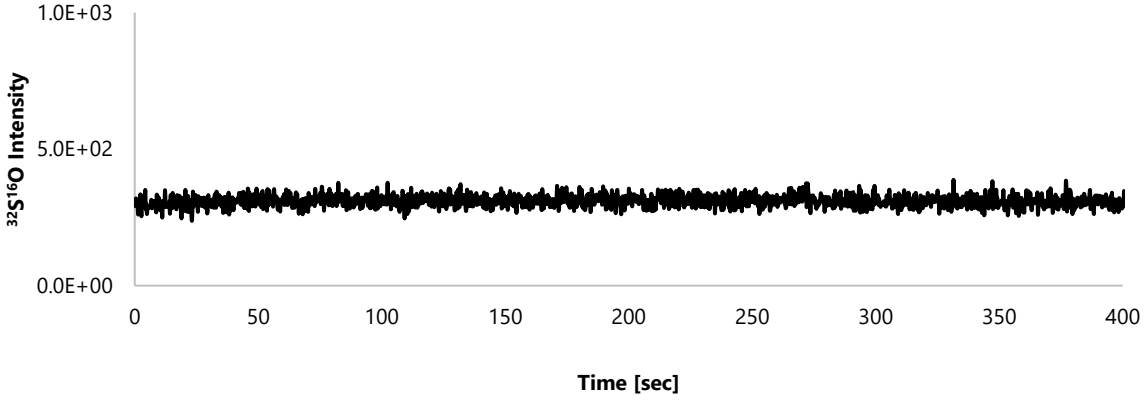

Figure 3.23: Analysis of eluted sample following immunoaffinity extraction of BSA with an anti-BSA ePrep cartridge. Sample was analysed using SEC-ICP-MS/MS for detection of $^{32}S^{16}O$.

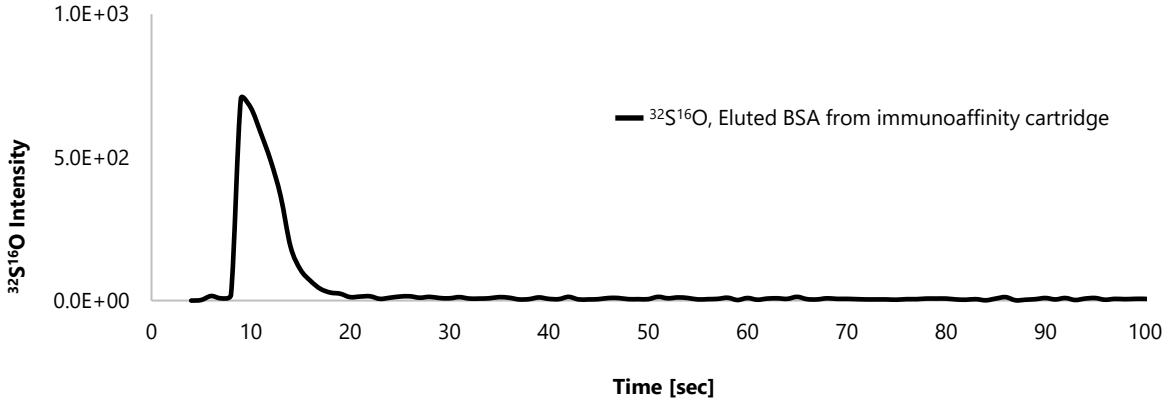

Figure 3.24: Analysis of eluted sample following immunoaffinity extraction of BSA with an anti-BSA ePrep cartridge. Sample was analysed using FI-ICP-MS/MS for detection of $^{32}S^{16}O$.

3.5 Combination of the immunoaffinity and IMER µSPE cartridges for an automated workflow

3.5.1 µSPE workflow

The final µSPE sample workflow developed for protein biomarkers consisted of the combination of the immunoaffinity extraction using antibodies, and IMER protein digestion cartridge (see Figure 3.1). Using the ePrep workstation, the samples, reagents and buffers for both cartridges were placed on the workstation bed and the immunoaffinity extraction and digestion method was setup to run sequentially, thus creating an automated workflow method combining the two cartridges. Additionally, these methods were repeated within the software allowing multiple samples to be prepared. Using BSA as the model protein, BSA standards (20 ng/µL) and BSA spiked into human serum samples (20 ng/µL) were subjected to an immunoaffinity isolation followed immediately by trypsin digestion, and finally analysed by LC-OT-MS.

3.5.2 Results and Discussion

After evaluating the immunoaffinity and trypsin enzymatic reactor cartridges separately, the next approach was to combine the two µSPE methods and run both in sequence to form an automated protein capture and digestion workflow as seen in Figure 3.1. This was performed using 20 ng/µL BSA standard (n=3) and a human serum sample (n=3) where BSA was also the target analyte and the BSA standard spiked into the sample matrix also at 20 ng/µL. For BSA standards, the observed protein sequence coverages for immunoaffinity captured BSA in the BSA standards were 87 ± 1% (n=3) (see Table 3.9, 1st use of the affinity cartridge). Additionally, after immunoaffinity extraction, the cartridge was immediately reconditioned to pH 8 twice with 500 µL of wash buffer to prevent antibody denaturation for further use. The regeneration of the immunosorbent was assessed using the same affinity cartridge twice where BSA protein coverage of 86 ± 8% (n=3) was observed showing the reusability of the cartridge (see Table 3.9, 2nd use of the affinity cartridge). For BSA spiked in human serum samples, protein sequence coverage was 25 ± 1% (n=3) (see Figure 3.25). Whilst the BSA sequence coverage was low in the human serum sample, BSA protein identification in both samples demonstrated the capability of the developed workflows to isolate the protein of interest from a complex matrix

followed by a successful tryptic digestion of the isolated protein. However due to the low sequence coverage obtained in comparison to the BSA standard, the human serum was seen to negatively impact the immunoaffinity isolation which may be due to interfering proteins within the complex biological matrix.

Table 3.9: Obtained BSA protein coverage after immunoaffinity extraction followed by tryptic digestion using three affinity cartridge twice.

IMER	**Protein Coverage [%] (1st use of the affinity cartridge)**	**Protein Coverage [%] (2nd use of the affinity cartridge)**
1	88	86
2	86	96
3	86	81
Average	87 ± 1 (n=3)	86 ± 8 (n=3)

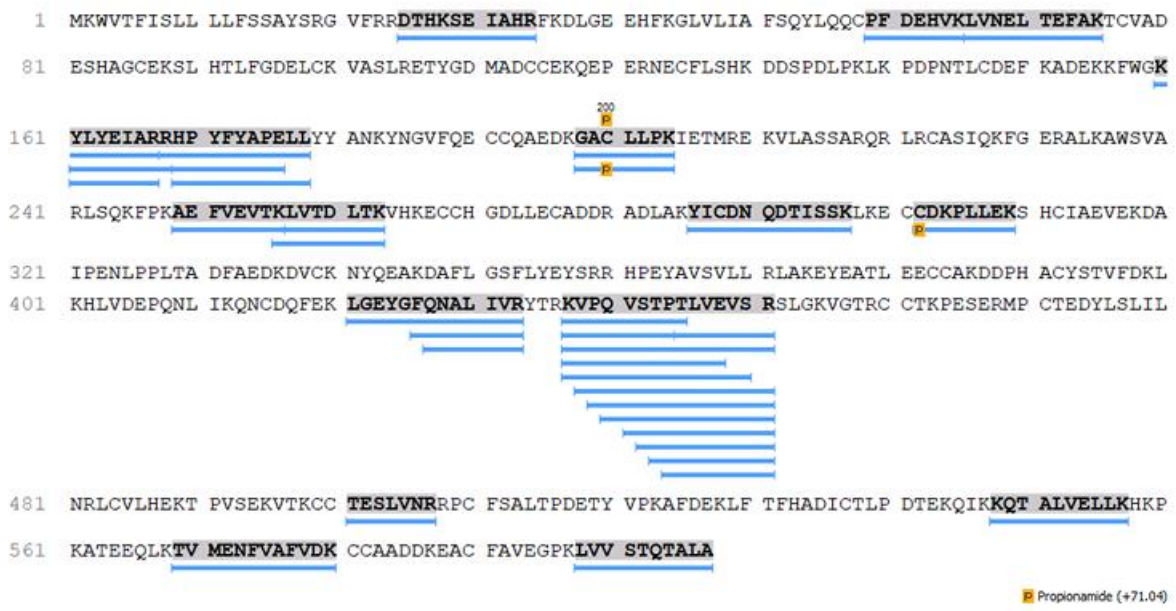

Figure 3.25: BSA protein coverage (26%) obtained by LC-OT-MS of the spiked human sample after protein isolation followed by tryptic digestion.

3.6 Conclusion

This chapter detailed the development of an immunoaffinity extraction μSPE cartridge and an IMER protein digestion μSPE cartridge. Using the silica-CMD support developed in Chapter 2, anti-BSA and trypsin were immobilised *in-situ* using an automated μSPE sample preparation platform. Optimisation of the immobilisation conditions were performed to ensure removal of excess non-specific binding ligands using salt buffers.

An immunoaffinity capture μSPE cartridge was prepared through *in-situ* covalent immobilisation of anti-BSA to the silica-CMD support, and captured BSA was analysed using SEC-ICP-MS/MS. Exogenous tagging of BSA through Maxpar™ polymer containing ^{166}Er to improve protein ICP MS detection was achieved, however due to the undesirable interactions between the polymer and μSPE cartridge, exogenous tagging was not used for final BSA quantification. Furthermore, attempts to quantify the amount of BSA captured by the antibodies were unsuccessful as the protein levels fell below the limit of detection of the SEC-ICP-MS/MS when analysing for $^{32}S^{16}O$ (*m/z* 48). The presence of sulphur in the final eluted BSA sample was detected when FI-ICP-MS/MS was used however, species information was lost. Therefore, in its current form, the binding capacity of the immunoaffinity μSPE cartridges are unknown.

In a similar way, an IMER μSPE cartridge was developed through *in-situ* covalent immobilisation of trypsin to the silica-CMD support. Using the BAEE substrate, the immobilised cartridge was tested for activity, effects of incubation time, digest reproducibility and removal of non-specifically bound trypsin. Good cartridge reproducibility with BAEE was observed at 5% RSD (n=6) and that increased incubation time resulted in more digestion products. The IMER was suitable for rapid protein digestion within 10 minutes at room temperature, with similar digestion performance of BSA and Cyt c to that of an in-solution digestion performed for 18 hours at 37°C. However, for the larger Tg protein, in-solution digestion was more efficient. Digestion of a human serum sample using the trypsin μSPEed cartridge also observed comparable protein hits as that obtained by in-solution digestion. Despite the promising results presented in this work, the developed IMER could be further optimised by adapting temperature, incubation time and/or protein load which will be discussed in the following chapter.

When combining the immunoaffinity and IMER μSPE cartridge into an automated workflow, BSA standard and BSA spiked into human serum samples resulted in reproducible sequence coverages of 87 ± 1% (n=3) and 25 ± 1% (n=3) respectively. However, the complex human serum sample was seen to negatively impact the immunoaffinity isolation and thus IMER digestion results in comparison. Whilst the results are promising, further optimisation and development into the μSPE cartridges must be performed and will be discussed in further detail in the final chapter.

Chapter 4:

Overall Conclusions and Future Work

This Thesis investigated the importance of improved sample preparation for protein biomarker quantification. Currently, quantitative determination is predominantly achieved through immunoassays, however, this technique is subject to limited dynamic range, cross-reactivity and interferences, and difficult to multiplex. As a result, there has been a transition towards the development of MS approaches. Quantification by MS is challenged due to length workflows which are difficult to automate and highly complex biological samples. Therefore, in partnership with ePrep, this work focused on the development of a generic automated sample preparation workflow for the targeted quantification of protein biomarkers using µSPE technology.

Objective 1:

In Chapter 2, sample preparation using customised solid-phase materials was introduced. Customised solid supports allowed choice of ligand binding for selective, fast, and automated sample preparation where biological compounds immobilised to supports allowed specific sample preparation tasks such as catalytic reactions using enzymes, and affinity separations using antibodies. In this chapter, a generic material using silica and CMD was developed with silica providing chemical and mechanical stability for use with the ePrep automated syringe drivers, and CMD providing a biocompatible surface for ligand binding for low non-specific protein interactions. The biological ligand, HRP, was successfully immobilised through covalent linkages and provided a more stable bond with minimal enzyme leakage compared to non-covalent adsorption as enzyme activity remained stable under ionic buffer conditions. Ligand immobilisation through the commonly used carbodiimide chemistry provided a simple one-step linkage. Immobilisation was improved with materials of greater surface area as greater -COOH groups are available for ligand binding as calculated by conductometric titrations, and unwanted ligand adsorption was minimised due to modifications of the surface with CMD which reduced electrostatic interactions. However further investigation into pore size and surface area relationship must be performed. Whilst the 120 Å provided a larger surface area compared to 300 Å and 1000 Å material, and thus increased -COOH concentration due to CMD coating, no results regarding the capability of the pore to sufficiently accommodate larger proteins was explored. Larger batch production (5 g) was possible however batch sizes >50 g must be evaluated for commercialisation.

Objectives 2-4

Using the material developed in Objective 1, Chapter 3 presented the development of an immunoaffinity extraction cartridge, an IMER cartridge, and its combination into a workflow using the ePrep automated sample preparation solutions for rapid protein isolation and digestion. Antibody and enzyme immobilisation to customised µSPE cartridges were explored for selective extraction and protein digestion. Anti-BSA and trypsin were successfully immobilised *in-situ*, and trace levels of protein and digested peptides were isolated and analysed by ICP-MS/MS and LC-OT-MS. The µSPE technology allows for a choice of bio-ligands to be used, increasing user flexibility and simplification of workflows. Although not explored in this thesis with a potential for future work, the *in-situ* immobilisation offers the opportunity for facile preparation of customisable IMERs with enzymes such as pepsin, or affinity sample preparation using antibodies for either depletion of HAPs, or enrichment of peptides.

Objective 2:

As mentioned in the development of the affinity cartridge, attempts to quantify the amount of BSA captured by the antibodies were unsuccessful as the protein levels fell below the limit of detection on the SEC-ICP-MS/MS, thus the cartridge extraction capacity is unknown and must be evaluated. Since biomarkers can be present at trace and even ultra-trace concentrations in biological samples, it is a requirement for an extraction cartridge to specifically retain and pre-concentrate the desired analyte to a level suitable for detection and quantification. Therefore, future experiments include assessing the amount of ligand being immobilised onto the material, antibody binding capacity of the immunoaffinity extraction cartridge, and enzyme kinetics for the IMERs. It was difficult to determine the amount of ligand being immobilised *in-situ*, therefore future approaches could involve pre-immobilising the material with biological ligands before packing, and therefore allowing easier characterisation and determination of the material. Methods such as the bicinchoninic acid (BCA) assay have been successfully used [359]. Pre-packing material would also require the evaluation of the µSPE material packing process to ensure the ligand stability and activity is retained. Additionally, studies on cartridge expiry, stability and storage must be performed for potential commercialisation.

Objective 3:

The IMER µSPE cartridge resulted in rapid digestion where 1 µg of protein and human serum sample were digested in 10 minutes but observed lower sequence coverages and protein identifications compared to the overnight in-solution digests. However, further optimisations to ligand immobilisation approaches, protein loading and incubation times must be explored to improve the performance of the µSPE method. These can include pre-immobilising the enzyme prior to packing, and comparison studies of the developed silica-CMD material to commercially available material that can be packed into the µSPE cartridge. Furthermore, in its current state, the ePrep sample preparation station lacks heating capabilities, therefore future work involves introducing heating elements to allow digestions at 37°C for improved digestion efficiency.

Objective 4:

Finally, the immunoaffinity and IMER cartridge were combined to form an automated workflow method for protein isolation and digestion of model protein BSA. The workflow was successfully applied for BSA extraction followed by digestion. The total workflow time was 45 minutes for one sample, thus showing improvement over conventional methods. The potential for cartridge reusability was briefly shown where regeneration of the immunoaffinity cartridge was achieved, further adding to improving overall workflow times as well as well as cost reduction. Whilst the work shows promise, the complex human serum sample matrix was seen to have a negative effect on BSA isolation compared to a neat BSA standard. Therefore, potential future work includes incorporating a HAP depletion cartridge as well as a peptide immunoaffinity extraction following protein digestion to minimise the effects of the sample matrix. Following this, the workflow must then be applied to a real-life clinical sample to determine usability for targeted protein biomarker quantification.

Overall, this work in partnership with ePrep demonstrated the potential for an automated µSPE platform for protein sample preparation. The customisable material developed in Chapter 2 allowed covalent immobilisation of three different biological ligands, HRP, trypsin and anti-BSA. Using simple crosslinking reagents such as EDC/NHS, there is potential to immobilise a wide range of bio-ligands for targeted sample preparation. Whilst this work showed promise for protein capture, immobilisation and digestion, further work needs to be performed to

establish it as a possible method used for clinical samples. In clinical settings where high volume of samples is observed, the use of an automated system allows for reproducible sample preparation which is crucial for protein biomarker quantification where several preparation processes and steps are performed. If developed, and validated, automated sample preparation methods can assist in routine analysis by minimising human intervention, increase sample throughput and provide patient safety.

References

1. Burckart, G.J. and D.J. Green, *Chapter 7 - Regulatory Aspects of Pediatric Biomarkers for Assessing Medication Response*, in *Personalizing Asthma Management for the Clinician*, S.J. Szefler, F. Holguin, and M.E. Wechsler, Editors. 2018, Elsevier. p. 69-86.

2. Khan, T.K., *Chapter 1 - Introduction to Alzheimer's Disease Biomarkers*, in *Biomarkers in Alzheimer's Disease*, T.K. Khan, Editor. 2016, Academic Press. p. 3-23.

3. Gromiha, M.M., *Chapter 1 - Proteins*, in *Protein Bioinformatics*, M.M. Gromiha, Editor. 2010, Academic Press: Singapore. p. 1-27.

4. Pollock, V., *Proteins*, in *xPharm: The Comprehensive Pharmacology Reference*, S.J. Enna and D.B. Bylund, Editors. 2007, Elsevier: New York. p. 1-11.

5. Fung, K.Y.C., et al., *Blood-Based Protein Biomarker Panel for the Detection of Colorectal Cancer.* PLOS ONE, 2015. 10(3): p. e0120425.

6. Lomnytska, M., et al., *Platelet protein biomarker panel for ovarian cancer diagnosis.* Biomarker Research, 2018. 6: p. 2.

7. Molina-Romero, C., E. Vergara, and O. Arrieta, *A novel biomarker protein panel for lung cancer, a promising first step.* Translational Lung Cancer Research, 2018. 7(Suppl 4): p. S304-S307.

8. Halbgebauer, S., et al., *Protein biomarkers in Parkinson's disease: Focus on cerebrospinal fluid markers and synaptic proteins.* Movement Disorders, 2016. 31(6): p. 848-860.

9. Gozes, I., *Specific protein biomarker patterns for Alzheimer's disease: improved diagnostics in progress.* EPMA Journal, 2017. 8(3): p. 255-259.

10. Hathout, Y., et al., *Large-scale serum protein biomarker discovery in Duchenne muscular dystrophy.* Proceedings of the National Academy of Sciences of the United States of America, 2015. 112(23): p. 7153-7158.

11. Wollert, K.C., T. Kempf, and L. Wallentin, *Growth Differentiation Factor 15 as a Biomarker in Cardiovascular Disease.* Clinical Chemistry, 2017. 63(1): p. 140-151.

12. Messina, R., et al., *Serum surfactant protein D is a potential biomarker of lung damage in systemic sclerosis.* European Respiratory Journal, 2016. 48(suppl 60): p. PA4888.

13. McMahon, B.A. and P.T. Murray, *Urinary liver fatty acid-binding protein: another novel biomarker of acute kidney injury.* Kidney International, 2010. 77(8): p. 657-659.

14. Schiess, R., B. Wollscheid, and R. Aebersold, *Targeted proteomic strategy for clinical biomarker discovery.* Molecular Oncology, 2009. 3(1): p. 33-44.

15. Drabovich, A.P., E. Martínez-Morillo, and E.P. Diamandis, *Toward an integrated pipeline for protein biomarker development.* Biochimica et Biophysica Acta (BBA) - Proteins and Proteomics, 2015. 1854(6): p. 677-686.

16. Makawita, S. and E.P. Diamandis, *The Bottleneck in the Cancer Biomarker Pipeline and Protein Quantification through Mass Spectrometry-Based Approaches: Current Strategies for Candidate Verification.* Clinical Chemistry, 2010. 56(2): p. 212-22.

17. Füzéry, A.K., et al., *Translation of proteomic biomarkers into FDA approved cancer diagnostics: issues and challenges.* Clinical Proteomics, 2013. 10(1): p. 13.

18. Anderson, N.L., *The clinical plasma proteome: a survey of clinical assays for proteins in plasma and serum.* Clinical Chemistry, 2010. 56(2): p. 177-185.

19. Selleck, M.J., M. Senthil, and N.R. Wall, *Making Meaningful Clinical Use of Biomarkers.* Biomarker Insights, 2017. 12.

20. Steffen, P., et al., *Protein species as diagnostic markers.* Journal of Proteomics, 2016. 134: p. 5-18.

21. Frantzi, M., A. Bhat, and A. Latosinska, *Clinical proteomic biomarkers: relevant issues on study design & technical considerations in biomarker development.* Clinical and Translational Medicine, 2014. 3(1): p. 7-7.

22. Hottenstein, C., et al., *Platforms and techniques used for biomarker assays: where are we now?* Bioanalysis, 2017. 9(14): p. 1029-1031.

23. Bults, P., N.C. van de Merbel, and R. Bischoff, *Quantification of biopharmaceuticals and biomarkers in complex biological matrices: a comparison of liquid chromatography coupled to tandem mass spectrometry and ligand binding assays.* Expert Review of Proteomics, 2015. 12(4): p. 355-374.

24. Aydin, S., *A short history, principles, and types of ELISA, and our laboratory experience with peptide/protein analyses using ELISA.* Peptides, 2015. 72: p. 4-15.

25. Kato, K., et al., *Use of Rabbit Antibody IgG Bound onto Plain and Aminoalkylsilyl Glass Surface for the Enzyme-Linked Sandwich Immunoassay.* The Journal of Biochemistry, 1977. 82(1): p. 261-266.

26. Lindstöm, P. and O. Wager, *IgG Autoantibody to Human Serum Albumin Studied by the ELISA-Technique.* Scandinavian Journal of Immunology, 1978. 7(5): p. 419-425.

27. Yorde, D.E., et al., *Competitive enzyme-liked immunoassay with use of soluble enzyme/antibody immune complexes for labeling. I. Measurement of human choriogonadotropin.* Clinical Chemistry, 1976. 22(8): p. 1372-1377.

28. Seitz, H. and S. Schumacher, *Biomarkers: From Discovery to Commercialization*, in *Biomarker Validation: Technological, Clinical and Commercial Aspects*. 2015, John Wiley & Sons, Incorporated: Somerset, Germany.

29. Van Gool, A., et al., *Analytical techniques for multiplex analysis of protein biomarkers.* Expert Review of Proteomics, 2020. 17(4): p. 257-273.

30. Hoofnagle, A.N. and M.H. Wener, *The fundamental flaws of immunoassays and potential solutions using tandem mass spectrometry.* Journal of Immunological Methods, 2009. 347(1): p. 3-11.

31. Wang, P., J.R. Whiteaker, and A.G. Paulovich, *The evolving role of mass spectrometry in cancer biomarker discovery.* Cancer Biology & Therapy, 2009. 8(12): p. 1083-1094.

32. Haab, B.B., et al., *A Reagent Resource to Identify Proteins and Peptides of Interest for the Cancer Community: A WORKSHOP REPORT*.* Molecular & Cellular Proteomics, 2006. 5(10): p. 1996-2007.

33. Li, H., et al., *General LC-MS/MS Method Approach to Quantify Therapeutic Monoclonal Antibodies Using a Common Whole Antibody Internal Standard with Application to Preclinical Studies.* Analytical Chemistry, 2012. 84(3): p. 1267-1273.

34. Maunsell, Z., D.J. Wright, and S.J. Rainbow, *Routine isotope-dilution liquid chromatography-tandem mass spectrometry assay for simultaneous measurement of the 25-hydroxy metabolites of vitamins D2 and D3.* Clin Chem, 2005. 51(9): p. 1683-90.

35. Rashed, M.S., et al., *Diagnosis of inborn errors of metabolism from blood spots by acylcarnitines and amino acids profiling using automated electrospray tandem mass spectrometry.* Pediatric Research, 1995. 38(3): p. 324-331.

36. Ombrone, D., et al., *Expanded newborn screening by mass spectrometry: New tests, future perspectives.* Mass Spectrometry Reviews, 2016. 35(1): p. 71-84.

37. Banerjee, S., *Empowering Clinical Diagnostics with Mass Spectrometry.* ACS Omega, 2020. 5(5): p. 2041-2048.

38. Kiyonami, R., et al., *Increased Selectivity, Analytical Precision, and Throughput in Targeted Proteomics.* Molecular & Cellular Proteomics, 2011. 10(2): p. M110.002931.

39. Büyükköroğlu, G., et al., *Chapter 15 - Techniques for Protein Analysis*, in *Omics Technologies and Bio-Engineering*, D. Barh and V. Azevedo, Editors. 2018, Academic Press. p. 317-351.

40. Twyman, R.M., *MASS SPECTROMETRY | Multidimensional*, in *Encyclopedia of Analytical Science (Second Edition)*, P. Worsfold, A. Townshend, and C. Poole, Editors. 2005, Elsevier: Oxford. p. 430-438.

41. Pan, S., et al., *Application of Targeted Quantitative Proteomics Analysis in Human Cerebrospinal Fluid Using a Liquid Chromatography Matrix-Assisted Laser Desorption/Ionization Time-of-Flight Tandem Mass Spectrometer (LC MALDI TOF/TOF) Platform*. Journal of Proteome Research, 2008. 7(2): p. 720-730.

42. Lin, S., T.A. Shaler, and C.H. Becker, *Quantification of Intermediate-Abundance Proteins in Serum by Multiple Reaction Monitoring Mass Spectrometry in a Single-Quadrupole Ion Trap*. Analytical Chemistry, 2006. 78(16): p. 5762-5767.

43. Brun, V., et al., *Isotope-labeled Protein Standards*. Toward Absolute Quantitative Proteomics, 2007. 6(12): p. 2139-2149.

44. Anderson, N.L., et al., *Mass Spectrometric Quantitation of Peptides and Proteins Using Stable Isotope Standards and Capture by Anti-Peptide Antibodies (SISCAPA)*. Journal of Proteome Research, 2004. 3(2): p. 235-244.

45. Selevsek, N., et al., *Systematic quantification of peptides/proteins in urine using selected reaction monitoring*. Proteomics, 2011. 11(6): p. 1135-1147.

46. Hüttenhain, R., et al., *Reproducible Quantification of Cancer-Associated Proteins in Body Fluids Using Targeted Proteomics*. Science Translational Medicine, 2012. 4(142): p. 142ra94-142ra94.

47. Toth, C.A., et al., *On-column trypsin digestion coupled with LC-MS/MS for quantification of apolipoproteins*. Journal of Proteomics, 2017. 150: p. 258-267.

48. Hoofnagle, A.N., et al., *Multiple-reaction monitoring-mass spectrometric assays can accurately measure the relative protein abundance in complex mixtures*. Clinical Chemistry, 2012. 58(4): p. 777-781.

49. Chen, Y.-T., et al., *Multiplexed quantification of 63 proteins in human urine by multiple reaction monitoring-based mass spectrometry for discovery of potential bladder cancer biomarkers*. Journal of Proteomics, 2012. 75(12): p. 3529-3545.

50. Peterson, A.C., et al., *Parallel Reaction Monitoring for High Resolution and High Mass Accuracy Quantitative, Targeted Proteomics*. Molecular & Cellular Proteomics, 2012. 11(11): p. 1475-1488.

51. Gallien, S., et al., *Targeted Proteomic Quantification on Quadrupole-Orbitrap Mass Spectrometer*. Molecular & Cellular Proteomics, 2012. 11(12): p. 1709-1723.

52. Schilling, B., et al., *Multiplexed, Scheduled, High-Resolution Parallel Reaction Monitoring on a Full Scan QqTOF Instrument with Integrated Data-Dependent and Targeted Mass Spectrometric Workflows*. Analytical Chemistry, 2015. 87(20): p. 10222-10229.

53. Thomas, S.N., et al., *Multiplexed Targeted Mass Spectrometry-Based Assays for the Quantification of N-Linked Glycosite-Containing Peptides in Serum.* Analytical Chemistry, 2015. 87(21): p. 10830-10838.

54. Kim, H.-J., et al., *Quantitative profiling of protein tyrosine kinases in human cancer cell lines by multiplexed parallel reaction monitoring assays.* Molecular & Cellular Proteomics, 2015: p. mcp.O115.051813.

55. Tsuchiya, H., K. Tanaka, and Y. Saeki, *The parallel reaction monitoring method contributes to a highly sensitive polyubiquitin chain quantification.* Biochemical and Biophysical Research Communications, 2013. 436(2): p. 223-229.

56. Michalski, A., et al., *Mass Spectrometry-based Proteomics Using Q Exactive, a High-performance Benchtop Quadrupole Orbitrap Mass Spectrometer.* Molecular & Cellular Proteomics, 2011. 10(9): p. M111.011015.

57. Rauniyar, N., *Parallel Reaction Monitoring: A Targeted Experiment Performed Using High Resolution and High Mass Accuracy Mass Spectrometry.* International Journal of Molecular Sciences, 2015. 16(12): p. 28566-28581.

58. Kitteringham, N.R., et al., *Multiple reaction monitoring for quantitative biomarker analysis in proteomics and metabolomics.* Journal of Chromatography B, 2009. 877(13): p. 1229-1239.

59. Wei, R., G. Li, and A.B. Seymour, *High-Throughput and Multiplexed LC/MS/MRM Method for Targeted Metabolomics.* Analytical Chemistry, 2010. 82(13): p. 5527-5533.

60. Vallverdú-Queralt, A., et al., *Straightforward Method To Quantify GSH, GSSG, GRP, and Hydroxycinnamic Acids in Wines by UPLC-MRM-MS.* Journal of Agricultural and Food Chemistry, 2015. 63(1): p. 142-149.

61. Zakett, D., R.G.A. Flynn, and R.G. Cooks, *Chlorine isotope effects in mass spectrometry by multiple reaction monitoring.* The Journal of Physical Chemistry, 1978. 82(22): p. 2359-2362.

62. Whiteaker, J.R., et al., *A targeted proteomics–based pipeline for verification of biomarkers in plasma.* Nature Biotechnology, 2011. 29: p. 625.

63. Hoofnagle, A.N., et al., *Multiple-Reaction Monitoring–Mass Spectrometric Assays Can Accurately Measure the Relative Protein Abundance in Complex Mixtures.* Clinical Chemistry, 2012. 58(4): p. 777-781.

64. Pitt, J.J., *Principles and applications of liquid chromatography-mass spectrometry in clinical biochemistry.* The Clinical biochemist. Reviews, 2009. 30(1): p. 19-34.

65. Kuzyk, M.A., et al., *Development of MRM-based assays for the absolute quantitation of plasma proteins.* Methods in molecular biology (Clifton, N.J.), 2013. 1023: p. 53-82.

66. Fu, Q., et al., *An Empirical Approach to Signature Peptide Choice for Selected Reaction Monitoring: Quantification of Uromodulin in Urine.* Clinical Chemistry, 2016. 62(1): p. 198-207.

67. Zhou, W., S. Yang, and P.G. Wang, *Matrix effects and application of matrix effect factor.* Bioanalysis, 2017. 9(23): p. 1839-1844.

68. Calderón-Celis, F., J.R. Encinar, and A. Sanz-Medel, *Standardization approaches in absolute quantitative proteomics with mass spectrometry.* Mass Spectrometry Reviews, 2018. 37(6): p. 715-737.

69. Larraga-Urdaz, A.L., et al., *Signal amplification strategies for clinical biomarker quantification using elemental mass spectrometry.* Analytical and Bioanalytical Chemistry, 2021.

70. Thomas, S.N., *Chapter 10 - Mass spectrometry*, in *Contemporary Practice in Clinical Chemistry (Fourth Edition)*, W. Clarke and M.A. Marzinke, Editors. 2019, Academic Press. p. 171-185.

71. Cid-Barrio, L., et al., *Assessment of the Potential and Limitations of Elemental Mass Spectrometry in Life Sciences for Absolute Quantification of Biomolecules Using Generic Standards.* Analytical Chemistry, 2020. 92(19): p. 13500-13508.

72. Calderón-Celis, F., et al., *Elemental Mass Spectrometry for Absolute Intact Protein Quantification without Protein-Specific Standards: Application to Snake Venomics.* Analytical Chemistry, 2016. 88(19): p. 9699-9706.

73. Calderón-Celis, F., et al., *Enhanced Universal Quantification of Biomolecules Using Element MS and Generic Standards: Application to Intact Protein and Phosphoprotein Determination.* Analytical Chemistry, 2019. 91(1): p. 1105-1112.

74. Yan, X., et al., *Absolute quantification of intact proteins via 1,4,7,10-tetraazacyclododecane-1,4,7-trisacetic acid-10-maleimidoethylacetamide-europium labeling and HPLC coupled with species-unspecific isotope dilution ICPMS.* Anal Chem, 2010. 82(4): p. 1261-9.

75. Hann, S., K. Boeck, and G. Koellensperger, *Immunoaffinity assisted LC-ICP-MS—a versatile tool in biomedical research.* Journal of Analytical Atomic Spectrometry, 2010. 25(1): p. 18-20.

76. Striegel, A., et al., *Modern Size-Exclusion Liquid Chromatography : Practice of Gel Permeation and Gel Filtration Chromatography*. 2009, Hoboken, UNITED STATES: John Wiley & Sons, Incorporated.

77. Aires-Barros, M.R. and A.M. Azevedo, *7 - Fundamentals of Biological Separation Processes*, in *Current Developments in Biotechnology and Bioengineering*, A. Pandey and J.A.C. Teixeira, Editors. 2017, Elsevier. p. 187-237.

78. Liu, F., et al., *Simultaneous determination of nitrated and oligomerized proteins by size exclusion high-performance liquid chromatography coupled to photodiode array detection.* Journal of Chromatography A, 2017. 1495: p. 76-82.

79. Campanella, B. and E. Bramanti, *Detection of proteins by hyphenated techniques with endogenous metal tags and metal chemical labelling.* Analyst, 2014. 139(17): p. 4124-4153.

80. Fernández, L.L., et al., *Initial studies on quantitative DNA induced oxidation by gel electrophoresis (GE)-ICP-MS.* Journal of Analytical Atomic Spectrometry, 2011. 26(1): p. 195-200.

81. Lothian, A. and B.R. Roberts, *Standards for Quantitative Metalloproteomic Analysis Using Size Exclusion ICP-MS.* Journal of visualized experiments : JoVE, 2016(110): p. 53737.

82. Pröfrock, D. and A. Prange, *Inductively Coupled Plasma–Mass Spectrometry (ICP-MS) for Quantitative Analysis in Environmental and Life Sciences: A Review of Challenges, Solutions, and Trends.* Applied Spectroscopy, 2012. 66(8): p. 843-868.

83. Cid-Barrio, L., et al., *Advances in absolute protein quantification and quantitative protein mapping using ICP-MS.* TrAC Trends in Analytical Chemistry, 2018. 104: p. 148-159.

84. Sanz-Medel, A., et al., *Elemental mass spectrometry for quantitative proteomics.* Analytical and Bioanalytical Chemistry, 2008. 390(1): p. 3-16.

85. Jarvis, K.E., A.L. Gray, and R.S. Houk, *Handbook of Inductively Coupled Plasma Mass Spectrometry*. 2003: Viridian Publishing.

86. Wang, M., et al., *ICP-MS-Based strategies for protein quantification.* Mass Spectrometry Reviews, 2010. 29(2): p. 326-348.

87. Møller, L.H., et al., *Quantification of pharmaceutical peptides in human plasma by LC-ICP-MS sulfur detection.* Journal of Analytical Atomic Spectrometry, 2016. 31(9): p. 1877-1884.

88. Sanz-Medel, A., "*Heteroatom-tagged*" *quantification of proteins via ICP-MS*. 2016. p. 5393-5395.

89. McCurdy, E., N. Yamada, and N. Sugiyama, *'Agilent's New 8800 Triple Quadrupole ICP-MS: Hardware and Technology Introduction''.* Agilent ICP-MS Journal, 2012. 49: p. 2-3.

90. Balcaen, L., et al., *Inductively coupled plasma – Tandem mass spectrometry (ICP-MS/MS): A powerful and universal tool for the interference-free determination of (ultra)trace elements – A tutorial review.* Analytica Chimica Acta, 2015. 894: p. 7-19.

91. Fernández, S.D., et al., *Triple Quad ICPMS (ICPQQQ) as a New Tool for Absolute Quantitative Proteomics and Phosphoproteomics.* Analytical Chemistry, 2012. 84(14): p. 5851-5857.

92. Lee, H.-S., et al., *Sulfur-based absolute quantification of proteins using isotope dilution inductively coupled plasma mass spectrometry.* Metrologia, 2015. 52(5): p. 619-627.

93. Tholey, A. and D. Schaumlöffel, *Metal labeling for quantitative protein and proteome analysis using inductively-coupled plasma mass spectrometry*. TrAC Trends in Analytical Chemistry, 2010. 29(5): p. 399-408.

94. Jakubowski, N., et al., *Labelling of proteins with 2-(4-isothiocyanatobenzyl)-1,4,7,10-tetraazacyclododecane-1,4,7,10-tetraacetic acid and lanthanides and detection by ICP-MS*. Journal of Analytical Atomic Spectrometry, 2008. 23(11): p. 1497-1507.

95. Fluidigm, *Maxpar Antibody Labeling Kit*. 2018.

96. Bishop, D.P., et al., *Applications of liquid chromatography-inductively coupled plasma-mass spectrometry in the biosciences: A tutorial review and recent developments*. TrAC Trends in Analytical Chemistry, 2018. 104: p. 11-21.

97. Lou, X., et al., *Polymer-Based Elemental Tags for Sensitive Bioassays*. Angewandte Chemie International Edition, 2007. 46(32): p. 6111-6114.

98. Clases, D., et al., *SEC-ICP-MS and on-line isotope dilution analysis for characterisation and quantification of immunochemical assays*. Analytical and Bioanalytical Chemistry, 2019. 411(16): p. 3553-3560.

99. Anderson, N.L., et al., *Mass spectrometric quantitation of peptides and proteins using Stable Isotope Standards and Capture by Anti-Peptide Antibodies (SISCAPA)*. J Proteome Res, 2004. 3(2): p. 235-44.

100. Bylda, C., et al., *Recent advances in sample preparation techniques to overcome difficulties encountered during quantitative analysis of small molecules from biofluids using LC-MS/MS*. Analyst, 2014. 139(10): p. 2265-2276.

101. Shen, S., B. An, and J. Qu, *Sample Preparation Methods for Targeted Biomarker Quantification by LC-MS*, in *Targeted Biomarker Quantitation by LC–MS*. 2017. p. 79-106.

102. Veenstra, T.D., *Proteomic Applications in Cancer Detection and Discovery*. 2013, Somerset, USA: John Wiley & Sons, Incorporated.

103. Borg, J., et al., *Spectral counting assessment of protein dynamic range in cerebrospinal fluid following depletion with plasma-designed immunoaffinity columns*. Clinical Proteomics, 2011. 8(1): p. 6-6.

104. Issaq, H.J., Z. Xiao, and T.D. Veenstra, *Serum and Plasma Proteomics*. Chemical Reviews, 2007. 107(8): p. 3601-3620.

105. Jones, K., *Affinity Separation*, in *Encyclopedia of Separation Science*, I.D. Wilson, Editor. 2000, Academic Press: Oxford. p. 3-17.

106. Hage, D.S., *Affinity Separations*, in *Reference Module in Chemistry, Molecular Sciences and Chemical Engineering*. 2015, Elsevier.

107. Aryal, U.K., A.R.S. Ross, and J.E. Krochko, *Enrichment and Analysis of Intact Phosphoproteins in Arabidopsis Seedlings.* PLOS ONE, 2015. 10(7): p. e0130763.

108. Reichelt, S., et al., *Amino-functionalized monolithic spin-type columns for high-throughput lectin affinity chromatography of glycoproteins.* Analyst, 2012. 137(11): p. 2600-2607.

109. Kijewska, M., et al., *An Optimised Di-Boronate-ChemMatrix Affinity Chromatography to Trap Deoxyfructosylated Peptides as Biomarkers of Glycation.* Molecules (Basel, Switzerland), 2020. 25(3): p. 755.

110. Donmez, M., H.A. Oktem, and M.D. Yilmaz, *Ratiometric fluorescence detection of an anthrax biomarker with Eu3+-chelated chitosan biopolymers.* Carbohydrate Polymers, 2018. 180: p. 226-230.

111. Zhao, C., et al., *Epitope mapping and targeted quantitation of the cardiac biomarker troponin by SID-MRM mass spectrometry.* Proteomics, 2014. 14(11): p. 1311-1321.

112. Ayyar, B.V., et al., *Affinity chromatography as a tool for antibody purification.* Methods, 2012. 56(2): p. 116-129.

113. Moser, A.C. and D.S. Hage, *Immunoaffinity chromatography: an introduction to applications and recent developments.* Bioanalysis, 2010. 2(4): p. 769-790.

114. Fung, E.N., P. Bryan, and A. Kozhich, *Techniques for quantitative LC–MS/MS analysis of protein therapeutics: advances in enzyme digestion and immunocapture.* Bioanalysis, 2016. 8(8): p. 847-856.

115. Adkins, J.N., et al., *Toward a Human Blood Serum Proteome.* Molecular & Cellular Proteomics, 2002. 1(12): p. 947.

116. Chromy, B.A., et al., *Proteomic Analysis of Human Serum by Two-Dimensional Differential Gel Electrophoresis after Depletion of High-Abundant Proteins.* Journal of Proteome Research, 2004. 3(6): p. 1120-1127.

117. El Rassi, Z. and C. Puangpila, *Liquid-phase based separation systems for depletion, prefractionation, and enrichment of proteins in biological fluids and matrices for in-depth proteomics analysis—An update covering the period 2014–2016.* Electrophoresis, 2017. 38(1): p. 150-161.

118. Ly, L. and V.C. Wasinger, *Protein and peptide fractionation, enrichment and depletion: Tools for the complex proteome.* Proteomics, 2011. 11(4): p. 513-534.

119. Lund, H., et al., *Immuno–MS Based Targeted Proteomics: Highly Specific, Sensitive, and Reproducible Human Chorionic Gonadotropin Determination for Clinical Diagnostics and Doping Analysis.* Analytical Chemistry, 2012. 84(18): p. 7926-7932.

120. Anderson, N.L., et al., *SISCAPA peptide enrichment on magnetic beads using an in-line bead trap device.* Molecular & cellular proteomics : MCP, 2009. 8(5): p. 995-1005.

121. Vidova, V. and Z. Spacil, *A review on mass spectrometry-based quantitative proteomics: Targeted and data independent acquisition.* Analytica Chimica Acta, 2017. 964: p. 7-23.

122. Dittrich, J., et al., *Sample preparation strategies for targeted proteomics via proteotypic peptides in human blood using liquid chromatography tandem mass spectrometry.* Proteomics – Clinical Applications, 2015. 9(1-2): p. 5-16.

123. Hustoft, H.K., et al., *Critical assessment of accelerating trypsination methods.* Journal of Pharmaceutical and Biomedical Analysis, 2011. 56(5): p. 1069-1078.

124. Vandermarliere, E., M. Mueller, and L. Martens, *Getting intimate with trypsin, the leading protease in proteomics.* Mass Spectrometry Reviews, 2013. 32(6): p. 453-465.

125. Oyler, J.M., B.Q. Tran, and D.P.A. Kilgour, *Rapid Denaturing Organic Digestion Method for Targeted Protein Identification and Characterization.* Analytical Chemistry, 2021. 93(12): p. 5046-5053.

126. Capelo, J.L., et al., *Overview on modern approaches to speed up protein identification workflows relying on enzymatic cleavage and mass spectrometry-based techniques.* Analytica Chimica Acta, 2009. 650(2): p. 151-159.

127. Hustoft, H., et al., *A Critical Review of Trypsin Digestion for LC-MS Based Proteomics*. 2012.

128. Havliš, J., et al., *Fast-Response Proteomics by Accelerated In-Gel Digestion of Proteins.* Analytical Chemistry, 2003. 75(6): p. 1300-1306.

129. López-Ferrer, D., J.L. Capelo, and J. Vázquez, *Ultra Fast Trypsin Digestion of Proteins by High Intensity Focused Ultrasound.* Journal of Proteome Research, 2005. 4(5): p. 1569-1574.

130. Wang, S., et al., *Infrared-Assisted On-Plate Proteolysis for MALDI-TOF-MS Peptide Mapping.* Analytical Chemistry, 2008. 80(14): p. 5640-5647.

131. Pramanik, B.N., et al., *Microwave-enhanced enzyme reaction for protein mapping by mass spectrometry: a new approach to protein digestion in minutes.* Protein science : a publication of the Protein Society, 2002. 11(11): p. 2676-2687.

132. Naldi, M., et al., *Towards automation in protein digestion: Development of a monolithic trypsin immobilized reactor for highly efficient on-line digestion and analysis.* Talanta, 2017. 167: p. 143-157.

133. Wassenaar, T.M., *Enzymes*, in *Bacteria: The Benign, the Bad, and the Beautiful*. 2011, Wiley-Blackwell.

134. Hartmann, M. and D. Jung, *Biocatalysis with enzymes immobilized on mesoporous hosts: the status quo and future trends.* Journal of Materials Chemistry, 2010. 20(5): p. 844-857.

135. Sheldon, R.A., *Enzyme Immobilization: The Quest for Optimum Performance.* Advanced Synthesis & Catalysis, 2007. 349(8-9): p. 1289-1307.

136. Safdar, M., J. Spross, and J. Jänis, *Microscale immobilized enzyme reactors in proteomics: latest developments.* Journal of Chromatography A, 2014. 1324: p. 1-10.

137. Meller, K., et al., *Preparation of an improved hydrophilic monolith to make trypsin-immobilized microreactors.* Journal of Chromatography B, 2016.

138. Ma, J., et al., *Immobilized enzyme reactors in proteomics.* TrAC Trends in Analytical Chemistry, 2011. 30: p. 691-702.

139. Sun, X., et al., *Immobilized trypsin on hydrophobic cellulose decorated nanoparticles shows good stability and reusability for protein digestion.* Analytical Biochemistry, 2015. 477: p. 21-27.

140. Kecskemeti, A. and A. Gaspar, *Particle-based immobilized enzymatic reactors in microfluidic chips.* Talanta, 2018. 180: p. 211-228.

141. Qiao, J., et al., *Trypsin immobilization in ordered porous polymer membranes for effective protein digestion.* Analytica Chimica Acta, 2016. 906: p. 156-164.

142. Nicoli, R., et al., *Trypsin immobilization on an ethylenediamine-based monolithic minidisk for rapid on-line peptide mass fingerprinting studies.* Journal of Chromatography A, 2009. 1216(13): p. 2695-2699.

143. Krenkova, J., N.A. Lacher, and F. Svec, *Highly Efficient Enzyme Reactors Containing Trypsin and Endoproteinase LysC Immobilized on Porous Polymer Monolith Coupled to MS Suitable for Analysis of Antibodies.* Analytical Chemistry, 2009. 81(5): p. 2004-2012.

144. Lee, J., et al., *Development of an Automated Digestion and Droplet Deposition Microfluidic Chip for MALDI-TOF MS.* Journal of the American Society for Mass Spectrometry, 2008. 19(7): p. 964-972.

145. Cingöz, A., F. Hugon-Chapuis, and V. Pichon, *Total on-line analysis of a target protein from plasma by immunoextraction, digestion and liquid chromatography–mass spectrometry.* Journal of Chromatography B, 2010. 878(2): p. 213-221.

146. Jiang, B., et al., *Hydrophilic immobilized trypsin reactor with magnetic graphene oxide as support for high efficient proteome digestion.* Journal of Chromatography A, 2012. 1254: p. 8-13.

147. Calleri, E., et al., *Trypsin-based monolithic bioreactor coupled on-line with LC/MS/MS system for protein digestion and variant identification in standard solutions and serum samples.* J Proteome Res, 2005. 4(2): p. 481-90.

148. Sassolas, A., L.J. Blum, and B.D. Leca-Bouvier, *Immobilization strategies to develop enzymatic biosensors.* Biotechnology Advances, 2012. 30(3): p. 489-511.

149. Jiang, H., et al., *A hydrophilic immobilized trypsin reactor with N-vinyl-2-pyrrolidinone modified polymer microparticles as matrix for highly efficient protein digestion with low peptide residue.* Journal of Chromatography A, 2012. 1246: p. 111-116.

150. Nicoli, R., et al., *Trypsin immobilization on three monolithic disks for on-line protein digestion.* Journal of Pharmaceutical and Biomedical Analysis, 2008. 48(2): p. 398-407.

151. Duan, J., et al., *Rapid protein identification using monolithic enzymatic microreactor and LC-ESI-MS/MS.* Proteomics, 2006. 6(2): p. 412-419.

152. Stigter, E.C.A., G.J. de Jong, and W.P. van Bennekom, *Pepsin immobilized in dextran-modified fused-silica capillaries for on-line protein digestion and peptide mapping.* Analytica Chimica Acta, 2008. 619: p. 231-8.

153. Kim, J.-H., et al., *Integrated Sample Preparation Methodology for Proteomics: Analysis of Native Proteins.* Analytical Chemistry, 2013. 85(17): p. 8039-8045.

154. Rivera-Burgos, D. and F.E. Regnier, *Native Protein Proteolysis in an Immobilized Enzyme Reactor as a Function of Temperature.* Analytical Chemistry, 2012. 84(16): p. 7021-7028.

155. Addona, T.A., et al., *Multi-site assessment of the precision and reproducibility of multiple reaction monitoring-based measurements of proteins in plasma.* Nature Biotechnology, 2009. 27: p. 633+.

156. Hoofnagle, A.N., *Quantitative clinical proteomics by liquid chromatography-tandem mass spectrometry: assessing the platform.* Clinical Chemistry, 2010. 56(2): p. 161-164.

157. Lee, M.S. and Q.C. Ji, *Protein Analysis Using Mass Spectrometry : Accelerating Protein Biotherapeutics from Lab to Patient*. 2017, New York, UNITED STATES: John Wiley & Sons, Incorporated.

158. Huck, C.W. and G.K. Bonn, *Recent developments in polymer-based sorbents for solid-phase extraction.* Journal of Chromatography A, 2000. 885(1–2): p. 51-72.

159. Andrade-Eiroa, A., et al., *Solid-phase extraction of organic compounds: A critical review. part ii.* TrAC Trends in Analytical Chemistry, 2016. 80: p. 655-667.

160. Silvestre, C.I.C., et al., *Liquid–liquid extraction in flow analysis: A critical review.* Analytica Chimica Acta, 2009. 652(1): p. 54-65.

161. Poole, C.F., *New trends in solid-phase extraction.* TrAC Trends in Analytical Chemistry, 2003. 22(6): p. 362-373.

162. Majors, R.E., *Solid-Phase Extraction*, in *Handbook of Sample Preparation*. 2010, John Wiley & Sons, Inc. p. 53-79.

163. Stevenson, D., *Immunoaffinity Extraction*, in *Encyclopedia of Separation Science*, I.D. Wilson, Editor. 2000, Academic Press: Oxford. p. 3060-3064.

164. Hage, D.S., *1 - Chromatography*, in *Principles and Applications of Clinical Mass Spectrometry*, N. Rifai, A.R. Horvath, and C.T. Wittwer, Editors. 2018, Elsevier. p. 1-32.

165. Moldoveanu, S. and V. David, *Chapter 7 - Solid-Phase Extraction*, in *Modern Sample Preparation for Chromatography*, S. Moldoveanu and V. David, Editors. 2015, Elsevier: Amsterdam. p. 191-286.

166. Buszewski, B. and M. Szultka, *Past, Present, and Future of Solid Phase Extraction: A Review.* Critical Reviews in Analytical Chemistry, 2012. 42(3): p. 198-213.

167. Rodrigues, C.A., et al., *Rapid extraction method followed by a d-SPE clean-up step for determination of phenolic composition and antioxidant and antiproliferative activities from berry fruits.* Food Chemistry, 2020. 309: p. 125694.

168. Peng, J., et al., *New techniques of on-line biological sample processing and their application in the field of biopharmaceutical analysis.* Acta pharmaceutica Sinica. B, 2016. 6(6): p. 540-551.

169. Ramos, L., *Critical overview of selected contemporary sample preparation techniques.* Journal of Chromatography A, 2012. 1221: p. 84-98.

170. Lucci, P., et al., *Current Trends in Sample Treatment Techniques for Environmental and Food Analysis*. 2012. p. 127-164.

171. Pena Pereira, F., *From Conventional to Miniaturized Analytical Systems*, in *Miniaturization in Sample Preparation*. 2014, Walter de Gruyter GmbH: Warschau/Berlin, Germany. p. 1-28.

172. Huang, Z. and H.K. Lee, *Materials-based approaches to minimizing solvent usage in analytical sample preparation*. 2012.

173. Płotka-Wasylka, J., et al., *Miniaturized solid-phase extraction techniques.* TrAC Trends in Analytical Chemistry, 2015. 73: p. 19-38.

174. Lord, H. and J. Pawliszyn, *Evolution of solid-phase microextraction technology.* Journal of Chromatography A, 2000. 885(1–2): p. 153-193.

175. Chen, J. and J.B. Pawliszyn, *Solid Phase Microextraction Coupled to High-Performance Liquid Chromatography.* Analytical Chemistry, 1995. 67(15): p. 2530-2533.

176. Ochiai, N., et al., *Solvent-assisted stir bar sorptive extraction by using swollen polydimethylsiloxane for enhanced recovery of polar solutes in aqueous samples: Application to aroma compounds in beer and pesticides in wine.* Journal of Chromatography A, 2016. 1455: p. 45-56.

177. Šafaříková, M. and I. Šafařík, *Magnetic solid-phase extraction.* Journal of Magnetism and Magnetic Materials, 1999. 194(1): p. 108-112.

178. Abdel-Rehim, M., *Microextraction by packed sorbent (MEPS): A tutorial.* Analytica Chimica Acta, 2011. 701(2): p. 119-128.

179. Naing, N.N., S.C. Tan, and H.K. Lee, *16 - Micro-solid-phase extraction*, in *Solid-Phase Extraction*, C.F. Poole, Editor. 2020, Elsevier. p. 443-471.

180. Telepchak, M.J., *Forensic and Clinical Applications of Solid Phase Extraction*, in *Forensic Science and Medicine*. 2004, Humana Press.

181. Alexandrou, L.D., et al., *Micro versus macro solid phase extraction for monitoring water contaminants: A preliminary study using trihalomethanes.* Science of The Total Environment, 2015. 512–513: p. 210-214.

182. Wei, D., et al., *Online and automated sample extraction.* Bioanalysis, 2015. 7(17): p. 2227-2233.

183. Said, R., et al., *Determination of four immunosuppressive drugs in whole blood using MEPS and LC–MS/MS allowing automated sample work-up and analysis.* Journal of Chromatography B, 2012. 897: p. 42-49.

184. Peters, S., et al., *An automated method for the analysis of phenolic acids in plasma based on ion-pairing micro-extraction coupled on-line to gas chromatography/mass spectrometry with in-liner derivatisation.* Journal of Chromatography A, 2012. 1226: p. 71-76.

185. Morris, B.D. and R.B. Schriner, *Development of an Automated Column Solid-Phase Extraction Cleanup of QuEChERS Extracts, Using a Zirconia-Based Sorbent, for Pesticide Residue Analyses by LC-MS/MS.* Journal of Agricultural and Food Chemistry, 2015. 63(21): p. 5107-5119.

186. Lant, M.S., J. Oxford, and L.E. Martin, *Automated sample preparation on-line with thermospray high-performance liquid chromatography—mass spectrometry for the determination of drugs in plasma.* Journal of Chromatography A, 1987. 394(1): p. 223-230.

187. ITSP Solutions. *ITSP's SmartSPE™*. 2016; Available from: https://www.itspsolutions.com/.

188. Lehotay, S.J., L. Han, and Y. Sapozhnikova, *Automated Mini-Column Solid-Phase Extraction Cleanup for High-Throughput Analysis of Chemical Contaminants in Foods by Low-Pressure Gas Chromatography—Tandem Mass Spectrometry.* Chromatographia, 2016. 79(17): p. 1113-1130.

189. Zhu, B., et al., *Simultaneous determination of 131 pesticides in tea by on-line GPC-GC–MS/MS using graphitized multi-walled carbon nanotubes as dispersive solid phase extraction sorbent.* Food Chemistry, 2019. 276: p. 202-208.

190. Sapozhnikova, Y., *High-throughput analytical method for 265 pesticides and environmental contaminants in meats and poultry by fast low pressure gas chromatography and ultrahigh-performance liquid chromatography tandem mass spectrometry.* Journal of Chromatography A, 2018. 1572: p. 203-211.

191. Zhong, M., et al., *Automated online solid-phase extraction liquid chromatography tandem mass spectrometry investigation for simultaneous quantification of per- and polyfluoroalkyl substances, pharmaceuticals and personal care products, and organophosphorus flame retardants in environmental waters.* Journal of Chromatography A, 2019. 1602: p. 350-358.

192. Lehmann, S., et al., *Determination of 74 new psychoactive substances in serum using automated in-line solid-phase extraction-liquid chromatography-tandem mass spectrometry.* Journal of Chromatography B, 2017. 1064: p. 124-138.

193. Marinova, M., et al., *Immunosuppressant therapeutic drug monitoring by LC-MS/MS: Workflow optimization through automated processing of whole blood samples.* Clinical Biochemistry, 2013. 46(16): p. 1723-1727.

194. Idder, S., et al., *Quantitative on-line preconcentration-liquid chromatography coupled with tandem mass spectrometry method for the determination of pharmaceutical compounds in water.* Analytica Chimica Acta, 2013. 805: p. 107-115.

195. Pan, J., et al., *Review of online coupling of sample preparation techniques with liquid chromatography.* Analytica Chimica Acta, 2014. 815: p. 1-15.

196. Quintana, J.B., et al., *Automated On-Line Renewable Solid-Phase Extraction-Liquid Chromatography Exploiting Multisyringe Flow Injection-Bead Injection Lab-on-Valve Analysis.* Analytical Chemistry, 2006. 78(8): p. 2832-2840.

197. Liska, I., *On-line versus off-line solid-phase extraction in the determination of organic contaminants in water: Advantages and limitations.* Journal of Chromatography A, 1993. 655(2): p. 163-176.

198. PerkinElmer. *Automated Liquid Handing*. [cited 2019 November 20]; Available from: https://www.perkinelmer.com/category/automation-liquid-handling-instruments.

199. Tecan. *Liquid Handling and Automation*. [cited 2019 November 20]; Available from: https://lifesciences.tecan.com/products/liquid_handling_and_automation.

200. Tomtec. *Quadra4™ Liquid Handling Workstation*. [cited 2019 November 20]; Available from: http://www.tomtec.com/quadra4.html.

201. Company, H. *Automated Liquid Handling*. 2019 [cited 2019 November 20]; Available from: https://www.hamiltoncompany.com/automated-liquid-handling.

202. Pichon, V., *Immunoaffinity Extraction*, in *Reference Module in Chemistry, Molecular Sciences and Chemical Engineering*. 2016, Elsevier.

203. Sellergren, B. and F. Lanza, *Chapter 15 - Molecularly imprinted polymers in solid phase extractions*, in *Techniques and Instrumentation in Analytical Chemistry*, B. Sellergren, Editor. 2001, Elsevier. p. 355-375.

204. Hennion, M.-C., *Solid-phase extraction: method development, sorbents, and coupling with liquid chromatography.* Journal of Chromatography A, 1999. 856(1–2): p. 3-54.

205. Augusto, F., et al., *New materials and trends in sorbents for solid-phase extraction.* TrAC Trends in Analytical Chemistry, 2013. 43: p. 14-23.

206. de Castro, M.D.L. and J.L.L. García, *Chapter 6 - High-pressure, high-temperature solvent extraction*, in *Techniques and Instrumentation in Analytical Chemistry*, M.D.L. de Castro and J.L.L. García, Editors. 2002, Elsevier. p. 233-279.

207. Gasilova, N., A.-L. Gassner, and H.H. Girault, *Analysis of major milk whey proteins by immunoaffinity capillary electrophoresis coupled with MALDI-MS.* ELECTROPHORESIS, 2012. 33(15): p. 2390-2398.

208. Wang, C., et al., *Development of immunoaffinity solid phase microextraction rods for analysis of three estrogens in environmental water samples.* Journal of Chromatography B, 2017. 1061-1062: p. 41-48.

209. Sun, S., et al., *Broad-spectrum immunoaffinity cleanup for the determination of aflatoxins B1, B2, G1, G2, M1, M2 in Ophiocordyceps sinensis and its pharmaceutical preparations by ultra performance liquid chromatography tandem mass spectrometry.* Journal of Chromatography B, 2017. 1068-1069: p. 112-118.

210. Pont, L., et al., *On-line immunoaffinity solid-phase extraction capillary electrophoresis mass spectrometry using Fab´antibody fragments for the analysis of serum transthyretin.* Talanta, 2017. 170: p. 224-232.

211. Panahi, Y., et al., *High sensitive and selective nano-molecularly imprinted polymer based electrochemical sensor for midazolam drug detection in pharmaceutical formulation and human urine samples.* Sensors and Actuators B: Chemical, 2018. 273: p. 1579-1586.

212. Scorrano, S., et al., *Synthesis of molecularly imprinted polymers for amino acid derivates by using different functional monomers.* International journal of molecular sciences, 2011. 12(3): p. 1735-1743.

213. Vasapollo, G., et al., *Molecularly imprinted polymers: present and future prospective*. International Journal of Molecular Sciences, 2011. 12(9): p. 5908-5945.

214. Sproß, J., et al., *Multidimensional nano-HPLC coupled with tandem mass spectrometry for analyzing biotinylated proteins*. Analytical and Bioanalytical Chemistry, 2013. 405(7): p. 2163-2173.

215. Minard-Basquin, C., et al. *Gold-nanoparticle-assisted oligonucleotide immobilisation for improved DNA detection*. IEE Proceedings - Nanobiotechnology, 2005. 152, 97-103.

216. Cao, L., *Immobilised enzymes: science or art?* Current Opinion in Chemical Biology, 2005. 9(2): p. 217-226.

217. Delaunay-Bertoncini, N. and M.C. Hennion, *Immunoaffinity solid-phase extraction for pharmaceutical and biomedical trace-analysis—coupling with HPLC and CE—perspectives*. Journal of Pharmaceutical and Biomedical Analysis, 2004. 34(4): p. 717-736.

218. Ikeda, T., et al., *Automated enzyme-linked immunosorbent assay using beads in a single tip (BIST) technology coupled with a novel anchor protein for oriented antibody immobilization*. Analytical Methods, 2014. 6(16): p. 6232-6235.

219. Asuri, P., et al., *Water-soluble carbon nanotube-enzyme conjugates as functional biocatalytic formulations*. Biotechnol Bioeng, 2006. 95(5): p. 804-11.

220. Atiroğlu, V., A. Atiroğlu, and M. Özacar, *Immobilization of α-amylase enzyme on a protein @metal–organic framework nanocomposite: A new strategy to develop the reusability and stability of the enzyme*. Food Chemistry, 2021. 349: p. 129127.

221. Hanefeld, U., L. Gardossi, and E. Magner, *Understanding enzyme immobilisation*. Chemical Society Reviews, 2009. 38(2): p. 453-468.

222. Zdarta, J., et al., *A General Overview of Support Materials for Enzyme Immobilization: Characteristics, Properties, Practical Utility*. Catalysts, 2018. 8(2): p. 92.

223. Zucca, P. and E. Sanjust, *Inorganic Materials as Supports for Covalent Enzyme Immobilization: Methods and Mechanisms*. Molecules, 2014. 19(9): p. 14139-14194.

224. Haider, T. and Q. Husain, *Immobilization of β galactosidase from Aspergillus oryzae via immunoaffinity support*. Biochemical Engineering Journal, 2009. 43(3): p. 307-314.

225. Dahiya, J., D. Singh, and P. Nigam, *Decolourisation of molasses wastewater by cells of Pseudomonas fluorescens immobilised on porous cellulose carrier*. Bioresource Technology, 2001. 78(1): p. 111-114.

226. Moreno-Mendieta, S.A., et al., *A novel antigen-carrier system: The Mycobacterium tuberculosis Acr protein carried by raw starch microparticles.* International Journal of Pharmaceutics, 2014. 474(1): p. 241-248.

227. Brewster, J.D., *Isolation and concentration of Salmonellae with an immunoaffinity column.* Journal of Microbiological Methods, 2003. 55(1): p. 287-293.

228. Yang, Y., et al., *Preparation and characterization of chitosan microparticles for immunoaffinity extraction and determination of enrofloxacin.* International Journal of Biological Macromolecules, 2016. 93: p. 783-788.

229. Zhu, D., et al., *Polyethyleneimine-grafted collagen fiber as a carrier for cell immobilization.* Journal of Industrial Microbiology & Biotechnology, 2015. 42(2): p. 189-196.

230. Afaq, S. and J. Iqbal, *Immobilization and stabilization of papain on chelating sepharose: a metal chelate regenerable carrier.* Electronic Journal of Biotechnology, 2001. 4: p. 1-2.

231. Wu, S., et al., *Preparing a metal-ion chelated immobilized enzyme reactor based on the polyacrylamide monolith grafted with polyethylenimine for a facile regeneration and high throughput tryptic digestion in proteomics.* Analytical and Bioanalytical Chemistry, 2012. 402(2): p. 703-710.

232. Černigoj, U., et al., *Characterization of methacrylate chromatographic monoliths bearing affinity ligands.* Journal of Chromatography A, 2016. 1464: p. 72-78.

233. Isgrove, F.H., et al., *Enzyme immobilization on nylon–optimization and the steps used to prevent enzyme leakage from the support.* Enzyme and Microbial Technology, 2001. 28(2–3): p. 225-232.

234. Dai, J., et al., *Phenanthroline method for quantitative determination of surface carboxyl groups on carboxylated polystyrene particles with high sensitivity.* Surface and Interface Analysis, 2009. 41(7): p. 577-580.

235. Yan, F., et al., *Polymer materials for enzyme immobilization and their application in bioreactors.* BMB Reports, 2011. 44(2): p. 087-095.

236. Claessens, H.A., M.A. van Straten, and J.J. Kirkland, *Effect of buffers on silica-based column stability in reversed-phase high-performance liquid chromatography.* Journal of Chromatography A, 1996. 728(1): p. 259-270.

237. Jaćkowska, M., et al., *Polymeric Functionalized Stationary Phase for Separation of Ionic Compounds by IC.* Chromatographia, 2010. 72(7): p. 611-616.

238. Qi, L. and Y. Ito, *Immunoaffinity centrifugal precipitation chromatography.* J Chromatogr A, 2007. 1151(1-2): p. 121-5.

239. Chefalo, P., et al., *Heme-regulated eIF-2α kinase purifies as a hemoprotein.* European journal of biochemistry / FEBS, 1999. 258: p. 820-30.

240. Hartmann, M. and X. Kostrov, *Immobilization of enzymes on porous silicas – benefits and challenges.* Chemical Society Reviews, 2013. 42(15): p. 6277-6289.

241. Magner, E., *Immobilisation of enzymes on mesoporous silicate materials.* Chemical Society Reviews, 2013. 42(15): p. 6213-6222.

242. Gustafsson, H., et al., *Immobilization of lipase from Mucor miehei and Rhizopus oryzae into mesoporous silica—The effect of varied particle size and morphology.* Colloids and Surfaces B: Biointerfaces, 2012. 100: p. 22-30.

243. Trevisan, H.C., L.H.I. Mei, and G.M. Zanin, *Preparation of silica with controlled pore sizes for enzyme immobilization.* Brazilian Journal of Chemical Engineering

2000. 17(1): p. 71-77.

244. Johnsson, B., S. Löfås, and G. Lindquist, *Immobilization of proteins to a carboxymethyldextran-modified gold surface for biospecific interaction analysis in surface plasmon resonance sensors.* Analytical Biochemistry, 1991. 198(2): p. 268-277.

245. Heurich, M., M.K.A. Kadir, and I.E. Tothill, *An electrochemical sensor based on carboxymethylated dextran modified gold surface for ochratoxin A analysis.* Sensors and Actuators B: Chemical, 2011. 156: p. 162-168.

246. Kamra, T., et al., *Covalent immobilization of molecularly imprinted polymer nanoparticles on a gold surface using carbodiimide coupling for chemical sensing.* Journal of Colloid and Interface Science, 2016. 461: p. 1-8.

247. Pensa, E., et al., *The Chemistry of the Sulfur–Gold Interface: In Search of a Unified Model.* Accounts of Chemical Research, 2012. 45(8): p. 1183-1192.

248. Wu, H., et al., *Titania and Alumina Sol−Gel-Derived Microfluidics Enzymatic-Reactors for Peptide Mapping: Design, Characterization, and Performance.* Journal of Proteome Research, 2004. 3(6): p. 1201-1209.

249. Thörn, C., H. Gustafsson, and L. Olsson, *QCM-D as a method for monitoring enzyme immobilization in mesoporous silica particles.* Microporous and Mesoporous Materials, 2013. 176: p. 71-77.

250. Falahati, M., et al., *The effect of functionalization of mesoporous silica nanoparticles on the interaction and stability of confined enzyme.* International Journal of Biological Macromolecules, 2012. 50(4): p. 1048-1054.

251. Zheng, Y., et al., *Mussel-inspired surface capping and pore filling to confer mesoporous silica with high loading and enhanced stability of enzyme.* Microporous and Mesoporous Materials, 2012. 152: p. 122-127.

252. Schrader, A.M., et al., *Surface chemical heterogeneity modulates silica surface hydration.* Proceedings of the National Academy of Sciences of the United States of America, 2018. 115(12): p. 2890-2895.

253. Emami, F.S., et al., *Prediction of Specific Biomolecule Adsorption on Silica Surfaces as a Function of pH and Particle Size.* Chemistry of Materials, 2014. 26(19): p. 5725-5734.

254. Mathé, C., et al., *Structural determinants for protein adsorption/non-adsorption to silica surface.* PLOS ONE

2013. 8(11): p. e81346-e81346.

255. Peng, G., et al., *Immobilized trypsin onto chitosan modified monodisperse microspheres: A different way for improving carrier's surface biocompatibility.* Applied Surface Science, 2012. 258: p. 5543-5552.

256. Piehler, J., et al., *A high-density poly(ethylene glycol) polymer brush for immobilization on glass-type surfaces.* Biosensors and Bioelectronics, 2000. 15(9): p. 473-481.

257. Paribok, I.V., A.E. Solomyanskii, and G.K. Zhavnerko, *Patterns of the adsorption of bovine serum albumin on carboxymethyl dextran and carboxymethyl cellulose films.* Russian Journal of Physical Chemistry A, 2016. 90(2): p. 466-469.

258. Markovic, G., et al., *Application of surface acoustic waves for optimisation of biocompatibility of carboxymethylated dextran surfaces.* Surface and Coatings Technology, 2006. 201: p. 1282-1288.

259. Piehler, J., et al., *Surface modification for direct immunoprobes.* Biosensors and Bioelectronics, 1996. 11(6): p. 579-590.

260. Hoffman, A.S. and J.A. Hubbell, *Chapter I.2.17 - Surface-Immobilized Biomolecules*, in *Biomaterials Science (Third Edition)*, B.D. Ratner, et al., Editors. 2013, Academic Press. p. 339-349.

261. Cao, L., *Carrier-bound Immobilized Enzymes: Principles, Application and Design*. Carbohydrate Polymers. Vol. 64. 2006. 603.

262. Roessl, U., J. Nahálka, and B. Nidetzky, *Carrier-free immobilized enzymes for biocatalysis.* Biotechnology Letters, 2010. 32(3): p. 341-50.

263. Cao, L., F. van Rantwijk, and R.A. Sheldon, *Cross-Linked Enzyme Aggregates: A Simple and Effective Method for the Immobilization of Penicillin Acylase.* Organic Letters, 2000. 2(10): p. 1361-1364.

264. Li, S., *Chapter 11 - Fundamentals of Biochemical Reaction Engineering*, in *Reaction Engineering*, S. Li, Editor. 2017, Butterworth-Heinemann: Boston. p. 491-539.

265. Labus, K., K. Wolanin, and Ł. Radosiński, *Comparative Study on Enzyme Immobilization Using Natural Hydrogel Matrices—Experimental Studies Supported by Molecular Models Analysis*. Catalysts, 2020. 10(5): p. 489.

266. Homaei, A.A., et al., *Enzyme immobilization: an update*. Journal of chemical biology, 2013. 6(4): p. 185-205.

267. Koutsopoulos, S., et al., *Adsorption of Trypsin on Hydrophilic and Hydrophobic Surfaces*. Langmuir, 2007. 23(4): p. 2000-2006.

268. Zhou, Z., et al., *Ion-exchange-membrane-based enzyme micro-reactor coupled online with liquid chromatography–mass spectrometry for protein analysis*. Analytical and Bioanalytical Chemistry, 2012. 403(1): p. 239-246.

269. Dismer, F., M. Petzold, and J. Hubbuch, *Effects of ionic strength and mobile phase pH on the binding orientation of lysozyme on different ion-exchange adsorbents*. Journal of Chromatography A, 2008. 1194(1): p. 11-21.

270. Fuentes, M., et al., *Reversible and strong immobilization of proteins by ionic exchange on supports coated with sulfate-dextran*. Biotechnol Prog, 2004. 20(4): p. 1134-9.

271. Reddy, K.R.C. and A.M. Kayastha, *Improved stability of urease upon coupling to alkylamine and arylamine glass and its analytical use*. Journal of Molecular Catalysis B: Enzymatic, 2006. 38(2): p. 104-112.

272. Pierre, S.J., et al., *Covalent Enzyme Immobilization onto Photopolymerized Highly Porous Monoliths*. Advanced Materials, 2006. 18(14): p. 1822-1826.

273. Sun, J., et al., *Stability and activity of immobilized trypsin on carboxymethyl chitosan-functionalized magnetic nanoparticles cross-linked with carbodiimide and glutaraldehyde*. Journal of Chromatography B, 2017. 1054: p. 57-63.

274. Misra, A. and P. Dwivedi, *Immobilization of oligonucleotides on glass surface using an efficient heterobifunctional reagent through maleimide–thiol combination chemistry*. Analytical Biochemistry, 2007. 369(2): p. 248-255.

275. Edupuganti, S.R., et al., *Use of T-2 toxin-immobilized amine-activated beads as an efficient affinity purification matrix for the isolation of specific IgY*. Journal of Chromatography B, 2013. 923-924: p. 98-101.

276. Chiou, S.-H. and W.-T. Wu, *Immobilization of Candida rugosa lipase on chitosan with activation of the hydroxyl groups*. Biomaterials, 2004. 25(2): p. 197-204.

277. Zhang, D.-H., L.-X. Yuwen, and L.-J. Peng, *Parameters Affecting the Performance of Immobilized Enzyme*. Journal of Chemistry, 2013. 2013: p. 7.

278. Rusmini, F., Z. Zhong, and J. Feijen, *Protein Immobilization Strategies for Protein Biochips*. Biomacromolecules, 2007. 8(6): p. 1775-1789.

279. Sisson, T.H. and C.W. Castor, *An improved method for immobilizing IgG antibodies on protein A-agarose*. J Immunol Methods, 1990. 127(2): p. 215-20.

280. Hage, D.S. and J. Cazes, *Handbook of Affinity Chromatography*. 2005: CRC Press.

281. Li, G. and R.E. Moellering, *A Concise, Modular Antibody-Oligonucleotide Conjugation Strategy Based on Disuccinimidyl Ester Activation Chemistry*. Chembiochem : a European journal of chemical biology, 2019. 20(12): p. 1599-1605.

282. Li, L., J. Yan, and M.-P. Zhao, *Improvement of the performance of an immunoaffinity extraction method via region-specific immobilization of IgG*. Journal of Chromatography A, 2006. 1103(2): p. 350-355.

283. Thermo Scientific, *Avidin-Biotin Technical Handbook*. 2009.

284. Pfister, D., L. Nicoud, and M. Morbidelli, *Continuous Biopharmaceutical Processes: Chromatography, Bioconjugation, and Protein Stability*. Cambridge Series in Chemical Engineering. 2018, Cambridge: Cambridge University Press.

285. Gunnoo, S.B. and A. Madder, *Bioconjugation – using selective chemistry to enhance the properties of proteins and peptides as therapeutics and carriers*. Organic & Biomolecular Chemistry, 2016. 14(34): p. 8002-8013.

286. Barth, B.M., et al., *Bioconjugation of Calcium Phosphosilicate Composite Nanoparticles for Selective Targeting of Human Breast and Pancreatic Cancers In Vivo*. ACS Nano, 2010. 4(3): p. 1279-1287.

287. Geyik, C., et al., *Bioconjugation and Applications of Amino Functional Fluorescence Polymers*. Macromolecular Bioscience, 2017. 17(3): p. 1600232.

288. Salimi, K., et al., *Protein A and protein A/G coupled magnetic SiO2 microspheres for affinity purification of immunoglobulin G*. International Journal of Biological Macromolecules, 2018. 111: p. 178-185.

289. Pfister, D. and M. Morbidelli, *Process for protein PEGylation*. Journal of Controlled Release, 2014. 180: p. 134-149.

290. Foubert, A., et al., *Bioconjugation of quantum dots: Review & impact on future application*. TrAC Trends in Analytical Chemistry, 2016. 83.

291. Hermanson, G.T., *Chapter 5 - Homobifunctional Crosslinkers*, in *Bioconjugate Techniques (Third Edition)*, G.T. Hermanson, Editor. 2013, Academic Press: Boston. p. 275-298.

292. Hermanson, G.T., *Chapter 6 - Heterobifunctional Crosslinkers*, in *Bioconjugate Techniques (Third Edition)*, G.T. Hermanson, Editor. 2013, Academic Press: Boston. p. 299-339.

293. Avrameas, S. and T. Ternynck, *The Cross-linking of Proteins with Glutaraldehyde and its use for the preparation of immunoadsorbents.* Immunochemistry, 1969. 6(1): p. 53-66.

294. Lalli, E., G.C. Sarti, and C. Boi, *Effect of the spacer arm on non-specific binding in membrane affinity chromatography.* MRS Communications, 2018. 8(1): p. 65-70.

295. Hermanson, G.T., *Chapter 4 - Zero-Length Crosslinkers*, in *Bioconjugate Techniques (Third Edition)*, G.T. Hermanson, Editor. 2013, Academic Press: Boston. p. 259-273.

296. Hoare, D.G. and D.E. Koshland, *A Procedure for the Selective Modification of Carboxyl Groups in Proteins.* Journal of the American Chemical Society, 1966. 88(9): p. 2057-2058.

297. Thermo Scientific, *Crosslinking Reagents Technical Handbook*. 2012, Thermo Scientific: USA.

298. Williams, A. and I.T. Ibrahim, *Carbodiimide chemistry: recent advances.* Chemical Reviews, 1981. 81(6): p. 589-636.

299. Staros, J.V., R.W. Wright, and D.M. Swingle, *Enhancement by N-hydroxysulfosuccinimide of water-soluble carbodiimide-mediated coupling reactions.* Analytical Biochemistry, 1986. 156(1): p. 220-222.

300. Wilchek, M. and T. Miron, *Limitations of N-hydroxysuccinimide esters in affinity chromatography and protein immobilization.* Biochemistry, 1987. 26(8): p. 2155-2161.

301. Karyakin, A.A., et al., *Oriented Immobilization of Antibodies onto the Gold Surfaces via Their Native Thiol Groups.* Analytical Chemistry, 2000. 72(16): p. 3805-3811.

302. Ho, J.-a.A., et al., *Ultrasensitive electrochemical detection of biotin using electrically addressable site-oriented antibody immobilization approach via aminophenyl boronic acid.* Biosensors and Bioelectronics, 2010. 26(3): p. 1021-1027.

303. Makaraviciute, A. and A. Ramanaviciene, *Site-directed antibody immobilization techniques for immunosensors.* Biosensors and Bioelectronics, 2013. 50: p. 460-471.

304. Ying, L.-L., et al., *Poly(glycidyl methacrylate) nanoparticle-coated capillary with oriented antibody immobilization for immunoaffinity in-tube solid phase microextraction: Preparation and characterization.* Journal of Chromatography A, 2017. 1509: p. 1-8.

305. Hermanson, G.T., *Chapter 20 - Antibody Modification and Conjugation*, in *Bioconjugate Techniques (Third Edition)*, G.T. Hermanson, Editor. 2013, Academic Press: Boston. p. 867-920.

306. Iqbal, S.S., et al., *A review of molecular recognition technologies for detection of biological threat agents.* Biosensors and Bioelectronics, 2000. 15(11): p. 549-578.

307. Płotka-Wasylka, J., et al., *Modern trends in solid phase extraction: New sorbent media.* TrAC Trends in Analytical Chemistry, 2016. 77: p. 23-43.

308. Dubiel, E.A., et al., *In vitro morphogenesis of PANC-1 cells into islet-like aggregates using RGD-covered dextran derivative surfaces.* Colloids and Surfaces B: Biointerfaces, 2012. 89: p. 117-125.

309. Lorimer, J.P., et al., *Effect of ultrasound on the degradation of aqueous native dextran.* Ultrasonics Sonochemistry, 1995. 2(1): p. S55-S57.

310. Piehler, J., et al., *Protein interactions in covalently attached dextran layers.* Colloids and Surfaces B: Biointerfaces, 1999. 13(6): p. 325-336.

311. Penzol, G., et al., *Use of dextrans as long and hydrophilic spacer arms to improve the performance of immobilized proteins acting on macromolecules.* Biotechnology and Bioengineering, 1998. 60(4): p. 518-523.

312. Johnsson, B., et al., *Comparison of methods for immobilization to carboxymethyl dextran sensor surfaces by analysis of the specific activity of monoclonal antibodies.* Journal of Molecular Recognition, 1995. 8(1-2): p. 125-131.

313. Hajdukiewicz, J., et al., *An enzyme-amplified amperometric DNA hybridisation assay using DNA immobilised in a carboxymethylated dextran film anchored to a graphite surface.* Biosensors and Bioelectronics, 2010. 25: p. 1037-42.

314. ePrep. *Robotic Analytical Syringe Sample Preparation*. 2020 [cited 2020; Available from: https://www.eprep-analytical.com/.

315. Porto-Figueira, P., et al., *A fast and innovative microextraction technique, μSPEed, followed by ultrahigh performance liquid chromatography for the analysis of phenolic compounds in teas.* Journal of Chromatography A, 2015. 1424: p. 1-9.

316. Moein, M.M., A. Abdel-Rehim, and M. Abdel-Rehim, *Microextraction by packed sorbent (MEPS).* TrAC Trends in Analytical Chemistry, 2015. 67: p. 34-44.

317. Wu, H.-X., et al., *Effects of −COOH Groups on Organic Particle Surface on Hydrous Alumina Heterogeneous Coating.* Industrial & Engineering Chemistry Research, 2007. 46(13): p. 4363-4367.

318. Prior, R.L., X. Wu, and K. Schaich, *Standardized Methods for the Determination of Antioxidant Capacity and Phenolics in Foods and Dietary Supplements.* Journal of Agricultural and Food Chemistry, 2005. 53(10): p. 4290-4302.

319. Jodeh, S., et al., *Synthesis of 1-(Pyrrol-2-yl) imine modified silica as a new sorbent for the removal of hexavalent chromium from water*. 2015. 1-2.

320. Purama, R.K., et al., *Structural analysis and properties of dextran produced by Leuconostoc mesenteroides NRRL B-640.* Carbohydrate Polymers, 2009. 76(1): p. 30-35.

321. Ayala, V., et al., *Effect of surface charge on the colloidal stability and in vitro uptake of carboxymethyl dextran-coated iron oxide nanoparticles.* Journal of Nanoparticle Research, 2013. 15(8): p. 1874.

322. Aylward, G.H. and T.J.V. Findlay, *SI Chemical Data*. 2008: Wiley.

323. Finholt, J.E., *Basic Physical Chemistry (Moore, Walter J.).* Journal of Chemical Education, 1984. 61(7): p. A208.

324. Wagner, B.M., et al., *Superficially porous particles with 1000Å pores for large biomolecule high performance liquid chromatography and polymer size exclusion chromatography.* Journal of chromatography. A, 2017. 1489: p. 75-85.

325. Trevisan, H.C., L.H.I. Mei, and G.M. Zanin, *Preparation of silica with controlled pore sizes for enzyme immobilization.* Brazilian Journal of Chemical Engineering, 2000. 17: p. 71-77.

326. Bayne, L., R.V. Ulijn, and P.J. Halling, *Effect of pore size on the performance of immobilised enzymes.* Chemical Society Reviews, 2013. 42(23): p. 9000-9010.

327. Osaka Soda Co., L., *DAISOGEL™ High Resolution Chromatography Products*. 2006.

328. Bonichon, M., et al., *Online coupling of immunoextraction, digestion, and microliquid chromatography-tandem mass spectrometry for the analysis of sarin and soman-butyrylcholinesterase adducts in human plasma.* Analytical and Bioanalytical Chemistry, 2018. 410(3): p. 1039-1051.

329. Wei, Z.-H., et al., *Construction of a microfluidic platform integrating online protein fractionation, denaturation, digestion, and peptide enrichment.* Talanta, 2021. 224: p. 121810.

330. Li, Y., et al., *Integrated proteomic sample preparation with combination of on-line high-abundance protein depletion, denaturation, reduction, desalting and digestion to achieve high throughput plasma proteome quantification.* Analytica Chimica Acta, 2021. 1154: p. 338343.

331. Šlechtová, T., et al., *Performance comparison of three trypsin columns used in liquid chromatography.* Journal of Chromatography A, 2017. 1490: p. 126-132.

332. Hinterwirth, H., W. Lindner, and M. Lämmerhofer, *Bioconjugation of trypsin onto gold nanoparticles: Effect of surface chemistry on bioactivity.* Analytica Chimica Acta, 2012. 733: p. 90-97.

333. Sun, L., et al., *High efficiency and quantitatively reproducible protein digestion by trypsin-immobilized magnetic microspheres.* Journal of Chromatography A, 2012. 1220: p. 68-74.

334. Wei, L., et al., *Immobilization of enzyme on detonation nanodiamond for highly efficient proteolysis.* Talanta, 2010. 80(3): p. 1298-1304.

335. Yuan, H., L. Zhang, and Y. Zhang, *Preparation of high efficiency and low carry-over immobilized enzymatic reactor with methacrylic acid–silica hybrid monolith as matrix for on-line protein digestion.* Journal of Chromatography A, 2014. 1371: p. 48-57.

336. Thakur, V.K. and M.K. Thakur, *Handbook of Polymers for Pharmaceutical Technologies, Biodegradable Polymers*. 2015: Wiley.

337. Xu, F., et al., *Facile trypsin immobilization in polymeric membranes for rapid, efficient protein digestion.* Analytical chemistry, 2010. 82(24): p. 10045-10051.

338. Liu, Y., et al., *Assessment of the enzymatic activity and inhibition using HPFA with a microreactor, trypsin, absorbed on immobilized artificial membrane.* J Chromatogr Sci, 2010. 48(2): p. 150-5.

339. Bernevic, B., et al., *Online immunocapture ICP-MS for the determination of the metalloprotein ceruloplasmin in human serum.* BMC Research Notes, 2018. 11(1): p. 213.

340. Wang, M., et al., *Quantitative Analysis of Proteins via Sulfur Determination by HPLC Coupled to Isotope Dilution ICPMS with a Hexapole Collision Cell.* Analytical Chemistry, 2007. 79(23): p. 9128-9134.

341. Kinter, M. and N.E. Sherman, *Protein Sequencing and Identification Using Tandem Mass Spectrometry*. 2000, New York: John Wiley. 301.

342. Regnier, F.E., *Bonded carbohydrate stationary phases for chromatography*. 1976, Google Patents.

343. Janson, J.-C., *Protein Purification : Principles, High Resolution Methods, and Applications*. 2011, Hoboken, USA: John Wiley & Sons, Incorporated.

344. GE Healthcare Life Sciences, *Ion Exchange Chromatography Principles and Methods*. 2016.

345. Kotormán, M., et al., *Effects of Ca2+ on catalytic activity and conformation of trypsin and α-chymotrypsin in aqueous ethanol.* Biochemical and Biophysical Research Communications, 2003. 304(1): p. 18-21.

346. Gilliland, G.L. and A. Teplyakov, *Structural Calcium (Trypsin, Subtilisin)*, in *Handbook of Metalloproteins*.

347. Horak, J., S. Hofer, and W. Lindner, *Optimization of a ligand immobilization and azide group endcapping concept via "Click-Chemistry" for the preparation of adsorbents for antibody purification.* Journal of Chromatography B, 2010. 878(32): p. 3382-3394.

348. Schwert, G.W. and Y. Takenaka, *A spectrophotometric determination of trypsin and chymotrypsin.* Biochimica et Biophysica Acta, 1955. 16: p. 570-575.

349. Šlechtová, T., et al., *Performance comparison of three trypsin columns used in liquid chromatography.* Journal of chromatography. A, 2017. 1490: p. 126-132.

350. Proc, J.L., et al., *A quantitative study of the effects of chaotropic agents, surfactants, and solvents on the digestion efficiency of human plasma proteins by trypsin.* Journal of proteome research, 2010. 9(10): p. 5422-5437.

351. Sechi, S. and B.T. Chait, *Modification of cysteine residues by alkylation. A tool in peptide mapping and protein identification.* Anal Chem, 1998. 70(24): p. 5150-8.

352. Thermo Scientific, *NanoDrop 2000/2000c Spectrophotometer V1.0 User Manual*. 2009.

353. Chang, S.G. and C.J. Guidos, *Method for Tagging Antibodies with Metals for Mass Cytometry Experiments*, in *Mass Cytometry: Methods and Protocols*, H.M. McGuire and T.M. Ashhurst, Editors. 2019, Springer New York: New York, NY. p. 47-54.

354. Some, D., et al., *Characterization of Proteins by Size-Exclusion Chromatography Coupled to Multi-Angle Light Scattering (SEC-MALS).* Journal of Visualized Experiments, 2019.

355. Janeway, C., et al., *The structure of a typical antibody molecule.*, in *Immunobiology: The Immune System in Health and Disease*. 2001, Garland Pub.

356. Feng, R., Y. Konishi, and A.W. Bell, *High accuracy molecular weight determination and variation characterization of proteins up to 80 ku by ionspray mass spectrometry.* Journal of the American Society for Mass Spectrometry, 1991. 2(5): p. 387-401.

357. GE Healthcare Life Sciences, *Affinity Chromatography Principles and Methods*. 2007.

358. Thornton, K., et al., *A Model System for Fast Screening of Optimal Protein Purification Conditions*. 2018, Bio-Rad Laboratories, Inc: California, USA.

359. Bonichon, M., et al., *Development of immunosorbents coupled on-line to immobilized pepsin reactor and micro liquid chromatography–tandem mass spectrometry for analysis of butyrylcholinesterase in human plasma.* Journal of Chromatography A, 2017. 1526: p. 70-81.